Design of Stable Nanocrystalline Materials for Extreme Applications

by

Mansa Rajagopalan

A Dissertation Presented in Partial Fulfillment
of the Requirements for the Degree
Doctor of Philosophy

Approved October 2016 by the
Graduate Supervisory Committee:

Kiran N. Solanki, Chair
Terry Alford
Yang Jiao
Kris A. Darling

ARIZONA STATE UNIVERSITY

December 2016

ABSTRACT

Nanocrystalline (NC) materials experience inherent microstructural instability when exposed to elevated temperature, deformation rates or loads over long periods of time which limits its applications as well as processing. The instability arises due to the predominance of grain boundary (GB) diffusional processes which hastens coarsening. This dissertation aims to provide a solution for the very first time, through the development and characterization of a bulk NC alloy system. The NC-Cu-Ta discussed here offers exceptional thermal stability in addition to superior strength and creep resistance. The systematic study of the behavior of this material will pave the way for future development of NC materials with a multitude of optimized properties for extreme applications.

In-situ and ex-situ TEM characterization, multiple strain-rate compression testing and atomistic modeling were employed to investigate the behavior of NC-Cu-Ta under intense heating, stress/strain-rate and creep conditions. Results reveal, that temperature influences the misfit strain, leading to a significant change in flow stress, despite which (strength) remains greater than all known NC metals. Further, this alloy was found to achieve and retain strengths which were over two orders of magnitude higher than most NC metals under elevated temperature conditions. Dislocation-based slip was found to predominate at elevated temperatures for both high- and low-strain rate testing whereas twinning was favored during low temperature high-strain rate testing. The solute concentration was also found to play a role in dictating the deformation where heterogeneous twinnability was found to decrease with an increase in Ta concentration.

A paradigm-shift in the creep response of NC-materials with unprecedented property combinations is also reported, i.e., high strength with extremely high temperature creep resistance (6-8 orders higher than other NC materials), in this NC-Cu-Ta-alloy. The unique combination of properties in these NC-alloys is achieved through a processing route that creates distinct GB-pinning nanoclusters of the solute that favor kinetic stability of grains.

Overall, this dissertation provides an understanding of the mechanical response of a stable alloy system to extreme conditions, which was previously unattainable, and a perspective on the design of a new class of NC alloys exhibiting a multitude of optimized high temperature properties.

DEDICATION

I dedicate this dissertation to my family – parents Padma and Rajagopalan who have been a constant source of inspiration and have always been there for me, my sister Prasanna who pushes me to be a better person and my in-laws who feel a sense of joy in my work. Last but not least, to my husband Rahul for his unwavering support and encouragement.

ACKNOWLEDGMENTS

This dissertation would have not been possible without the support of many people. First and foremost, I would like to thank my advisor Prof. K.N. Solanki, for his invaluable support, motivation and guidance throughout my Ph.D. journey. He gave me the opportunity to tackle various challenging projects, and has indeed helped to push me beyond what I thought my limits were.

I would also like to thank my other committee members: Dr. Kris A. Darling, Prof. Terry Alford and Prof. Yang Jiao for their insightful comments and helpful remarks related to the research.

I thank the other members of Multiphysics Lab - Dr. Mehul Bhatia, Dr. Ilaksh Adlakha, Benyamin Gholami, Scott Turnage, Pulkit Garg, Chaitanya Kale, and Soundarya Srinivasan for the stimulating discussions, sleepless nights while we were working before deadlines and the fun we had as a group in the last five years. I would also like to express my thankfulness to Dr. Billy Hornbuckle at ARL for the help extended.

Further, there are no words to describe the constant support from my friends here who made Tempe a home away from home. Their love and encouragement has helped me in so many ways.

I would like to acknowledge the support of Army Research Laboratory through grant W911NF-15-2-0038 for the research. The use of facilities of ASU Leroy Eyring Center for Solid State Science is also gratefully acknowledged.

TABLE OF CONTENTS

CHAPTER Page

LIST OF FIGURES

Figure Page

Figure Page

Figure Page

Figure Page

Figure Page

Figure Page

Figure Page

CHAPTER 1

1 MOTIVATION

Nanocrystalline (NC) materials with mean grain size (d) less than 100 nm have received significant attention due to the enhanced mechanical properties compared to coarse-grained (CG) materials ($d > 1$ μm). Therefore, NC alloys are very attractive for multiple engineering and structural applications (R. Z. Valiev et al. 2007; Ruslan Z. Valiev, Xia, and Langdon 2009). However, the high interfacial energy of the boundaries lead to instability. For instance, NC Cu samples exhibited dramatic grain growth even at room temperature. Addition of stress alleviates the problem even at sub-zero temperatures. The plastic instability (Kumar, Van Swygenhoven, and Suresh 2003a; Meyers, Mishra, and Benson 2006; Ovid'ko 2007; Dao et al. 2007) due to loss in the strain hardening behavior and grain growth (under both monotonic and cyclic loading) (Gianola et al. 2006; Malow and Koch 1997; Hibbard et al. 2002) observed in various pure NC materials at small grain sizes at low homologous temperatures has been well documented. Furthermore, the effect of coarsening is elevated under conditions of prolonged exposure to temperature and stress which is typical of the conditions experienced by structural materials. In addition, the processing of these NC materials also take a hit where the processing routes involve extended periods of exposure to high temperatures. As a result, for the past 30 years, basic deformation research has been restricted to lower temperatures because of this short fall.

While challenges remain, recent advanced in experimental, computation and theoretical capability have allowed for the synthesis of thermally and mechanically stabilized bulk specimens to be produced that have heretofore been pursued only on a very limited basis. The addition of solutes to minimize coarsening is considered to stabilize the nanocrystalline materials. This thermal stability is critically important for producing *bulk* NC specimens using mechanical alloying, whereby a subsequent high temperature consolidation step is required to produce a fully dense, bulk NC sample (Carl C Koch 2007; Carl C. Koch et al. 2013; Frolov et al. 2012; K. A. Darling, Tschopp, VanLeeuwen, et al. 2014a; Andrew J Detor and Schuh 2007; Ma 2004). Synthesis of one such material based on thermodynamic and kinetic modes of stabilization, NC-Cu-10at.%Ta has paved way for the emergence of development of such stable alloys.

Despite significant gains in knowledge related to the development and engineering of plasticity in nanomaterials, there still persist a sizeable gap in the fundamental understanding of how the stable nanostructured materials respond at highly elevated temperatures and stress levels. Specifically, isolation and identification of microstructural features that influence the deformation and stability in these alloys. This complete understanding is to satisfactorily address the current need for stronger structural materials in many important technologies.

Therefore, in this work the focus is on the understanding the mechanical response and deformation behavior of stable NC alloys with NC-Cu-10at.%Ta as a model system which will aid in design and development of super-strong advanced NC materials.

CHAPTER 2

2 BACKGROUND AND RESEARCH OBJECTIVE

2.1 Background

Nanocrystalline (NC) metals and alloys have received significant attention over the past couple of decades owing to their interesting properties. As their name suggests, polycrystalline materials with their average grain size (d) below 100 nm, are classified as NC materials. These materials possess a large volume fraction of grain boundaries (GBs), which play a more dominant role in determining the behavior in comparison to their coarse grained (CG) counterparts (>1 micron average grain size). The upper limit of their regime defined by the term “ultra-fine” grain (UFG) is applicable for metals and alloys whose average grain size is between 250 to 1000 nm. Properties such as superior strength, improved toughness, enhanced diffusivity and wear resistance in comparison to CG metals make NC alloys very attractive for multiple engineering applications (R. Z. Valiev et al. 2007; Ruslan Z. Valiev, Xia, and Langdon 2009). The strengthening due to grain refinement in CG and UFG metals and alloys is depicted by the Hall-Petch relationship which indicates that dislocation pileup at the GBs is responsible for the resistance to plastic deformation (Hall 1954; Petch 1953). However, as grain sizes approach the NC regime the relationship is valid however it breaks down at around 15 nm (Gleiter 2000; Meyers, Mishra, and Benson 2006) beyond which there is a plateau/negative slope exists for grain sizes below a critical size (e.g., 8-15 nm for Cu (Schiøtz, Di Tolla, and Jacobsen 1998; Van Swygenhoven, Caro, and Farkas 2001)). This inverse Hall-Petch effect has been attributed to a change in deformation mechanism e.g., from dislocation pileups to processes such as GB sliding or the occurrence of coble creep (A. H. Chokshi et al. 1989; Xiao et al. 2001). The strain rate and pressure dependence of deformation was determined to be the largest at the same average grain size for the onset of the Hall-Petch breakdown (Van Swygenhoven, Caro, and Farkas 2001; Schiøtz, Di Tolla, and Jacobsen 1998; Trelewicz and Schuh 2007). In addition, NC metals and alloys also exhibit high strain rate sensitivity, plastic strain recovery (J. Rajagopalan, Han, and Saif 2007; Y. Wei, Bower, and Gao 2008a) and creep deformation (Meyers, Mishra, and Benson 2006; Dao et al. 2007) at relatively low temperatures. An illustration of the Hall-Petch relation and breakdown is in Fig 1.

Several studies, both experimental and computational, have documented in great detail the deformation mechanisms and mechanical behavior of NC and UFG materials (Kumar, Van Swygenhoven, and Suresh 2003a; Meyers, Mishra, and Benson 2006; Ovid'ko 2007; Ii and Boyce 2010; Dao et al. 2007; Q. Wei et al. 2008; Q. Wei et al. 2003; Connolley, Mchugh, and Bruzzi 2005; Rinaldi et al. 2008). These mechanisms and properties are influenced by the inherent microstructure and not the grain size solely. In the case of CG metals, the movement of the dislocations contributes to the plastic deformation and microstructural features such as solutes, GBs also interact with the dislocations and are responsible for annihilation of dislocations (Hirth and Lothe 1982). However, NC metals have limited plasticity due to the small grain size and lack of dislocation sources to contribute towards plasticity (Saada 2005; Marc Legros, Gianola, and Hemker 2008). Experimentally observed deformation mechanisms include deformation twinning in NC face centered cubic (FCC) metals, GB rotation/sliding and dislocation glide (X. Liao et al. 2003; B. Q. Li et al. 2009; M. Chen et al. 2003; X. Z.

Liao et al. 2004; Zhu, Liao, and Wu 2012; Zhu et al. 2011; Wu et al. 2011; Cheng et al. 2009). Plastic instability (Kumar, Van Swygenhoven, and Suresh 2003a; Meyers, Mishra, and Benson 2006; Ovid'ko 2007; Ii and Boyce 2010; Dao et al. 2007) due to loss in the strain hardening behavior and grain growth (under both monotonic and cyclic loading) (T. J. Rupert et al. 2009; Gianola et al. 2006; Fan et al. 2006; Carl C Koch 2007; Malow and Koch 1997; Hibbard et al. 2002) have also been observed in various pure NC materials. In-situ and ex-situ transmission electron microscopy (TEM) studies have been instrumental in characterizing the nanoscale deformation behavior of NC metals and alloys. These studies have indicated that the dislocation mediated plasticity is a dominant mechanism for grain sizes above 30 nm (Kumar et al. 2003; Hugo et al. 2003). The deformation mechanisms in NC metals and alloys are not only dependent on the material properties but the external variables such as the temperature and also the mode of loading. In particular, the mechanisms associated with deformation for high strain rate loading is different in NC metals and alloys as compared to their CG counterparts. That is, hardening due to forest dislocations is unlikely in NC materials with FCC structure (Duhamel, Brechet, and Champion 2010). Simulations in addition to the experimental observations have contributed to the understanding of deformation mechanisms of NC metals and alloys. Molecular dynamics (MD) studies have indicated that GBs serve as a nucleation sites and provide trapping sinks for the dislocations. That is, the dislocations once nucleated, travel across the grain and get absorbed in the opposite GB. These GBs are also responsible for pinning the dislocations ultimately obstructing the motion of the dislocations and thermal energy is required to unpin the dislocations (Schiøtz and Jacobsen 2003b; Van Swygenhoven, Caro, and Farkas 2001; Swygenhoven and Caro

1997; Van Swygenhoven, Derlet, and Hasnaoui 2002). Thus the availability of advanced processing and characterization tools enables us to fabricate, inspect the structure and mechanical behavior of NC metals and alloys for various applications.

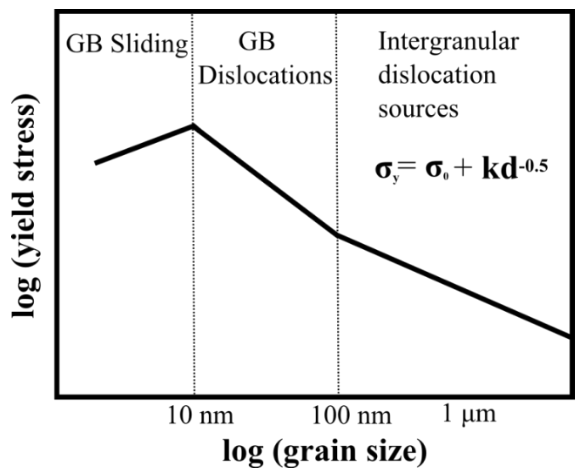

Figure 1: Illustration of Hall- Petch behavior and breakdown adapted from (Kumar, Van Swygenhoven, and Suresh 2003b)

Defects in NC metals and alloys play a critical role in controlling the deformation processes and mechanical properties. GBs, triple junctions (TJs) and stacking faults (SFs) contribute toward emission (especially GBs), nucleation and annihilation of dislocations.

Furthermore GBs are a major contributor towards deformation mechanisms including slip transfer capability and their local atomic structure has a lot of significance in terms of dictating the properties in NC metals and alloys. Furthermore, these “defect” regions (GBs) act as a sink for dislocations, vacancies, impurities and SFs. Processing NC through mechanical alloying and consolidation introduces many non-equilibrium GBs in the microstructure which also possess excess free volume that can accommodate these defects (X. Z. Liao et al. 2004; Van Swygenhoven, Derlet, and Frøseth 2004). For smaller grain sizes GBs act as dislocation sources where a dislocation is nucleated then it travels along the grains and gets absorbed at the opposite GB. Another mechanism namely, GB sliding occurs due to the dislocation climb mechanism or glide for smaller grain sizes. Temperature has an influence on the structural state of the GBs and determines the interactions between various defects. Several MD computational studies have ascertained the role of GBs on dislocation emission and also the role of temperature on the activation mechanism (Duhamel, Brechet, and Champion 2010; Van Swygenhoven, Derlet, and Frøseth 2004; Van Swygenhoven, Derlet, and Frøseth 2006a). Thermally active de-pinning of dislocations is also considered to be a rate controlling process(Van Swygenhoven, Derlet, and Frøseth 2006a; Kato 2009). In addition, with the application of temperature, a relaxation process was found to occur in the non-equilibrium GBs where the atoms rearrange into a structure and remove the “excess” defects that are present. This “new” structure is ordered and energetically favorable (Hasnaoui, Van Swygenhoven, and Derlet 2002). That is, this is due to the fact that the energy required to create relaxed GBs (GB energy) is lower than the non-equilibrium GBs. Moreover, this process has an impact on the mechanical properties of these NC metals and alloys where enhanced strengthening is observed due to the relaxed GBs. Therefore, identification of the structure and properties of the GB is critical while designing systems for high strength applications.

In addition to GBs, TJs also act as sinks for vacancies, impurities and dislocations due to their excess volume unlike the bulk which has a low energetic preference to segregate. Also, the diffusion is faster in comparison to the GBs (Chellali et al. 2011; Ames et al. 2008). This has a higher significance in the case of NC metals and alloys due to the high volume fraction of GBs and TJs in a given volume (Chellali et al. 2011). This is why the diffusional deformation based mechanisms are dominant for NC materials (B. Cai et al. 1999; Y. Wei, Bower, and Gao 2008b).

It is known that SFs are created in the case of FCC metal systems such as Cu and Ni where only one partial dislocation is emitted. Interestingly, in case of FCC NC metals and alloys, the nucleation event also consist of formation of a leading partial and then a trailing partial as the presence of a SF in between partial dislocations is more favorable compared to a full dislocation. Such SFs leading to deformation twins are more predominant in smaller grained FCC NC systems (M. Chen et al. 2003; X. Liao et al. 2003; X. Z. Liao et al. 2004; Zhu et al. 2011; Zhu, Liao, and Wu 2012). For example, in a low stacking fault energy(STFE) NC metal aluminum a twin or a full dislocation is formed due to the accompanying trailing partial(Yamakov et al. 2004; Van Swygenhoven, Derlet, and Frøseth 2006a; Zhu et al. 2011).

Thus, these observations have ascertained that the rate of creation/removal or modifications of the defects such as GBs, TJs and SFs control the deformation process and in turn the mechanical behavior of the NC metals and alloys. For instance, the role of alloying additions/impurities towards strengthening has been thoroughly studied. The presence of solutes at either substitutional or interstitial positions of the parent lattice can either cause softening or hardening of the alloy (solid-solution strengthening). In the case of CG metals and alloys, the resistance to dislocation motion due to the alloying elements causes the strengthening. However for NC metals and alloys, the strengthening is dependent on not only the solid solution strengthening but also GB strengthening where the GBs display a higher tendency to segregate the solute (Shen and Koch 1996). For grain sizes below 15 nm, dislocation activity is negligible and the effect of solutes on solid solution strengthening is difficult to probe.

Understanding the influence of external loading on these defects is also critical as mechanical loading such as indentation, tension/compressive uniaxial loading, cyclic fatigue etc. has been shown to have an impact on the structure of the NC metals and alloys where the stress state provides a stimulus for grain growth and changes in GB structure (T. J. Rupert et al. 2009; Ii and Boyce 2010; Mughrabi and Höppel 2010; Gianola et al. 2006). Several studies have pointed out that grain growth is affected by temperature as well as loads applied in NC FCC metals and alloys such as Al, Ni, Cu etc. The changes in the microstructure have been characterized through in-situ as well as ex-situ TEM observations. GB sliding and grain rotation is said to be responsible for the mechanically-induced grain growth behavior (Hall 1954; Marc Legros, Gianola, and Hemker 2008). In the case of GB sliding, the local atomic structure is said to influence the motion for both High Angle GBs (HAGBs) and Low Angle GBs (LAGBs) (Gutkin and Ovid'ko † 2004; Boyce and Ii 2011). The atom shuffling induces the GB motion perpendicular to the GB plane and this has been linked to shear stresses (Cahn and Taylor 2004; Cahn, Mishin, and Suzuki 2006). Also, the local atomic structures at the GBs and TJs are sensitive to the external load and have been observed to re-arrange for NC metals and alloys thereby reducing the volume fraction and energy. With the application of the stress, the GBs are also observed to exhibit similar behavior when a thermal stimulus is present. Several studies have reported these phenomena in Ni, Al and Cu metals and alloys (Jin et al. 2004; Shan et al. 2004). During mechanical loading, grain rotation is also said to occur where grains rotate and coalesce to form larger grains. This inevitably leads to instability as the properties of NC metals and alloys are not retained post-deformation. GB network and texture has also been observed to undergo changes with the application of load. Cyclic loading has been found to induce several twin boundaries and simultaneous applying loading as well as temperature was found to induce change in GB network in Ni (Panzarino, Ramos, and Rupert 2015).

Several studies have pointed out the feasibility of the role of solutes on stabilizing the microstructure under applied stress/temperature to retain the nanocrystallinity. Two approaches have been put forth to achieve thermal/plastic stability, viz a viz Thermodynamics and Kinetic methods. The operative mechanisms under thermodynamic approach deals with thermodynamic reduction in driving force for grain growth, whereas kinetic approach revolves around the use of second-phase particles for Zener pining and either impurity/solute drag or TJ drag to take into account(K. A. Darling et al. 2015a). In the case of thermodynamic stabilization of grain size, the segregation of the impurity/solute is said to be responsible for the reduction in driving force for grain growth. These solutes are said to stabilize the grain size over a range of temperatures and several alloys have demonstrated the thermal stability(K. A. Darling et al. 2013; Dake and Krill III 2012; K. A. Darling et al. 2010; A.J. Detor and Schuh 2007; J. Weissmüller et al. 1992; K. W. Liu and Mücklich 2001; Terwilliger and Chiang 1995; Färber et al. 2000; C.C. Koch et al. 2008). The basic assumptions and derivations can be looked up in these references (Saber et al. 2013a; Saber et al. 2013b; Carl C. Koch et al. 2013; Frolov et al. 2012; Andrew J Detor and Schuh 2007; Jörg Weissmüller 1994; J. Weissmüller 1993; Cserháti, Szabó, and Beke 1998; Millett, Selvam, and Saxena 2007;

Kirchheim 2002; F. Liu and Kirchheim 2004). Second-phase/Zener pining (Zener mechanism) is said to stem from the pinning of GBs and TJs due to the alloying elements which exert pressure that reduces the drive for the motion of the GBs (Andrew J Detor and Schuh 2007; Carl C Koch 2007; Carl C. Koch et al. 2013; K. A. Darling, Tschopp, VanLeeuwen, et al. 2014a; Saber et al. 2013a; Frolov et al. 2012; Saber et al. 2013b; M. A. Atwater, Scattergood, and Koch 2013).

This pressure is given by (Bate 2001):

$$P_Z = \frac{3f\gamma}{d}$$

where P_Z is the pressure exerted by the particles per unit area of the GB, f is the volume fraction of particles, d is the effective diameter of the particles, and γ is the GB energy. These particles are observed to be more effective in TJ pinning compared to GBs because of the removal of the high energy density at the TJs("Sina_Shahandeh_TMS2010.pdf" 2015). Stabilization of the grain growth at low and intermediate temperatures may be attributed to solute drag for systems with segregated impurities (Upmanyu et al. 2002; Humphreys and Hatherly 2004). However, the majority of the contribution to thermal stability is said to arise due to the reduction in GB energy caused by the segregated impurities rather than the solute drag itself (Z. Chen et al. 2009; Z. Chen et al. 2012; Zheng Chen et al. 2009; Gong, Liu, and Zhang 2011). Very small grain sizes have been observed to exhibit TJ drag and TJs themselves have a higher volume fraction for sizes lower than 5 nm in comparison to the GBs (Upmanyu et al. 2002; Palumbo, Thorpe, and Aust 1990). Thus, the major contributor to the kinetic based stabilization mechanism for these grain sizes is the TJ drag. However, a study on NC Pd (Ames et al. 2008) has elucidated that the TJs do not influence the stabilization of grain size (GS) for relatively moderate GS ranges. All in all, these mechanisms primarily rely on the incorporation of solutes into the microstructure which will stabilize and in turn provide sufficient strength at various loading/thermal conditions. Thus, using the thermodynamic and kinetic stabilization theory (K. A. Darling, Tschopp, VanLeeuwen, et al. 2014a; K. A. Darling et al. 2013; Saber et al. 2013a; Saber et al. 2013b; Frolov et al. 2012; Tschopp et al. 2014), it has been shown that grain coarsening at high temperatures could be suppressed through selective segregation of solute species to the interface. This thermal stability is also critically important for producing bulk NC specimens using mechanical alloying whereby a subsequent high temperature consolidation step is required to produce a fully dense, bulk NC sample (Carl C Koch 2007; Carl C. Koch et al. 2013; Frolov et al. 2012; K. A. Darling, Tschopp, VanLeeuwen, et al. 2014a; Andrew J Detor and Schuh 2007; Ma 2004).

The deformation mechanisms are said to be distinctly different than the un-alloyed/pure NC metals which experience instability under thermal/stress impetus. The emergence of such stable materials provides an exciting opportunity for uncovering novel plastic deformation mechanisms in nanocrystalline metals and alloys at high homologous temperatures ($T > 0.4T_m$) which until recently have not been possible to explore. Although the research efforts up to now have focused on developing a basis for creating thermally stable nanocrystalline materials, the systematic study involving the discovery and effect of microstructural parameters on active deformation modes in these materials is limited. The complex nature of the microstructure has prevented delineating the specific mode or modes of deformation (e.g., dislocation propagation, twin nucleation and growth, etc.) operating in these systems under a combination of loading and temperature. This process is complicated by the fact that extensive coupling of the various microstructural features. This dissertation will focus on understanding the interaction between various microstructural features which translate into the mechanical response of one such stable nanocrystalline alloy, NC-Cu-Ta at extreme conditions. The systematic evaluation of structure-property relationship will aid in designing materials with exceptional response at extreme conditions.

2.2 Research Objectives

Instability limits the application of conventional nanocrystalline materials for any practical applications. Understanding the fundamentals that are involved in the development of stable nanocrystalline material systems that can exhibit a multitude of properties at extreme conditions is still a work in progress. In fact, the limited understanding of the effect of microstructural features and deformation mechanisms that will contribute towards the exceptional performance of these materials affects the design of such materials. Therefore, this dissertation aim to address the critical need, building upon a full dense well characterized material complex material that exhibits high thermal and mechanical stability as well as exceptional high temperature performance under the evaluating conditions. The objectives are:

1. Assessment of microstructural stability in a nanocrystalline stable alloy.

A major concern with nanocrystalline materials is the thermal and plastic instability associated which restricts the practical utility of the high-strength materials. Grain coarsening leads to a rapid deterioration of properties at elevated temperature and stress levels. To overcome this problem, the convolution and competition of kinetic and thermodynamic stabilization mechanisms have led to the design of stable nanocrystalline duplex systems. One such material system, immiscible Cu-based alloy – NC Cu-Ta has shown promise. In-situ TEM heating experiments, atomistic modeling along with elevated temperature compression tests on a thermally stabilized nanostructured Cu–10at.% Ta alloy was used to assess the microstructural manifestations caused by changes in temperature as under intense heating and/or deformation, pure nanocrystalline (NC) metals exhibit significant grain coarsening, thus preventing the study of length scale effects on their physical response under such conditions (Chapter 3). In this section, three main observations were made and derived: a) thermal stability achieved with this NC Cu-10 at.% Ta diverges from those observed for conventional coarse-grained metals as well as other NC metals; b) Macroscopically, the microstructure (Cu grain and Ta based cluster size) of NC Cu-10at% Ta was morphologically stable in shape and (c) local structural changes at the interface between the Ta based clusters and the Cu matrix with temperature (i.e.) changes in the lattice misfit was said to influence the changes in flow stress.

2. Investigation of deformation behavior at extreme conditions of stress and temperature in a stable nanocrystalline alloy.

Since, their conception, there has been great interest in uncovering novel plastic deformation mechanisms in nanocrystalline metals and alloys which show unique properties which deviate from the behavior of coarse grained materials. Despite significant gains in knowledge related to the development and engineering of plasticity in nanomaterials, there still persists a sizeable gap in the fundamental understanding of how these very same nanostructured materials respond at highly elevated temperatures. This is mainly because their thermal and mechanical instability under such extreme conditions presents a significant obstacle to their proper evaluation. As a result, for the past 30 years, basic deformation research has been restricted to lower temperatures because of this short fall. The emergence of such materials provides an exciting opportunity for uncovering novel plastic deformation mechanisms in nanocrystalline metals and alloys at high homologous temperatures ($T > 0.4T_m$) which until recently have not been possible to explore. A range of deformation temperature is used to specifically investigate the strain rate sensitivity and activation volume as a function of temperature, e.g the signatures of the rate-limiting thermally activated deformation mechanisms accommodating the plastic flow at temperature. Such experimental evidence is highly valuable as the current understanding of deformation mechanisms in NC metals has been limited to low or room temperature analysis where thermally activated mechanisms may not be significant to allow the punching of mobile dislocations through the dense bundle of excess grain boundary dislocations, or the de-pinning and translation of propagating dislocations from GBs into the neighboring grains [E Ma], especially in the presence of a high density of Ta based clusters. These dislocation–grain boundary interaction-mediated mechanisms will become increasingly important to understand in nc metals stabilized to high homologous temperatures.

3. Investigation of long-term deformation behavior: creep resistance in a microstructurally stable nanocrystalline alloy.

Nanocrystalline metals, with a mean grain size of less than 100 nanometres, have greater room-temperature strength than their coarse-grained equivalents, in part owing to a large reduction in grain size(Gleiter 2000). However, this high strength generally comes with substantial losses in other mechanical properties, such as creep resistance, which limits their practical utility; for example, creep rates in nanocrystalline copper are about four orders of magnitude higher than those in typical coarse-grained copper(Mohamed and Li 2001; Atul H. Chokshi 2009). The degradation of creep resistance in nanocrystalline materials is in part due to an increase in the volume fraction of grain boundaries, which lack long-range crystalline order and lead to diffusional processes such as diffusional creep, sliding and rotation(Atul H. Chokshi 2009). In this section, nanocrystalline copper–tantalum alloys is reported to possess an unprecedented combination of properties: high strength combined with extremely high-temperature creep resistance, while maintaining mechanical and thermal stability. Precursory work on this family of immiscible alloys has previously highlighted their thermo-mechanical stability and strength(K. A. Darling, Tschopp, Guduru, et al. 2014; K. A. Darling et al. 2015b), which has motivated their study under the more extreme conditions of creep. A steady-state creep rate of less than 10^{-6} per second—six to eight orders of magnitude lower than most nanocrystalline metals—at various homologous temperatures between 0.5 and 0.64 times the melting temperature of the matrix (1073 degrees Celsius) under an applied stress ranging from 0.85 per cent to 1.2 per cent of the shear modulus was observed. The unusual combination of properties in this nanocrystalline alloy is achieved via a processing route that creates distinct nanoclusters of atoms that pin grain boundaries within the alloy. This pinning improves the kinetic stability of the grains by increasing the energy barrier for grain-boundary sliding and rotation and by inhibiting grain coarsening, under extremely long-term creep conditions. The processing approach should enable the development of microstructurally stable structural alloys with high strength and creep resistance for various high-temperature applications, including in the aerospace, naval, civilian infrastructure and energy sectors.

4. Evaluation of the effect of Ta concentration on deformation of stable nanocrystalline alloys.

Stable nanocrystalline materials offer exceptional thermal stability and mechanical response at elevated stress/temperature conditions. Nanostructured Cu–Ta alloys show promise as high strength materials in part due to their limited grain growth. In the present study, the role of Ta on the transition from deformation twinning to dislocation-mediated slip mechanisms in nanocrystalline Cu through atomistic simulations and TEM characterization is elucidated. In particular, computed generalized stacking fault energy curves show that as Ta content increases there is a shift from twinning to slip-dominated deformation mechanisms. Furthermore, heterogeneous twinnability from microstructural defects decreases with an increase in Ta. The computed effect of Ta on plasticity is consistent with the HRTEM observations.

In the end a future research idea is presented. The technological advances in material processing have made processing of such stable nanocrystalline materials a viable option. For realization in practical applications, it is imperative to design a nanocrystalline material system that offers a good strength-ductility tradeoff whilst retaining thermal and mechanical stability at elevated temperatures. A general methodology for the design of strong, and lightweight components necessitates the use of a model that can capture the physical aspects at the plastic deformation in order to design structural materials. The strength/ductility can be controlled in these stable nanocrystalline material systems through the effective control of solute addition. Thereby, the following key insights were accrued: a) a systematic methodology to study the effect of Ta on structural stability was developed; b) the effect of Ta concentration and processing on microstructure-property was determined and c) optimum Ta concentration which can offer a good balance between strength and ductility is predicted.

CHAPTER 3

3 MICROSTRUCTURAL EVOLUTION IN A NANOCRYSTALLINE CU-TA ALLOY: A COMBINED IN-SITU TEM AND ATOMISTIC STUDY

3.1 Introduction

Metals with a mean grain size *(d)* below 100 nm, i.e., nanocrystalline (NC) materials, have garnered significant interest due to their superior mechanical properties as compared to coarse-grained materials (Gleiter 2000) A large number of experimental and computational studies have explored how grain boundary mediated plasticity and microstructural size effects impact the mechanical behavior of NC materials (Meyers, Mishra, and Benson 2006; Dao et al. 2007; Q. Wei et al. 2008). For example, the Hall-Petch (Hall 1954; Petch 1953) relationship describes the experimentally-observed increase in yield strength with decreasing grain size down to grain diameters as small as 20 nm (Gleiter 2000; Meyers, Mishra, and Benson 2006); this behavior is generally followed by a plateau/negative slope region for grain sizes below a critical size (e.g., 8-15 nm for Cu (Schiøtz, Di Tolla, and Jacobsen 1998)). This inverse Hall-Petch effect has been directly attributed to changes in the governing deformation mechanisms away from traditional dislocation glide and pile-up processes (A. H. Chokshi et al. 1989). Fundamental changes in deformation mechanisms are also known to cause many other intriguing and unexpected physical responses of NC metals, including altered strain rate and pressure dependencies of deformation (Hornbuckle et al. 2015), superplasticity (Sherby and Wadsworth 1989), and low temperature creep (M. A. Bhatia, Mathaudhu, and Solanki 2015), to name a few (see (Tschopp et al. 2014; J. Li et al. 2016)). Generally, these unique deviations in behavior are solely attributed to a continual reduction in grain size and an increase in the fraction of grain boundaries and triple junctions, which leads to the experimentally reported mechanisms of deformation twinning, grain boundary (GB) rotation/sliding and viscous flow (M. Chen et al. 2003; X. Z. Liao et al. 2004; Zhu, Liao, and Wu 2012).

Despite significant gains in knowledge related to the development and engineering of plasticity in nanomaterials, there still persists a sizeable gap in the fundamental understanding of the mechanical behavior of these materials, especially under extreme conditions such as at ultra-high temperatures. This gap is critical as the material performance at high temperatures is significantly different from the room temperature (RT) behavior. Limited studies have explored the mechanical behavior of NC materials at room or moderately low temperatures where a drastic change in the microstructure (grain growth) has been reported. For example, Farrokh and Khan investigated the uniaxial compressive behavior of NC Cu and Al (grain size 32 nm and 82 nm, respectively) prepared through mechanical alloying at a strain rate of 0.01/s (Cu) and a significant effect of temperature on the strength was observed (Farrokh and Khan 2009a). At the homologous temperatures of 0.4 T_m and 0.56 T_m (T_m being the melting temperature), the strength was reported to be 40% and 72% of the RT strength for NC Cu and Al, respectively (Farrokh and Khan 2009a). In case of alloy systems such as NC multiphase Al alloys (Fe, Cr and Ti minor additions), a similar trend in loss of strength with temperature was reported for samples with the grain sizes of 50 and 80 nm tested at quasistatic rates. This significant loss in strength in the NC metal/alloy systems was attributed to the loss in nanocrystallinity (grain coarsening) (Malow and Koch 1997;

Gianola et al. 2006; Zhao et al. 2014; Zhou et al. 1997; Akbarpour and Kim 2015) which led to the dislocation-based mechanism to be a dominant deformation mechanisms at elevated temperatures (Shaw and Luo 2007).

In general, the thermal and mechanical stability of NC microstructures has been regarded low based on other experimental observations (Gianola et al. 2006; K. Zhang, Weertman, and Eastman 2005; Tao et al. 2013). For instance, under thermal heating experiments, the pure NC Cu exhibits rapid grain growth to the micron-scale at just 100 °C (Huang, Menovsky, and De Boer 1993; Sonia Simões et al. 2008; S. Simões et al. 2008). Further, indentation studies at liquid nitrogen temperature revealed that NC Cu undergoes rapid grain growth, where the microstructure consists of grains as large as 700 nm (with sizeable volume fraction) after 30 minutes of dwell time in liquid nitrogen temperatures as compared to an average grain size of 20 nm (K. Zhang, Weertman, and Eastman 2005). These examples illustrate that, for nominally pure NC metals, the nanoscale microstructure is an inherent barrier to experimental studies of their properties even under relatively low temperature conditions. It is expected that more intense conditions, either thermal or mechanical, will result in a more rapid grain coarsening and a sudden loss of the material's intrinsic physical and structural features. Recently, alternative methodologies have been successfully employed to impart greater stability to NC metals. These methodologies are based on thermodynamic considerations (K. A. Darling, Tschopp, VanLeeuwen, et al. 2014a; Saber et al. 2013b; Chookajorn, Murdoch, and Schuh 2012; Murdoch and Schuh 2013; Timothy J Rupert 2016) coupled with classical kinetic mechanisms (Carl C. Koch et al. 2013). Such techniques allow for the retention of the as-processed fine grain size, especially during high temperature consolidation. Hence, it may be stated that such methodologies establish the fabrication pathway and, thus the application of NC metals with desirable properties.

Recently, quasi-static and dynamic yield strengths of greater than 1 GPa were measured in bulk samples of a NC Cu–Ta alloys, which could not be explained by grain size strengthening alone (K. A. Darling, Tschopp, Guduru, et al. 2014). The increase in strength was attributed to the thermal decomposition of a non-equilibrium Cu rich Cu-Ta solid solution over a range of temperatures (700–900 °C), which led to the formation of a high density of small coherent Ta-rich nanoclusters (~2 nm in diameter) (K. A. Darling, Tschopp, Guduru, et al. 2014; K. A. Darling et al. 2016b). The presence of these Ta nanoclusters within grains and along grain boundaries resulted in strength levels approximately twice as high as those predicted by Hall–Petch hardening (K. A. Darling et al. 2015b). These studies suggest that the presence of Ta-based clusters play a commanding role in defining the deformation response as compared to the NC grain size alone. Therefore, in the present study, the microstructural evolution was examined, i.e., the underlying changes in the Cu matrix grain size and the corresponding Ta nanoclusters by in-situ transmission electron microscopy (TEM) heating experiments and atomistic simulations.

This work shows that the thermal stability achieved with this NC Cu-10 at.% Ta alloy diverges from those observed for conventional coarse-grained metals as well as other NC metals. That is, macroscopically, the microstructure (Cu grain and Ta based cluster size) of NC Cu-10at% Ta was morphologically stable in shape and size. However, local structural changes at the interface between the Ta based clusters and the Cu matrix have a significant effect on thermo-mechanical properties. Specifically, the misfit strain was found to decrease monotonically from 12.9% to 4.0% with increase in temperature, leading to a significant change in flow stress, despite which remains greater than all known NC metals.

3.2 Methodology

3.2.1 Experimental Details

High-energy cryogenic mechanical alloying was used to synthesize NC powders with a composition of Cu-10 at.% Ta using very high purity (99.9%), ~325 mesh size elemental Cu and Ta powders. The ball milling was carried out in a SPEX 8000M shaker mill at cryogenic temperatures (verified to be ~ -196 °C) using liquid nitrogen with a milling time of 4 hours. The milling medium was 440C stainless steel balls and a ball-to-powder ratio of 5-to-1 by weight was maintained. Cryogenic mechanical milling resulted in an un-agglomerated powder mass with a particulate size range of 20 µm to 100 µm. The as-milled powders were placed into nickel cans and sealed inside the glove box. Prior to Equal Channel Angular Extrusion (ECAE), the die assembly was heated to 350 °C. The nickel cans loaded with as-milled powders were equilibrated (for 40 min) in a box furnace purged with pure Ar cover gas at 700 °C. The equilibrated cans were then quickly removed from the furnace, dropped into the ECAE tooling, and extruded at an extrusion rate of 25.4 mm/s using 90° rotations for four passes. This process resulted in dense 12 mm diameter rod samples with a stable initial grain size distribution. To identify the impurity content in these alloys, atom probe tomography was performed on the as-milled powder as well as the NC Cu -10 at. % Ta ECAE sample processed at 700 °C where a minimal concentration of 1.25 at. % was detected for O. Fe contamination was detected using APT and varied between 0.05 at.% and 1 at.%, indicating a relatively impurity-free alloy (Hornbuckle et al. 2015).

Quasistatic compression tests were carried out over a temperature range from 25 °C to 400 °C using an INSTRON load frame with a 50 kN load capacity and a furnace rated up to 1800 °C. The pushrods of the load frame were constructed with precision machined ZrO_2 rods to minimize heat losses. The specimens were cylinders with a 3mm diameter and 3 mm in length, machined using an electric discharge machine from the same sample batch. Boron nitride lubricated polished WC-disks were used as platens. The system was held at the testing temperature for about 30 minutes to attain equilibrium and thermocouples were attached on the specimen to monitor the temperature. Specimens were loaded under strain control with a strain rate of 0.1 s^{-1}.

In-situ TEM heating experiments were carried out in the aberration corrected FEI-TITAN TEM at 300 kV using an Inconel heating holder and the temperature was monitored digitally. Aberration corrected ARM-200F operating at 200 kV was also used to acquire images, especially of the nanoclusters illustrated in the forthcoming sections. Multiple images were acquired in the bright field and the high resolution TEM mode to analyze the microstructure and quantify the statistics such as grain size distribution etc. Imaging was performed at the room temperature (25 °C) followed by imaging at temperatures 100 °C to 400 °C in 100 C° intervals. Each temperature level was achieved in approximately 20 minutes and a holding time of 20 minutes was maintained to reach equilibrium temperature and minimize sample drift. Due to the effects of beam on a thin area, a relatively thick reference area was chosen for studying the microstructural evolution under temperature. The samples for in-situ heating were prepared through conventional thinning procedures where a 3 mm disk was punched from the bulk specimen and thinned to about 100 μm followed by dimpling to about 5 μm thickness. Ion milling was performed under liquid nitrogen temperatures using Precision Ion Polishing System (PIPS) to obtain electron-transparent regions in the specimens. The samples were then plasma cleaned in Ar prior to heating to minimize contamination.

3.2.2 Computational Details

Interatomic interactions in the Cu-10 at.% Ta system were described by a semi-empirical angular-dependent atomistic potential developed by Pun et al. (Pun et al. 2015). This potential was parameterized using an extensive database of energies and configurations from density functional theory (DFT) calculations of energy differences between various crystal structures of pure Cu and pure Ta, the formation energies of coherent Cu-Ta interfaces, and the binding energy of several ordered compounds, such as $L1_2$-Cu_3Ta, $L1_0$-CuTa, $L1_1$-CuTa, B_2-CuTa, and $L1_2$-Ta_3Cu (Pun et al. 2015). More details on the validation of the potential at different temperatures can be found in (Pun et al. 2015). This potential was recently applied to study structural stability of Cu-Ta alloys and the Zener pinning of Cu grain boundaries by nano-scale Ta clusters (Koju et al. 2016). The simulations were performed using the large-scale atomic/molecular massively parallel simulator (LAMMPS) (Plimpton 1995).

To estimate the lattice misfit and coherency as functions of the cluster size and temperature, spherical Ta clusters were created inside cubic simulation blocks of pure FCC Cu with several different sizes up to 40 x 40 x 40 nm with periodic boundary conditions. The clusters were created by replacing Cu atoms by Ta atoms within a spherical region at the center of the block. Five different cluster radii ranging from 1.5 to 3.5 nm were studied in this work. Note that in this simulation scheme, the Ta atoms were initially arranged in FCC structure perfectly coherent with the surrounding Cu. The structure was then relaxed by molecular statics (total energy minimization), which resulted in a partial loss of coherency and transformation of certain regions inside the cluster from FCC to BCC. The cluster structure was examined using the visualization tool OVITO (Stukowski 2010). Besides FCC and BCC, a small fraction of other structures or unstructured regions was usually found in the cluster, especially near the Cu-Ta interface. The system was then slowly heated up to the temperature of 927 °C (1200 K) by molecular dynamics simulations and the structure evolution was monitored by periodically quenching the simulation block to -273 °C (0 K) and examining its structure with OVITO.

3.3 Results and discussion

The primary TEM microstructural characterization and XRD analysis (Figures 2 and 3) of the as-received Cu-10at.% Ta ECAE sample processed at 700 °C revealed the presence of Cu and Ta based phases, that is fcc Cu and bcc Ta. The orientations indexed through precession diffraction data for the fcc Cu and bcc Ta phase of the as-received sample indicates a random texture (Figure 3 (K. A. Darling et al. 2016b)). The TEM characterization along with grain size distributions is illustrated in Figure 2. The selected area diffraction pattern confirms the nanocrystallinity of the sample at RT. Surprisingly, even though our NC material was consolidated to bulk through sever plastic deformation at 700°C with a total accumulated strain of 4.6 (i.e., 460%), the as received averaged grain size was 52 ± 14.3 nm, still in the NC regime (Figure 2). In comparison, NC-materials have been reported to exhibit dramatic grain-coarsening even under low homologous temperatures, such as NC Cu which was found to coarsen to the micron regime at just 100 °C (Huang, Menovsky, and De Boer 1993; Sonia Simões et al. 2008; S. Simões et al. 2008). Therefore, this NC Cu-10 at.% Ta alloy exhibits a very stable microstructure. The processing conditions produced a wide range of Ta particle sizes, ranging from atomic nanoclusters to much larger precipitates (see Figures 1A to 1D). Further, Figures 2B, 2C and 2D shows histograms, taken from multiple images similar to Figures 2A, indicating that the larger Ta particle size distribution has an average diameter of 39 ± 19 nm while the smaller Ta based nanoclusters possess an average diameter of 3.18 ± 0.86 nm. Small aggregations of Ta atoms (e.g., ~10-50 atoms) as referred as nanoclusters and sizes larger than 14 nm (diameter) are considered as particles, although we recognize that there is no sharp boundary between the two. The energy of the interface (J. D. Eshelby 1957) between the nanocluster and the Cu matrix can be used to quantify the type of coherency of these nanoclusters, and the range of the grain sizes which correspond to them. Characterizing the coherency at RT has indicated that this material has coherent, semicoherent and incoherent nanoclusters (d < 3.898 nm, 3.898 to 15.592 nm, and >15.592 nm, respectively) (J. D. Eshelby 1957).

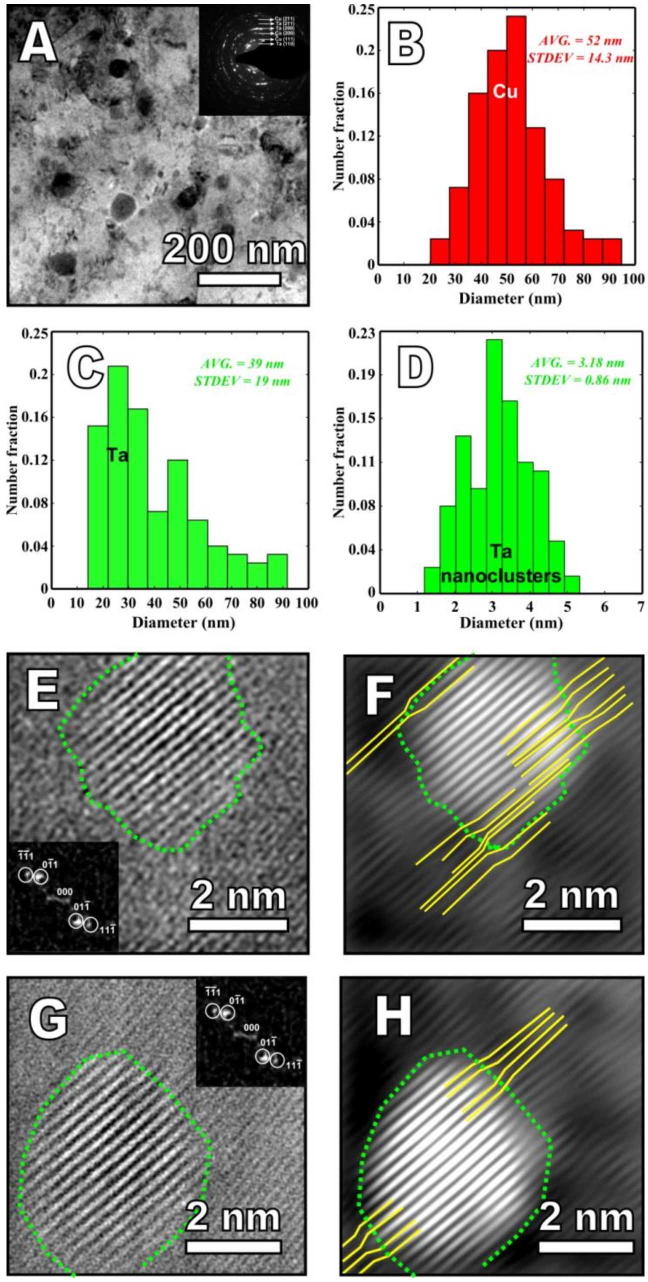

Figure 2: TEM characterization of as received NC Cu-10at.% Ta (**a**) bright field TEM image showing the microstructure consisting of a distinct Cu(fcc) and Ta(bcc) phase (inset: SAED pattern), size distributions of (**b**) Cu and **(c)** larger Ta grains based on TEM images (average 200 grains), **(d)** size distribution of Ta nanoclusters with an average size of 3.18 nm distributed along the grains and grain boundaries, and inverse Fourier filtered images (IFFT) of **(e-f)** an coherent (d = 3.47 nm) and **(g-h)** semicoherent nanocluster (d= 4.11 nm). The interface between the Ta nanocluster and the Cu matrix are highlighted using dashed green lines in (e-h). Inset: Indexed SAED patterns confirming nanocrystallinity (M. Rajagopalan et al. 2017).

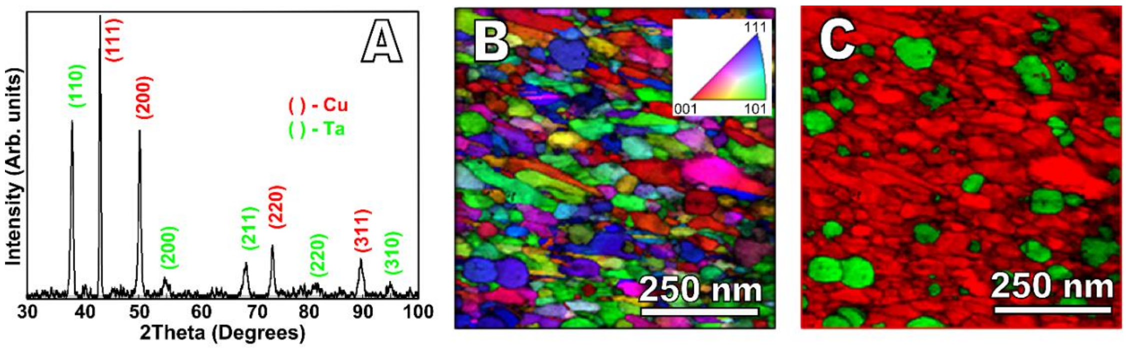

Figure 3: Characterization of as-received NC Cu-10at.%Ta. (a) X-Ray Diffraction pattern of the as-received NC-Cu-10at.%Ta bulk sample processed at 700 °C highlighting the Cu (fcc) and Ta (bcc) reflections, and (b) orientation imaging map of the as-received NC-Cu-10at.%Ta obtained through precession diffraction technique representing a random texture, (c) phase map of the region represented in (b) where red and green colors correspond to Cu and Ta phases respectively. Data from (K. A. Darling et al. 2016b).

Next, in-situ heating experiments were performed to probe and assess the microstructural manifestations caused by heat and/or changes in temperature as a fraction of the absolute melting point of Cu. Figure 4 shows a series of TEM bright field (BF) images captured at periodic temperature intervals along with the grain size distributions of Cu grains and Ta based nanoclusters. Each temperature level was achieved in 20 minutes with 20 minutes of hold time and 20 mins of imaging. Thus, at 400 °C, the time since the start of the test is approximately 240 minutes. Notably, the average grain size at 100 °C, 200 °C, 300 °C and 400 °C was evaluated based on statistical analysis as 55 nm (60 mins), 56.1 nm (120 mins), 59 nm (180 mins) and 61 nm (240 mins), respectively which corresponds to a change in grain size of 12 % at 0.5 T_m. The grain size distributions indicate limited grain growth in NC Cu-10 at. % Ta when subjected to annealing (Figure 4 and 5). While the average grain size is estimated to increase only by 12% for Cu phase, the full width half maximum values indicate an increase only about

4% for Cu grain and 10% for Ta nanoclusters at 0.5 T_m. However, the grain size of the larger Ta particles (Fig. 5) virtually remains unaffected indicating that their evolution does not play a major role in the behavior of this material. This suggests that the alloy is resistant to grain growth and there is no significant shift in the size distribution. From a practical perspective the small increase in grain size does not manifest a perceivable change in the mechanical properties as given by current Hall-Petch assessments of NC Cu (Tschopp et al. 2014). Furthermore, the limited growth observed may have more to do with enhanced surface diffusion kinetics related to the direct heating of the prepared TEM foil. The embedded nanoclusters also exhibit a strong resistance to coarsening, with the corresponding size distributions for these nanoclusters provided in Figure 4. The high stability is not completely unexpected as the initial consolidation temperature is 300°C higher than the maximum temperature of the in-situ heating experiments. Therefore, from a macro perspective under limited re-heating, the stability of the grain size and nanoclusters is very high in this alloy and diverges from those observed for conventional coarse-grained metals as well as other NC metals (Sonia Simões et al. 2008). While in general, the microstructure is morphologically stable in shape and scale, it is the fine changes in interfacial structure that dictate mechanical properties at elevated temperatures, owing to the dispersions initially coherent/semi-coherent nature with the Cu matrix at room temperature.

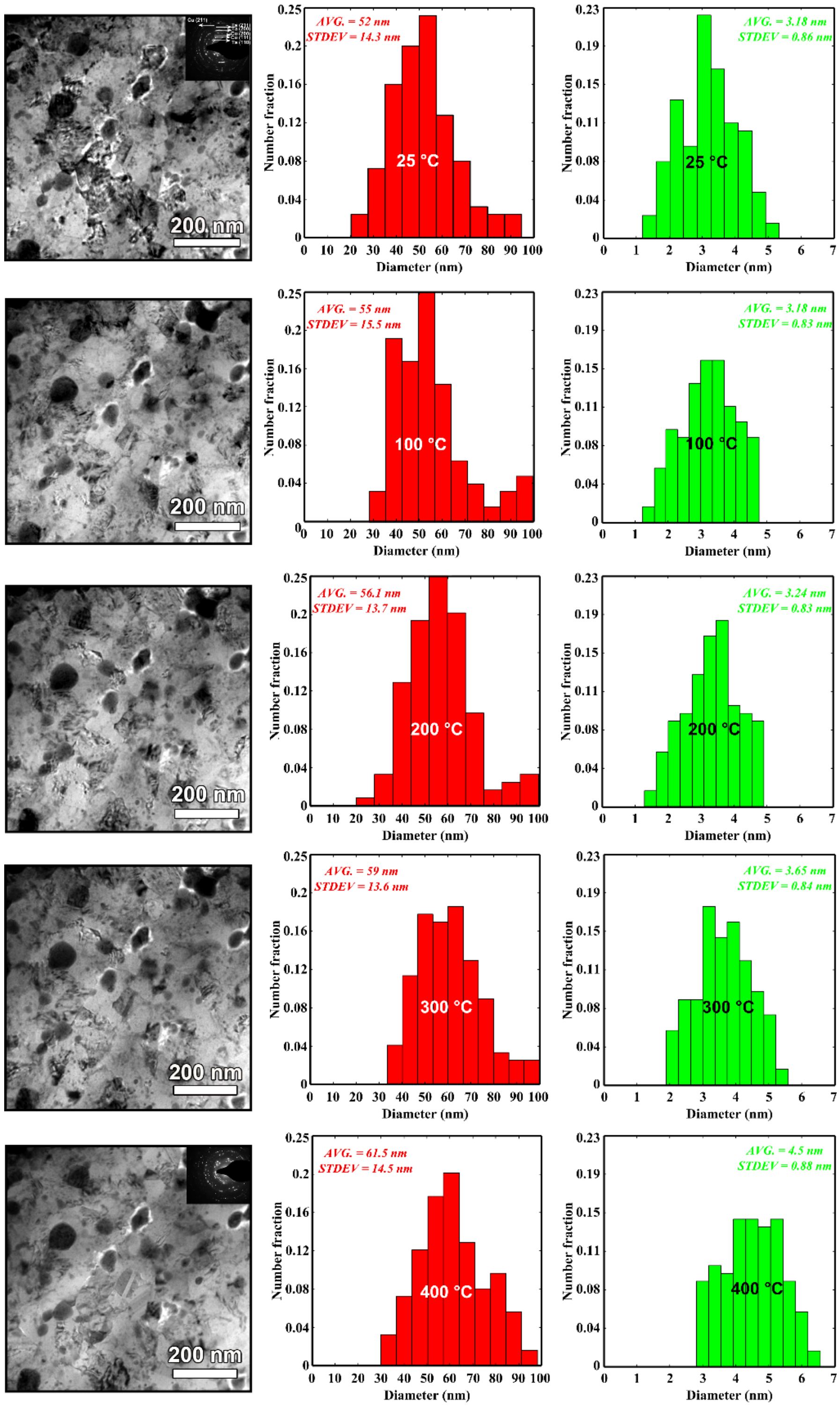

Figure 4: Microstructural evolution of NC Cu-10 at. % Ta subjected to in-situ heating and corresponding grain size distributions at each temperature level. The grain sizes for Cu and Ta nanoclusters do not change significantly indicating the stability of the alloy (M. Rajagopalan et al. 2017).

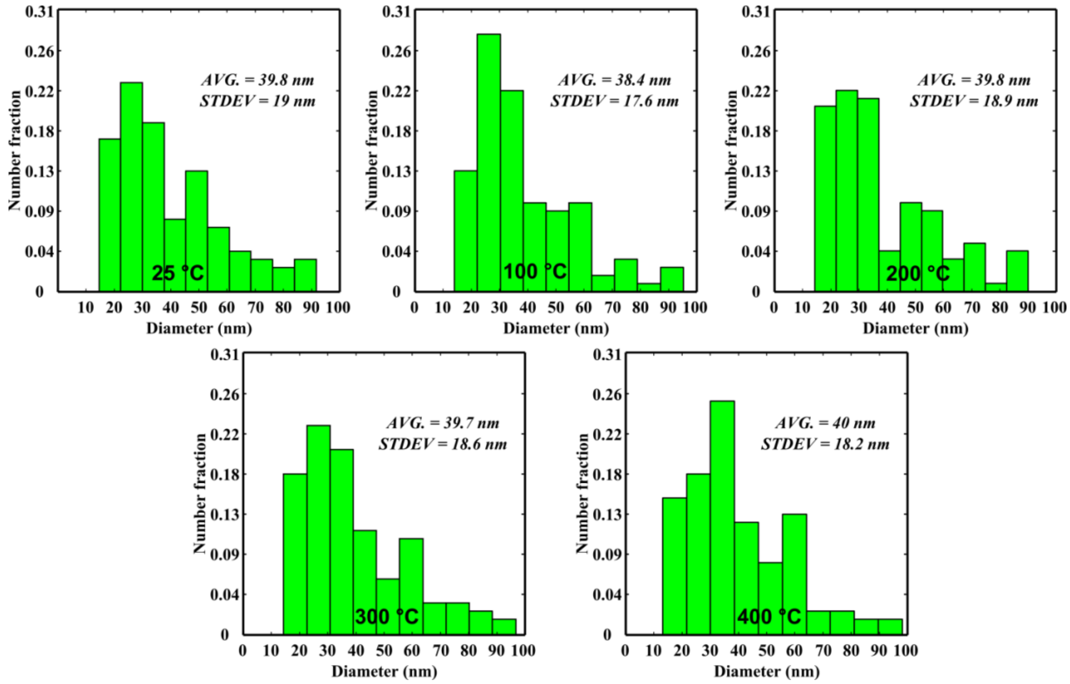

Figure 5: Ta particle size distribution as a function of temperature. The average size of Ta particle remains unchanged with the increase in temperature (M. Rajagopalan et al. 2017).

To understand the stability of this alloy at a finer length scale, the effect of temperature on the high density of coherent and semi-coherent nanoclusters (density = $6.5\times10^{23}/m^3$ (Rojhirunsakool et al. 2015)) distributed in the Cu matrix and along the grain boundaries was examined. In general, the coherency of the particle also determines the misfit strain at the interface. The misfit strain can be viewed as an indirect measurement of the interfacial bonding strength and is correlated with the material's thermal stability and mechanical properties. Coherent particles have a lower interfacial energy as compared to incoherent particles, therefore coherent particles are more energetically favorable to form below a critical diameter. Figures 2E and 2G illustrate the high resolution TEM (HRTEM) images of a semi/coherent nanoclusters in the as-received microstructure with diameters of 3.47 and 4.11 nm, respectively. The corresponding inverse fast Fourier transform (IFFT) images appear in 2F and 2H, where the yellow lines along the Cu-Ta interface in these images are indicative of where the lattice deviates from the bulk (i.e.) the presence of misfit dislocations. These misfit dislocations are introduced to minimize the strain at the interface between the clusters and matrix. The frequency of which can be seen to increase with the diameter of the clusters, see Figures 2F and 2H.

In order to characterize the change in misfit quantitatively, the average misfit strain from in-situ heating experiments (ε^*) was evaluated using the equation (Howe 1997)

$$\varepsilon^* = 2(d_2 - d_1)/(d_2 + d_1) \quad (1)$$

where d_1 and d_2 are the interplanar lattice spacings of the Ta based particles and Cu matrix computed from the fast Fourier transform (FFTs) at a particular temperature.

The strain values were averaged over the reference area (illustrated in Figure 2) and the average misfit value as a function of temperature is represented in Figure 5. In case of ODS steel, the misfit strain between the nano-sized oxide particle and matrix was also quantified to be relatively high, (i.e.) ~ 12.6% (Ribis and de Carlan 2012). Although the misfit strain in the as-received condition is high, i.e., 12.9% ± 2%, the microstructure appears to be relatively stable. With the increase in temperature, the average misfit strain was estimated to reduce to a value about 4%± 0.49%, at 400 °C. Partially, this can be explained by structural relaxation of the clusters, resulting in increased coherency and transformation to a more thermodynamically stable structure. Another factor is the difference in thermal expansion factors of Cu and Ta based clusters, which may reduce the lattice parameter difference at high temperatures.

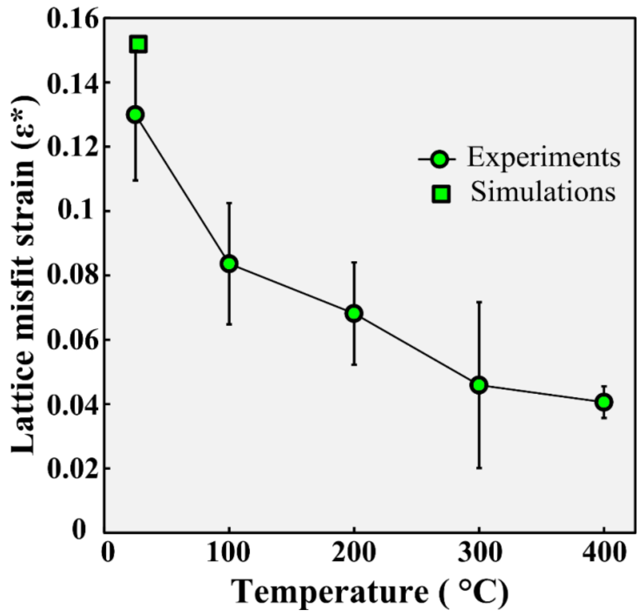

Figure 6: Average misfit strain evolution as a function of temperature for the Ta nanoclusters. With the increase in temperature the misfit strain decreases from 12.9% to 4% from experiments (M. Rajagopalan et al. 2017).

In order to gather more insight about the misfit dislocations and variation of misfit strain, atomistic simulations were performed. Figure 5 shows the lattice misfit strain calculated from atomistic simulations at room temperature which agrees quite well with experimental findings. However, because of the complex two-phase structures of the nanoclusters observed in atomistic simulations (see Figures 7a and 7b) and the thermal noise at high temperatures, it was not possible to accurately determine the interplanar spacing between Ta atoms from the atomistic simulations in this work. Hence, this precluded direct calculations using atomistic simulations of the temperature dependence of the lattice misfit defined by equation (1). Nevertheless, the misfit strain calculated from atomistic simulations at RT agrees well with in situ TEM experimental measurement.

Despite this limitation, atomistic simulations were able to reveal critical structural changes within the Ta based clusters which remained mostly (although not fully) coherent with the Cu matrix, see Figure 6. Since the clusters were initially created and statically relaxed at T = -273 °C/0 K when the lattice misfit was large, they were never perfectly coherent. Due to the partial loss of coherency, part of the initial FCC structure of the cluster always transformed to BCC and other structural forms (Figure 7a). In small clusters (e.g., with the radius of 1.5 nm), the fraction of the FCC structure was found to increase with temperature while the fraction of the BCC structure decreased. By contrast, in larger Ta clusters, most of the initial FCC structures transformed to BCC already during the static relaxation (Figure 7b). This resulted in nearly complete loss of coherency and during the subsequent high-temperature anneals, in which the fraction of the BCC structure in the cluster increased. The effects of the phase change on the behavior of the alloy and detailed analysis will be included in a follow up article. However, one important observation was that the loss of coherency was accompanied by emission of dislocation loops into the Cu matrix as illustrated in Figure 7c. Note the dislocation splitting into partials separated by a stacking fault. In Figure 7c, the FCC Cu atoms were removed for clarity. It is well known that a coherent nanocluster can lose coherency once it grows above a critical diameter. This happens when the elastic energy with the coherent nanocluster becomes large and it is energetically favorable for a dislocation to form at the matrix-nanocluster interface, see experimental Figures 7d and 7e. The generation of such dislocations is easier for an incoherent nanocluster in comparison to a coherent nanocluster. This dislocation raises the free energy of the system to an amount which equals to its formation energy but this increase in energy is compensated by the decrease in the self-energy of the nanocluster. Due to the presence of the misfit strain around nanocluster, the pinning-depinning of propagating dislocations during the deformation with in the matrix will be hindered (Van Swygenhoven, Derlet, and Frøseth 2006b). This hindrance will have a direct consequence on the mechanical behavior. Hence, the change in coherency can be linked to the change in mechanical properties (Alavudeen, Venkateshwaran, and Jappes 2006; Ashby, Bullough, and Hartley 2013).

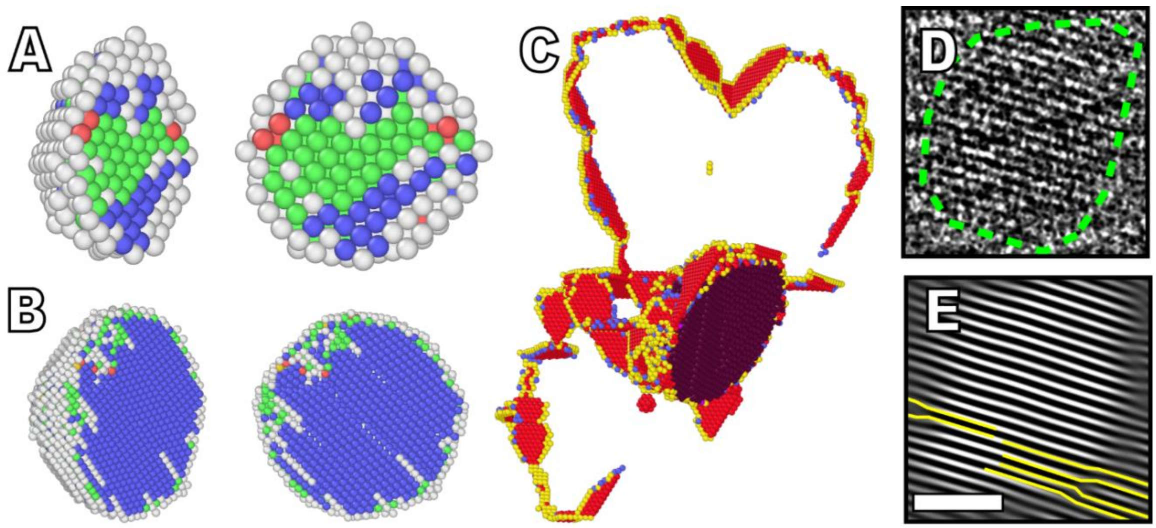

Figure 7: Cross sections of Ta clusters with a diameter of (a) 3 nm and (b) 7 nm at 426 °C (700 K). Ta atoms in FCC and BCC environments are shown in green and blue. The grey atoms represent other structural environments; (c) dislocation loops emitted by the Ta particle with d = 7 nm at 426 °C. Note the dislocation splitting into partials separated by a stacking fault. The FCC Cu atoms were removed for clarity. (d) HRTEM and (e) IFFT image of a semi-coherent particle with d = 5.0 $\pm$ 0.035 nm at 400 °C with misfit dislocations highlighted in yellow (The scale bar is identical for d and e and corresponds to 2 nm) (M. Rajagopalan et al. 2017).

Strength and stability of an alloy at elevated temperatures is controlled by not only the global microstructural changes but also the local changes in the microstructure. The high strength in alloys is influenced by the retention of the grain size as well as the nature of the particle-matrix interface (in our case, Ta nanocluster - Cu matrix) with the increase in temperature. To examine the effect, the compressive flow stress of the alloy at various temperatures was inspected. The flow stress was extracted at 10 % strain from the stress-strain response of samples subjected to quasistatic compression tests at 0.1 /s strain rate. The flow stress was found to decrease with the increase in temperature. It is critical to note that even the high-temperature of 400 °C (0.5 T_m) the flow strength is on par with pure NC Cu composed of 20 nm grain tested at room temperature (Saber et al. 2013b) and the strength at 400 °C for NC Cu-10 at. % Ta is 24% higher in comparison to the data reported for NC Cu (d = 32 nm) sample tested at 250 °C (Farrokh and Khan 2009a). This is understandable because the Ta nano-clusters distributed along the GBs and the matrix is believed to be responsible for the exceptional thermal stability and mechanical strength. That is, the stability arises from the nanoclusters that pin the grain boundaries by the Zener mechanism, thereby preventing significant grain coarsening and the strength arises from the endurance of the nanoclusters to dislocation motion and activation of twinning based mechanism (Koju et al. 2016; Manohar, Ferry, and Chandra 1998; M. Bhatia et al. 2016). Figure 8 highlights once such region in the sample at RT and at 0.5 T_m where a dense distribution of nanoclusters can be identified along the matrix and the GB. This observation confirms the presence and the interaction between the grain boundaries and the Ta nanoclusters that is responsible for the unique stability and strength exhibited by the alloy, also see (Koju et al. 2016).

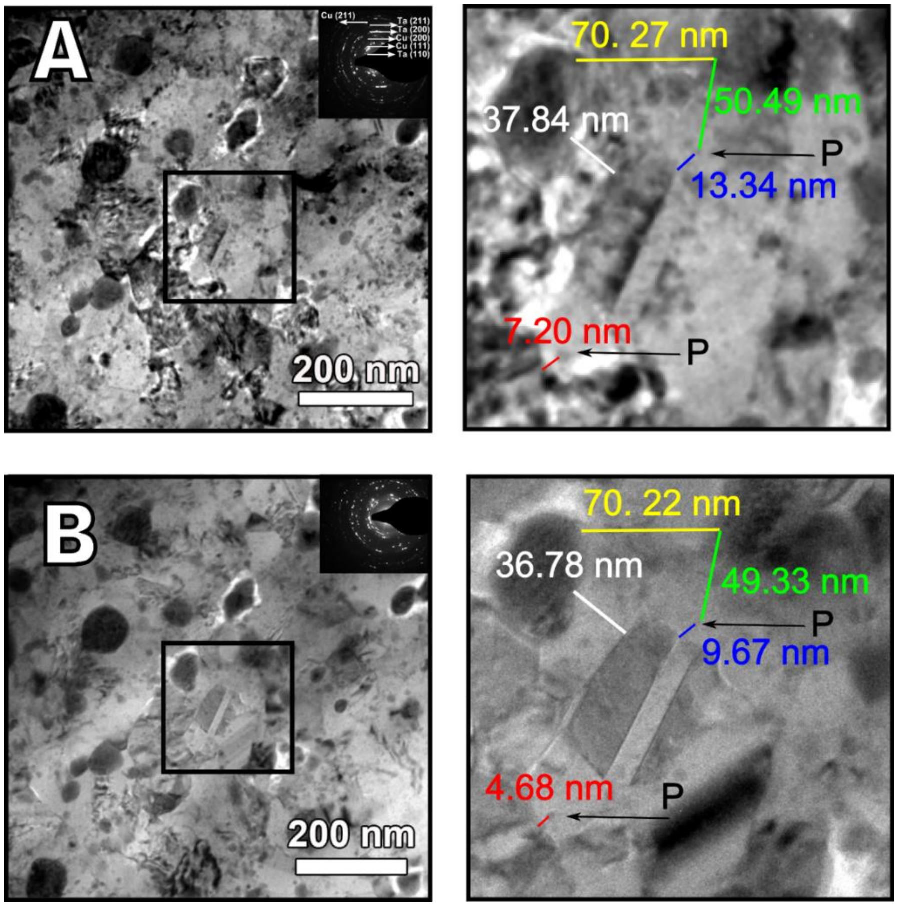

Figure 8: TEM bright field images in the (a) as-received condition and (b) 400 °C for NC Cu-10 at. % Ta alloy. The distances between large Ta particles, Ta nanocluster (P) and GB is highlighted for both the conditions. There is a significant Ta nanoclusters pinning the GB at both the conditions validating the Zener pinning theory (Koju et al. 2016) (M. Rajagopalan et al. 2017).

To address the reasoning behind the change in flow strength, the change in flow stress as a function of average misfit strain at the interface of the high density of nanoclusters and the matrix was probed. Figure 9 indicates the flow stress values plotted against the average misfit strain of the Ta nanoclusters-matrix interface in NC Cu-10 at. % Ta processed at 700 °C for three levels of temperature. The variation in flow stress was found to be strongly correlated with the average misfit strain, with high flow stress values observed at the RT which decrease with the decrease in misfit strain values. Other typical contributions to thermal softening including microstructural coarsening (Cu grain size and Ta based cluster) and changes in the elastic modulus may be excluded as their contributions are negligible over the given testing temperatures (24 - 400°C). The higher the coherency, the lower the misfit lattice strain and the lower the flow stress as the strain field surrounding the Ta based clusters decreases and interactions with dislocations become less prominent., i.e., the pinning-depinning of propagating dislocations during the deformation within in the matrix will be less hindered as the coherency increases (Van Swygenhoven, Derlet, and Frøseth 2006b). Additionally, as temperature increases, normal particles undergo coarsening and transition from a coherent to semi-coherent to incoherent state and strength is lost due to over-aging. In this case the particles gain coherency and at high enough temperatures may be more easily bypassed. However, in this class of materials, a significant coherency strain is retained (~4%), thereby providing significant resistance to high temperature deformation. This is identical with the data reported for superalloys, where lattice mismatch and coherency at the γ/γ' interface determines the resistance for dislocation propagation ultimately leading to superior thermal and mechanical properties for the superalloys (J. X. Zhang et al. 2005). Overall, the mechanical response of the NC Cu-10 at.% Ta alloy is still remains greater than all known NC metals and alloys. Further, the NC Cu-10 at.% Ta alloy exhibits negligible grain growth, which deviates from the conventional trend, thus resulting in a kinetically stable material with a superior flow strength even at 0.5 T_m.

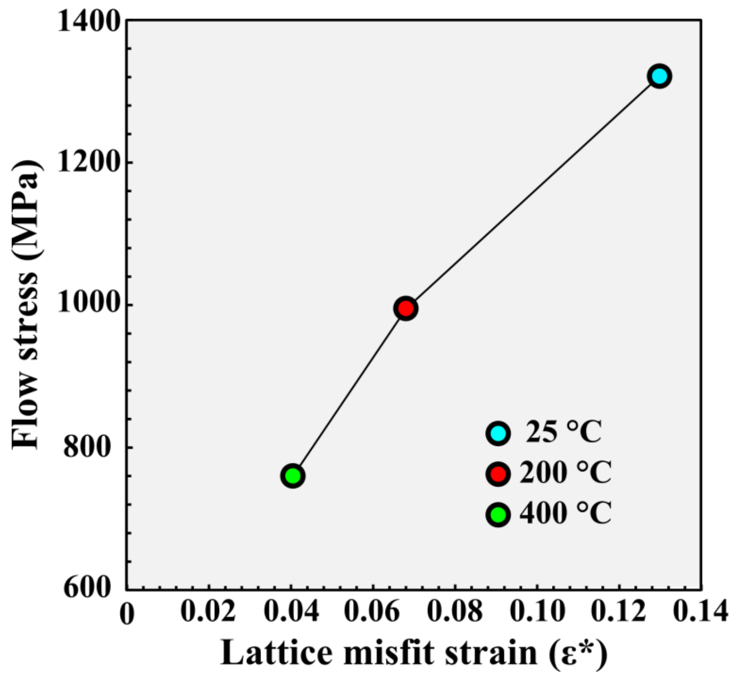

Figure 9: Flow stress as a function of average misfit strain of the Ta nanoclusters in NC Cu-10 at. % Ta processed at 700 °C. The flow stress was extracted at 10 % strain from the stress-strain response of samples subjected to quasistatic compression tests at 0.1 /s strain rate (M. Rajagopalan et al. 2017).

3.4 Conclusions

In this work, in-situ TEM heating experiments, atomistic modeling along with elevated temperature compression tests on a thermally stabilized nanostructured Cu–Ta alloy (Ta = 10 at. %) was used to probe and assess the microstructural manifestations caused by heat and/or changes in temperature. The results shows that the thermal stability achieved with this NC Cu-10 at.% Ta diverges from those observed for conventional coarse-grained metals as well as other NC metals. While the average grain size was estimated to increase only by 12% for Cu phase, the full width half maximum values indicate an increase of only about 4% for Cu grain and 10% for Ta nanoclusters at 0.5 T_m. This suggests that the alloy was resistant to coarsening and there was no significant shift in the size distribution. From a practical perspective, the small increase in grain size does not manifest a perceivable change in the mechanical properties as given by current Hall-Petch assessments of NC Cu. Therefore, macroscopically, the microstructure (Cu grain and Ta based cluster size) of NC Cu-10at% Ta was morphologically stable in shape and scale. However, local structural changes at the interface between the Ta based clusters and the Cu matrix have been observed. The lattice misfit between the Ta clusters and the matrix tends to decrease at high temperatures, promoting better coherency. In other words, the misfit strain was found to decrease monotonically from 12.9% to 4.0% with increase in temperature, leading to a significant change in flow stress, which remains greater than for all known NC metals. Overall, the evolution of such fine structures is critical the thermal-mechanical properties of this alloy.

CHAPTER 4

4 DESIGN AND SYNTHESIS OF ARCHETYPE ADVANCED MATERIALS WITH ANOMALOUS MECHANICAL BEHAVIOR UNDER EXTREME ENVIRONMENTS

4.1 Introduction

The relationship between grain size and strength suggests that with the decrease in grain size, the yield strength increases as defined by Hall-Petch relation. Due to which nanostructured metals (with grain sizes less than 100 nms) have garnered significant attention in the last few decades owing to their superior properties. Although NC materials are good contenders for many functional and structural applications theoretically, the practical application is plagued by the inability to withstand strengths over a range of service temperatures. Therefore, synthesizing nanocrystalline (NC) materials with microstructures that combats instability at elevated temperatures is one of the most fundamental issues in materials science as the microstructure predominantly influences the thermo-mechanical response of materials. For example, pure NC-Cu grains grow rapidly to the micron-scale at 100 °C (Huang, Menovsky, and De Boer 1993; Sonia Simões et al. 2008; S. Simões et al. 2008). Here, we demonstrate a new methodology to synthesize materials with tunable microstructures that are capable of withstanding very high stresses and temperatures, atypical of current generation nanomaterials and in par with structural materials in service. One obvious approach to improve the performance of NC materials is to minimize the delirious effect of grain growth through solute addition. However, the effect of these solutes on the deformation and behavior over a range of temperatures is rarely explored. Therefore, the current strategy explores the potential of creation of such nanocrystalline materials for structural components.

Microstructural stability through solute segregation (or Kinetic stability) is expected to have implications on the mechanical properties of materials. Here, we examine the potential of the concept, through a methodology that leads to the creation of bulk immscible material systems exploiting high-energy mechanical alloying and super-plastic deformation consolidation techniques such as equal channel angular extrusion. The synthesis of such multi-phase materials with a controlled density and size of nanocluster dispersions will serve as a road block for grain boundary migration. This ultimately will yield a material with promising combination of properties including elevated temperature dynamic strength and the process will also exercise control over the long-standing problem of thermal and mechanical instability. Furthermore, this inexpensive route favors mass-production that warrants commercial success of these super-strong materials.

It is demonstrated here that one such nanostructured binary phase material NC-Cu-10at.%Ta, achieves/retains strength that approach the values unlike any other pure NC or UFG structural material under extreme conditions. That is, yield and flow strength values of 600 MPa and 1.1 GPa at strain rates of 1 s^{-1} and 4,000 s^{-1}, respectively, were observed under a homologous temperature of 0.64 Tm (600 °C). The strength stems from the retention of nanocrystalline grain structure and presence of unique nano-clusters distributed homogeneously along the grain interiors and the boundaries. Furthermore, by controlling the density and size of these nanoclusters, the strengths close to theoretical limits can be achieved in these alloyed nanomaterials. This paves the way for revolutionizing structural materials field.

The alloy, NC Cu-10 at.% Ta, is produced through high energy ball milling followed by equal channel angular extrusion (ECAE) (M. Atwater and Darling 2012; K. A. Darling, Tschopp, VanLeeuwen, et al. 2014b; Kris A. Darling, Mathaudhu, and Kecskes 2012), (referred to herein as NC Cu-Ta). See the methodology section of Chapter 5 for details regarding processing procedures. The resultant billet consists of a binary structure of Cu and Ta nanometer sized grains. Importantly, the formation of these alloys rely on the thermal decomposition of non-equilibrium solid solutions and the formation a high density of coherent/semi-coherent Ta based atomic clusters. Preliminary TEM observations Cu has an average grain size of 50 nm, Ta has distinct distributions ranging from small atomic clusters which are embedded in the Cu to larger diameter particles. A range of deformation temperatures is used to specifically investigate the strain rate sensitivity and activation volume as a function of temperature, e.g. the signatures of the rate-limiting thermally activated deformation mechanisms accommodating the plastic flow at temperature. The isolation of factors contributing to deformation is complicated by the fact that extensive coupling of the various microstructural features occurs in these materials.

4.2 Methodology

Quasi-static tests were performed on an Instron load frame equipped with a 50 kN load cell and ATS clam shell furnace capable of reaching temperatures up to 1,200 ˚C. Tungsten carbide inserts were placed between the specimens and 718 Inconel extending rods. Specimens of 3 mm in diameter and 3 mm in length were compressed in at strain rates of 8 x 10^{-4}, 1 x 10^{-3}, 1 x 10^{-2}, 1 x 10^{-1}, and 1 s^{-1} and temperatures of 298 K, 473 K, 873 K, and 1073 K. A thermocouple embedded in the 718 Inconel rod was used to measure the temperature of the specimen. The specimens reached temperature within 30 minutes and were held at temperature for 30 minutes to ensure uniform temperature throughout the specimen before testing.

High strain rates were attained using a 12.7 mm diameter, 718 Inconel Kolsky bar. The Kolsky bar uses three rods of the same diameter and material to measure the stress-strain response of a material. These are the striker bar, incident bar, and transmitted bar. The striker bar impacts the incident bar generating a strain pulse which travels to the specimen sandwiched between the incident and transmitted bars. When the incident pulse hits the specimen, it splits into a reflected pulse and a transmitted pulse. The reflected pulse measured in the incident bar provides information on the strain in the specimen while the transmitted pulse measured in the transmitted bar provides information on the stress observed by the specimen. Further details of the Kolsky bar test method can be found in the work by Gamma et al.(Gama, Lopatnikov, and Gillespie 2004).

Elevated temperatures were applied using a tube furnace capable of reaching 900 ˚C placed around the specimen and ends of the Kolsky bar. Correction for the thermal gradient was applied.

As-received and post-deformed microstructures were characterized using JEOL-2010F, and ARM-200F operated at 200 Kilovolts. Samples for TEM characterization were prepared using conventional thinning procedures where 3 mm disc was punched out from the bulk sample, and subjected to grinding to 100 μm thickness. Dimpling was done to reduce the thickness to around 5 μm followed by ion-milling with Precision Ion Polishing System at liquid nitrogen temperatures (-195 ºC) to obtain electron transparent regions.

4.3 Results and Discussion

The strength evolution of the NC-Cu-10at.%Ta alloy in comparison to the other major NC and UFG metal systems is shown on the Ashby plot of strength (yield strength for quasistatic tests and flow stress for high strain rate conditions) versus temperature in Fig. 10. The yield strength is extracted at 0.2% offset whereas flow stress was extracted 10%. The upper and the lower bounds for the contour correspond to the stress response within the strain rate limits. The strength at 200 °C under compression was found to be 790 MPa and 1160 MPa for a strain rate of 0.001 s^{-1} and 4000 s^{-1}. These translate into a fraction of 64 % and 88 % of strength at RT. At even more intense conditions, this alloy demonstrates strength of 20 MPa at 1000 °C (0.001 s^{-1}). In contrast, conventional NC materials such as NC Cu exhibit a strength of 780 MPa at RT and 565 MPa at a rather low temperature of 250 °C which is only 0.38 T_m (Farrokh and Khan 2009b). In fact, the temperatures at which the current generation NC materials are tested can be deemed low as the service temperatures for the operation of structural components are significantly higher. From Fig. 10, it is evident that rate of decrease of stress with the increase in temperature is drastic with trend similar to exponential decay for conventional NC and UFG materials. However, NC Cu-10at.%Ta exhibits a higher resistance to the influence of temperature which is contrary to the conventional theory.

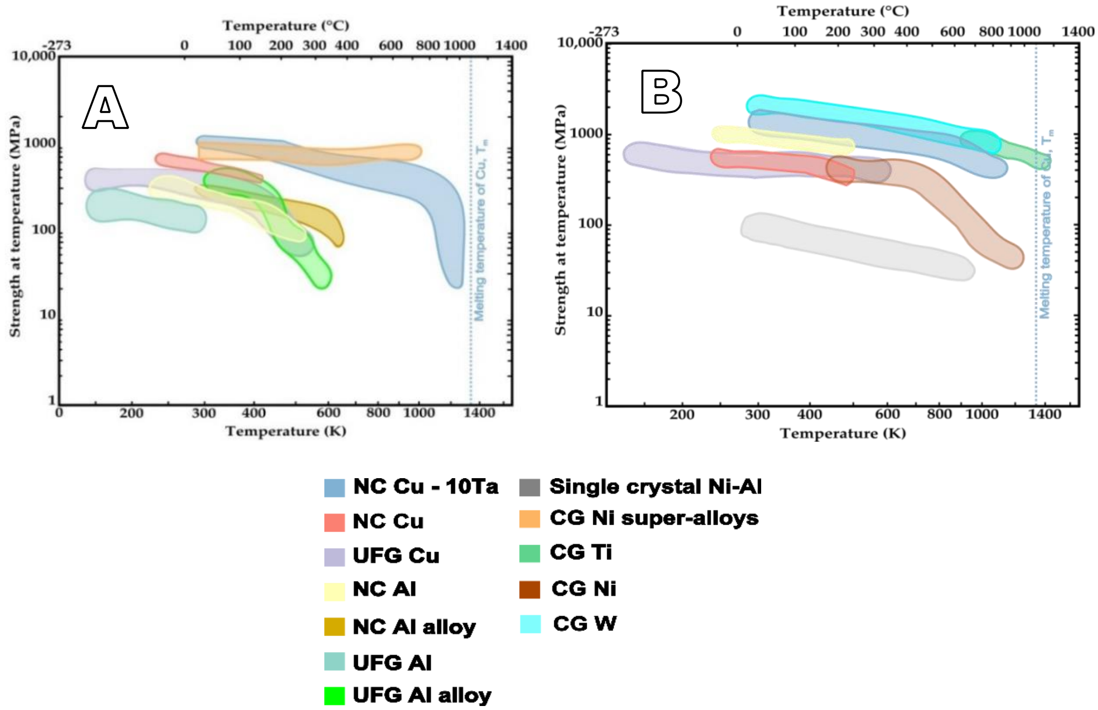

Figure 10: Strength at temperature versus applied temperature for NC and UFG metals and alloys. Yield strength and flow strength for NC-Cu-10at.%Ta's data along with NC and UFG data reported in the literature at (a) quasistatic and (b) high strain rates. The rate of change of strength with temperature is lower for NC-Cu-10at.% Ta as compared to other NC materials reported. NC Cu and Al from (Farrokh and Khan 2009b), UFG Cu from (Suo et al. 2013), UFG Al from (Sun et al., n.d.), UFG Al alloy from (Witkin, Han, and Lavernia, n.d.),NC Al alloy from (Shaw and Luo 2007), CG W from (Lennon and Ramesh 2000), CG Ti from (Lee and Lin 1998), Single crystal Ni-Al from (Ball and Smallman 1966), and CG Ni superalloys from (Yamashita and Kakehi 2006).

The plastic deformation in nanocrystalline materials occurs either through deformation twinning or dislocation slip. Studies have indicated that GBs serve as the origin for nucleation and provide a point for storing and the annihilation/absorption of dislocations after they transverse the grain under an applied stress. These GBs are also responsible for pinning the dislocations ultimately obstructing their motion by strongly influencing when and where cross-slip can occur and by increasing the energy to unpin and move across to the neighboring grains (Schiøtz and Jacobsen 2003b; Van Swygenhoven, Caro, and Farkas 2001; Swygenhoven and Caro 1997; Van Swygenhoven, Derlet, and Hasnaoui 2002). Quasistatic and high strain rate testing are fundamentally different processes, so the plasticity accommodation will be inherently different. To investigate the active deformation mechanisms and the reasoning behind the high temperature and stress response in these alloys, ex-situ microstructural characterization was also employed. In general, the emission of partial and full dislocations are competing mechanisms and their activation depends on the stress levels. From TEM observations, an appreciable dislocation density can be identified for quasistatic testing conditions implying the absence of dislocation absorption. In case of conventional nanocrystalline materials, grain boundaries act as source for dislocation generation which then runs freely and absorb at the opposite grain boundary sink. Here, the dislocations are emitted, interact with the high density nanoclusters and are pinned at various sites thereby reducing the mean free path for the propagation of the dislocations. The motions of dislocations are restricted and there exists a stress required to un-pin for the motion to resume. The other scenario includes the dislocation emission from the grain boundary, which travels to the opposite side and leaves behind two sides. The propensity of dislocation slip increases with the increase in testing temperature which helps in overcoming the energy barrier required for dislocation based activity in these systems. However, the mean free path for the dislocation motion is dependent on the grain size and density of the nanoclusters that are embedded in the material system. In case of high strain rate conditions, nucleation of partial dislocations is favored at RT due to the high applied stress which surpasses the barrier for twinning based deformation. This can be identified from the micrographs indicated in Fig.11 where twins with narrow widths can be identified. The growth of the twins is restricted due to the presence of Ta nanoclusters in Cu-10 at.% Ta. However, at elevated temperatures the deformation shifts from twin based to dislocation where the thermal energy favors the dislocation slip.

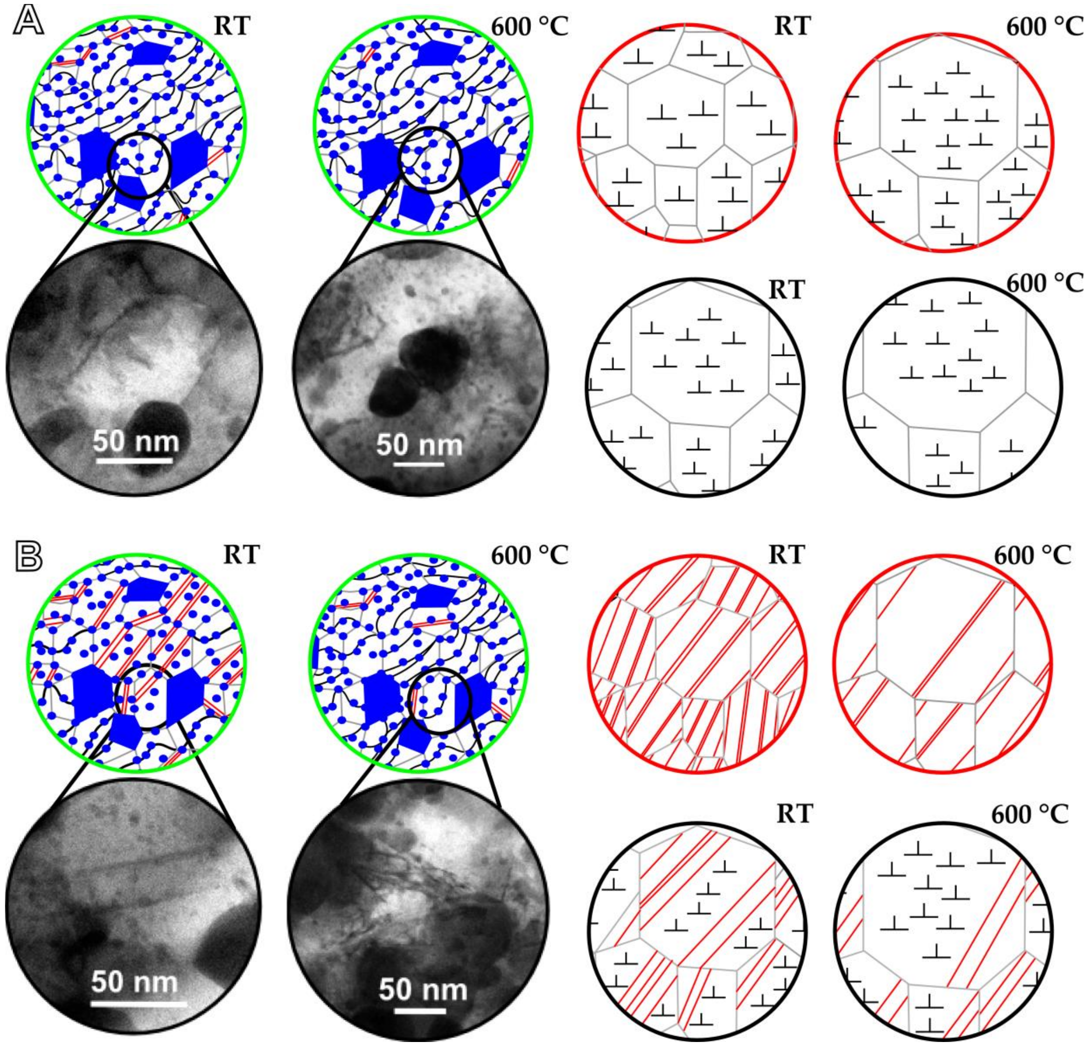

Figure 11: Microstructural characterization of post-deformed NC-Cu-10at.%Ta tested at various strain rates. Micrographs of NC-Cu-10at.%Ta (green circles), NC Cu (red circles), and CG Cu (black circles) corresponding to (a) quasistatic testing, and (b) high-strain rate testing highlighting the effects of temperature and strain rate on the deformation. The shift in deformation from twin based to slip dominated for high-strain rate testing is evident from the micrographs with the increase in temperature. Quasistatic testing results in slip based deformation at both RT and 600 °C. Ta nano-clusters are responsible for pinning the grain boundaries and dislocations imparting stability and strength.

Also, the stability of the Cu grains remains intact owing to the stability of the high density of coherent nanoclusters present in the microstructure (Fig. 12 and 13). The number distributions reveal that the increase in grain size increases from 48.5±16.1 nm in as-received condition to 83.3 ± 29.16 nm at 0.01 s^{-1} tested at 600 °C (0.64 T_m). Likewise, average grain size was observed to be 80 ± 39.93 nm post-600 °C and 4000 s^{-1} high-strain rate testing conditions. The relative size of the nanoclusters were also constant with the application of stress and temperature highlighting the ability to resist coarsening. Further, these nanoclusters pin the grain boundaries through Zener pinning mechanism thereby arresting diffusion which is responsible for grain growth (Fig. 12).

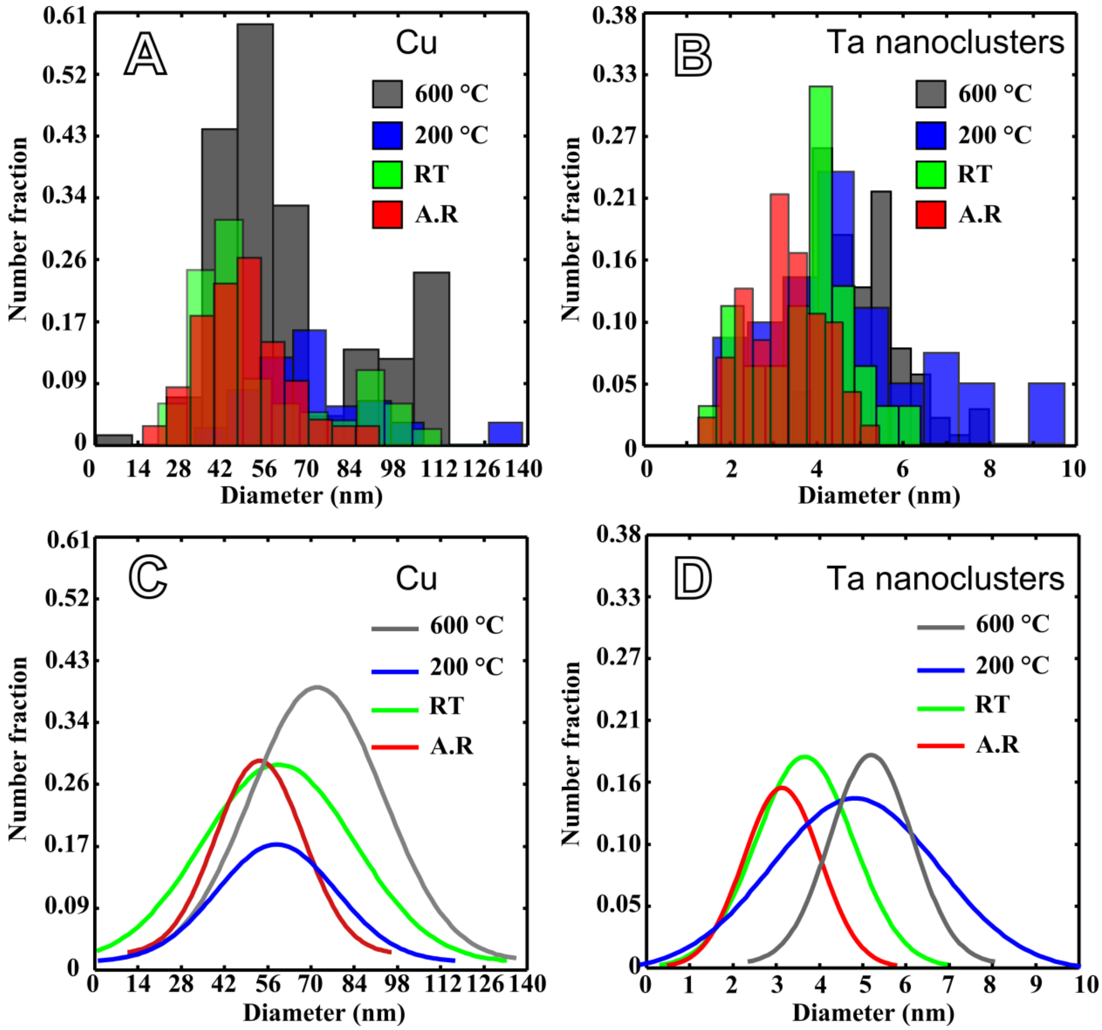

Figure 12: Grain size distribution of Cu and Ta nanoclusters obtained from as-received and quasistatic tested samples (at 0.01 s^{-1}). (a) The distributions indicate nominal increase in grain size for Cu with majority of the grains in the nanocrystalline regime. (b) Ta nanoclusters also exhibit stability with temperature. (c-d) Gaussian distributions confirm that the distributions do not shift significantly indicating negligible grain coarsening.

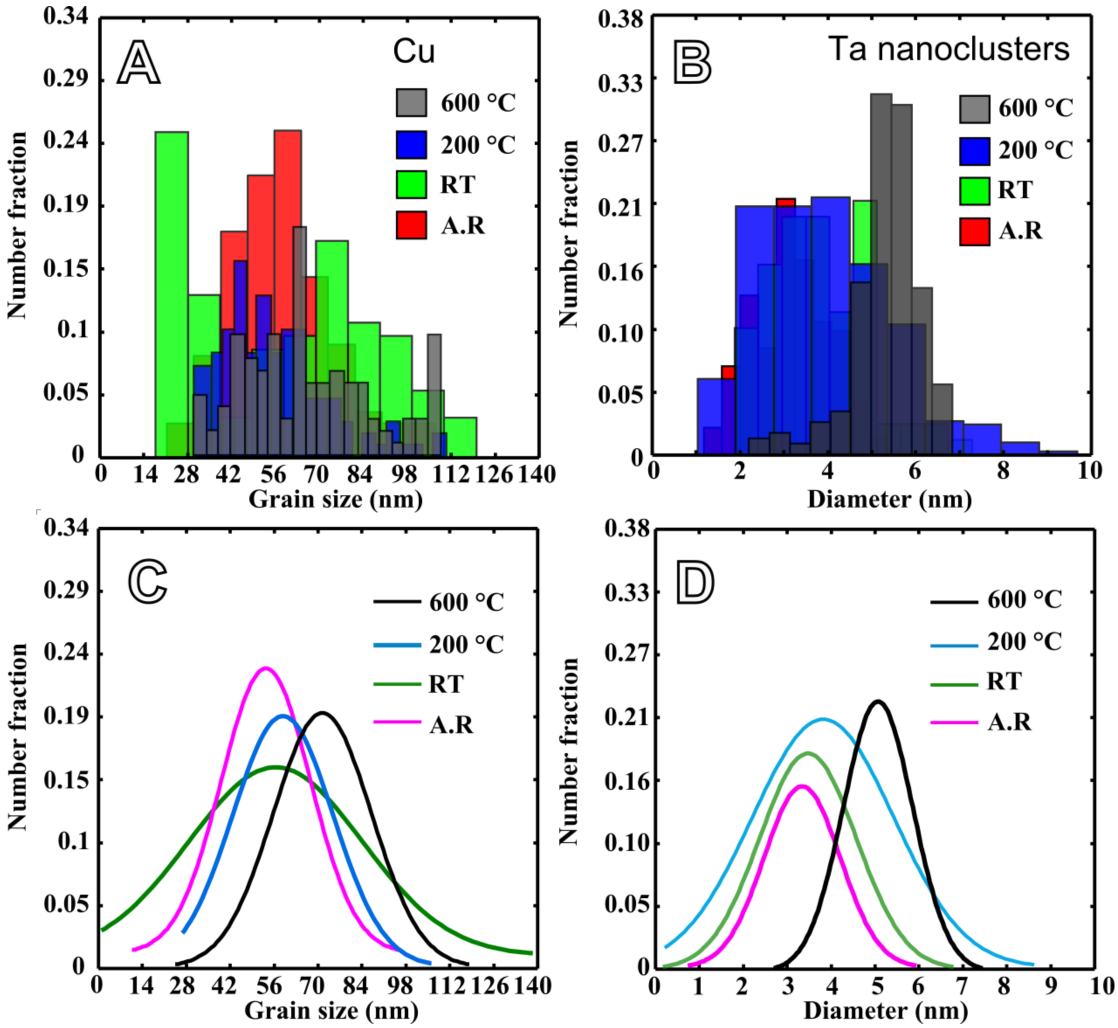

Figure 13: Grain size distribution of Cu and Ta nanoclusters obtained from as-received and high strain rate tested samples (at 4000 s^{-1}). (a) The distributions indicate nominal increase in grain size for Cu with majority of the grains in the nanocrystalline regime. (b) Ta nanoclusters also exhibit stability with temperature. (c-d) Gaussian distributions confirm that the distributions do not shift significantly indicating negligible grain coarsening.

Furthermore, these nanoclusters contribute towards strengthening which can be identified from the micrographs highlighting the interaction between the dislocations responsible for accommodating plasticity at elevated temperatures and nanoclusters (Fig. 11). The dislocations appear to bow owing to the strong interfacial bond between the nanoclusters and the Cu matrix. The interaction between the nanoclusters and dislocation reflect on the strength at various temperatures. Although these Ta-rich nanoclusters are considered spherical, interesting shape variations of the nanoclusters were identified through high-resolution transmission electron microscopy as well as bright field and high angle annular dark field scanning transmission electron microscopy. Fig. 14 indicates the different morphologies of the nanoclusters obtained from TEM as well as the atom probe data. Some coherent clusters appear to have strong diffraction spots confirming their crystallinity whereas others have distorted/ hollow ring like features which points to a plausibility of non-crystalline components in these structures. For instance, Fig. 14a illustrates a conjoined nanocluster of a completely crystalline nanocluster sharing an interface with another nanocluster with amorphous content. Fig. 14 b highlights one completely crystalline nanocluster whereas Fig. 14c and d represent shell type nanoclusters where the shell is Ta-rich and contrast variation between the shell and core supports the likelihood of defects present in the core. These nanoclusters are expected to pin the grain boundary at various conditions of stress and temperature. The pinning is responsible for imparting the extraordinary strength and stability in these alloys as verified by the atomistic simulations (Koju et al. 2016).

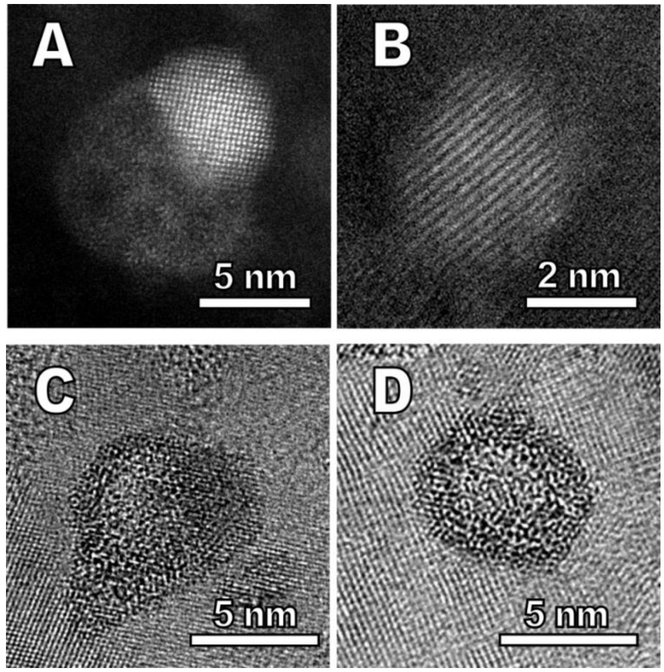

Figure 14: Characterization of the Ta-rich nanoclusters responsible for the unique stability and strength in the immiscible based alloy systems. (a) High Angle Annular Dark Field (HAADF) image of disordered-ordered nanocluster where one part exhibits a high degree of crystallinity and the other exhibits a disordered structure, (b) High Angle Annular Dark Field (HAADF) image of perfectly crystalline nanocluster, and High Resolution Transmission Electron Microscope image of (c-d) core shell type nanoclusters with a crystalline shell being rich in Ta, and the core consisting of defects such as vacancies (d from (K. A. Darling et al. 2016a)) .

4.4 Conclusions

We conclude that the binary NC Cu-Ta alloys displays remarkable mechanical strength at even temperatures over 0.5 T_m (melting temperature = 1356 K). The alloy has strength levels that are comparable to Ni superalloys. Furthermore, these alloys have outstanding combinations of strength and stability under extreme testing conditions such as high strain rate as well as creep. These unique combinations of properties draw our attention to the unique nano-clusters which control deformation and thus, deem these materials as excellent candidates for high temperature applications. This opens up the prospects of achieving super-strong alloys through tailoring the microstructure of any structural metal such as Ni with such nano-structures which will push the envelope of performance of current generation alloys towards theoretical limits.

CHAPTER 5

5 EXTREME CREEP RESISTANCE IN A MICROSTRUCTURALLY STABLE NANOCRYSTALLINE ALLOY

5.1 Introduction

Over the past 50 years, the reduction or elimination of intrinsic topological defects (grain or cell boundaries) has been central to the design of creep-resistant materials. Current designs enhance high-temperature creep performance through the use of single-crystal alloys, for example, nickel-based, single-crystal superalloys (Giamei 2013; Reed 2008). Nano-grained materials with grain sizes 7–8 orders of magnitude smaller than, and grain-boundary volume fractions 5–6 orders of magnitude higher than, the currently used single-crystal superalloys have never been considered viable for high-temperature creep applications. Moreover, nanocrystalline metals exhibit microstructural instability, that is, grain growth via diffusional processes such as diffusional creep, sliding and rotation, at moderately low and even room temperatures, sometimes in combination with deformation (Mohamed and Li 2001; Meyers, Mishra, and Benson 2006; Choi et al. 2013). Consequently, previous creep studies on nanocrystalline metals have reported creep-stress exponents of 1–3 resulting from grain-size effects on diffusional (Coble) creep (Mohamed and Li 2001).

Contrary to conventional wisdom, a divergent, bulk nanocrystalline copper–tantalum alloy (10 atomic per cent (at%) tantalum; hereafter Cu–10 at% Ta was developed, that is able to achieve and retain high strength and creep resistance at a high homologous temperature of $0.64T_m$ = 600 °C (where T_m is the melting temperature of the matrix), owing to its unique microstructural architecture. Initially synthesized through high-energy ball milling and subsequently consolidated via equal-channel angular extrusion (ECAE), the as-processed microstructure consists of a copper matrix with an average grain size of 50 ± 17.5 nm and tantalum based particles that range in size from atomic nanoclusters (average diameter of 3.18 ± 0.86 nm) to much larger precipitates (average diameter of 32 ± 7.5 nm). (For a macroscopic view of the microstructure and additional processing details, see Methods). It has been shown that such ranges in particle size give rise to an extremely stable microstructure; as compared to pure nanocrystalline copper, which exhibits rapid grain growth to the micrometre scale at only 100 °C (Huang, Menovsky, and De Boer 1993), Cu–10 at% Ta powders maintain a mean grain size of 167 nm after annealing at 1,040 °C for 4 h (K. A. Darling, Tschopp, Guduru, et al. 2014). N This highly stabilized microstructure could give rise to unusual combinations of mechanical properties, such as creep resistance under extreme conditions (high stress and temperature).

5.2 Methodology

5.2.1 Powder processing and consolidation via ECAE

For the preparation of nanocrystalline (NC) Cu–10 at % Ta powder, the powder was generated through high-energy cryogenic mechanical alloying. The desired composition was obtained by loading elemental Cu and Ta powders (–325 mesh and 99.9% purity) into a hardened steel vial along with the milling media (440C stainless steel balls) inside a glove box with an Ar atmosphere (oxygen and H_2O are <1 p.p.m.). The vials were loaded with 10 g of the Cu–Ta powder as well as the appropriate amount of media to ensure a ball-to-powder ratio of 5:1 by weight. A SPEX 8000 M shaker mill was used to perform the milling at cryogenic temperature (verified to be about −196 °C) for 4 h (14.4 ks) using liquid nitrogen. To ensure the vial remained at cryogenic temperature, a thick polymer sleeve was retrofitted to fit around the vial in the SPEX mill with an inlet and outlet vent to flow the liquid nitrogen. Before starting the milling process, the vial was placed in the polymer sleeve with the liquid nitrogen flowing for approximately 20 min (1.2 ks) to ensure the vial approached −196 °C. Once the milling was completed, the vials were placed back into the glove box, opened and stored. This milling procedure was performed until 100 g of NC Cu–10 at% Ta powder was generated. The resulting powder after cryogenic mechanical milling was an unagglomerated mass of powder with particulates ranging in size from about 20 μm to 100 μm.

For consolidating the NC Cu–10 at% Ta powder to bulk, equal-channel angular extrusion (ECAE) was selected as the consolidation process. Billets of Ni 201 with dimensions of 25.4 mm × 25.4 mm × 90 mm had cylindrical chambers with diameters of 10 mm and lengths of 50 mm made within them for housing the powder. The powder was loaded into the chamber followed by press-fitting a Ni 201 plug into the open end to seal the chamber. Both of these steps were performed within the glove box. Before starting the ECAE process, the die assembly used for processing the billets was preheated to 350 °C to minimize thermal loss during the ECAE processing. Additionally, the billets containing the powder were held at 700 °C in a box furnace purged with Ar for 40 min (2.4 ks) to ensure that they reach the desired extrusion temperature. The heated billets were dropped into the ECAE tooling as quickly as possible from the furnace and extruded at an extrusion rate of 25.5 mm s^{-1}. This step was repeated four times following route 'B_C' to prevent imparting a texture to the consolidated powder. As a result of the extrusion channel having an angle of 90°, a total strain of 460% was imparted onto the powder-containing billet as a result of processing. The creep specimens were then machined from these billets, within the region containing the consolidated powder, via a wire electric discharge machine. Finally, SEM imaging confirmed the creep specimens to be fully consolidated after the ECAE process with no porosity or as-milled particle boundaries being present. Note that a change in processing conditions or steps, such as in ECAE process temperatures, will result in different microstructural statistics such as grain-size distributions; however, as shown previously, the nanocluster density depends mainly on the Ta concentrations, which are the primary features resulting in an enhanced creep behaviour.

5.2.2 Mechanical characterization at creep conditions

Compressive cylindrical creep experiments were performed using a 2320 series lever arm creep tester (Applied test systems) with a 5:1 lever arm ratio. Both the diameter and the height of the cylindrical creep specimens were about 3 mm. The specimens were kept at the centre of a 3210 series split tube furnace to maintain a constant temperature across the sample height. A heating rate of 200 °C h^{-1} and a soak time of 0.5 h was used for the creep tests. For the best temperature measurement and control, a thermocouple was always wrapped around the creep specimens to maintain good contact. An ST 1278 incremental length gauge with ±1 μm accuracy was used to measure the conventional creep strain. The compression creep experiments were conducted in air at 873 K and with fractions of 0.45, 0.50, 0.55, 0.60 and 0.65 of the yield stress, at 773 K and with fractions of 0.70, 0.75 and 0.80 of the yield stress, and at 673 K and with fractions of 0.70, 0.80, 0.90 and 1.00 of the yield stress. The specimens were first coated with a thin layer of boron nitride for lubrication and then placed between the compression platens. Creep test temperatures were attained at a constant heating rate followed by soaking at the set temperature (for 0.5 h) to avoid the temperature fluctuation during the test. After the soaking stage, the loading begins automatically, followed by the start of the creep test. These tests were typical constant-force tests. All the creep data were recorded from the test start to finish. Further, specimens did not reach failure because tests were stopped before the strain rate exponentially increases with stress (before the tertiary creep domain), and our primary objective was to characterize the secondary creep rates. For most of the creep tests, the total strain values did not exceed about 6%. All the crept samples were quenched in water immediately after unloading to preserve the crept microstructure. The physical dimensions of the crept samples were measured after the test and compared with the extensometer measurements. Note that the stress was determined after the test by taking into account the amount of strain. Further, during initial loading to a desired constant creep load of the test specimen can include both elastic and plastic strains. The minimum creep rate was calculated from the slope of the curve of conventional creep strain versus time.

5.3 Results and Discussion

Compression creep tests were conducted over a wide range of applied stress and temperature conditions (see Methods Section), as shown in Fig. 15. The compression–creep-strain evolution curves shown in Fig. 15a consist of the primary creep region, where the creep strain rate decreased with time, and the secondary creep region, where the creep strain rate remained at steady state. The steady-state creep rates in nanocrystalline Cu–10 at% Ta were all found to be less than 10^{-6} s^{-1} at various homologous temperatures between $0.5T_m$ and $0.64T_m$ under a stress of 1.2%–0.85% of the shear modulus. Note that the creep rates reported for nanocrystalline Cu–10 at% Ta are minimum creep rates. The upper and lower fractions of the shear modulus equate to stress values of 576 MPa and 319 MPa, respectively, which represent 90% and 65% of the at-temperature (400 °C and 600 °C) yield strength. The yield stress values at various temperatures were quantified using a series of quasi-static compression tests with a strain rate of 8×10^{-4} s^{-1}. To further demonstrate the improvement in the creep resistance, a creep test was performed under 100% of the yield stress at $0.5T_m$ (400 °C), which resulted in a creep rate of 5.3×10^{-8} s^{-1}. By contrast, at a rather low homologous temperature—$0.4T_m$ or 275 °C, for example—a creep rate of 10^{-1} s^{-1} was reported for an applied stress of 0.12% of the shear modulus (57 MPa) with an average grain size of 25 nm in pure nanocrystalline copper (Mohamed and Li 2001). As compared to pure NC-Cu, NC-Cu-10at.%Ta at 1.5 to 2 times higher temperature and an order of magnitude higher stress has 6-8 orders of magnitude lower $\dot{\boldsymbol{\varepsilon}}$ (Atul H. Chokshi 2009). Such a response is reminiscent of, and more comparable to, that of the creep performance achieved by advanced single-crystal nickel-based superalloys (creep rate of about 10^{-8} s^{-1})(Pollock and Tin 2006).

In general, creep in nanocrystalline materials has been reported to follow the Coble creep mechanism (Coble 1963), whereby creep occurs through the transport of vacancies along grain boundaries (Ashby 1972; Coble 1963) with a low stress exponent (of the order of 1–3) (Atul H. Chokshi 2009; Mohamed and Li 2001). On the other hand, our nanocrystalline Cu–10 at% Ta alloy exhibits stress exponents that are substantially higher than those associated with the diffusional-creep- and grain-boundary-related mechanisms. Therefore, the creep resistance achieved with our nanocrystalline Cu–10 at% Ta alloy outperforms most nanocrystalline materials.

Figure 15: Creep response of NC-Cu-10at.%Ta. **(a)** Creep strain versus time curves for various applied temperatures and constant stress conditions, and **(b)** theoretical

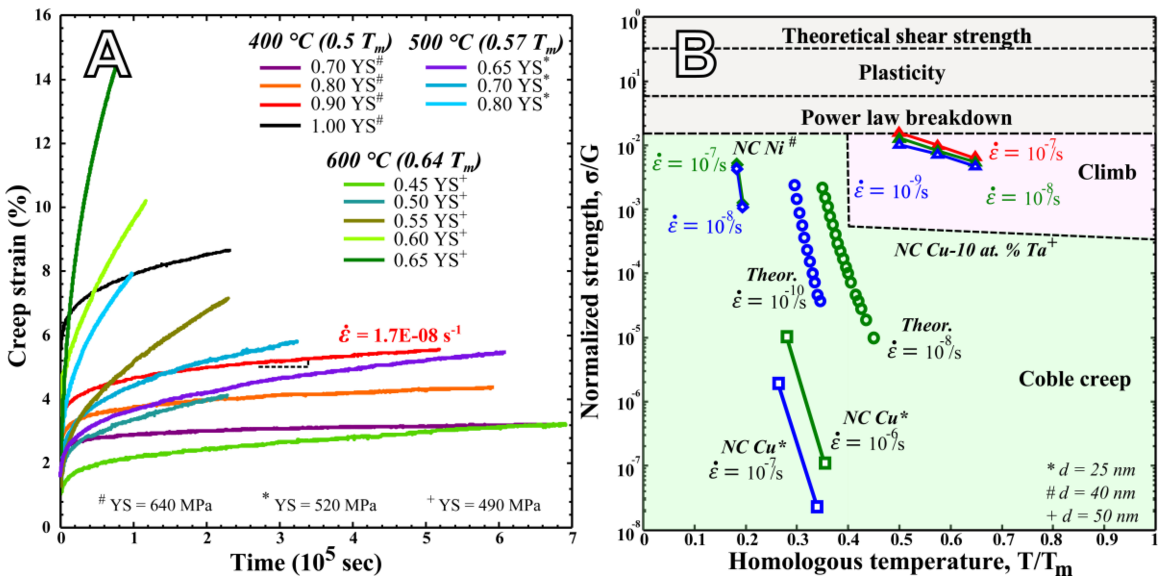

deformation mechanism map of a NC-Cu with an average grain size of 50nm along with recently published experimental creep rates (Mohamed and Li 2001) in NC-Cu and Ni are plotted in stark comparison to this work on NC-Cu-10at.%Ta. The theoretical constant Coble creep rate lines for a grain size of 50nm (green and blue circles) are also provided (K. A. Darling et al. 2016a).

To comprehend this improvement in creep resistance, a compilation of experimental and theoretical creep-rate data for various nanocrystalline materials is presented on an Ashby-type deformation mechanism map (Ashby 1972) in Fig. 15 b, which was derived on the basis of creep constants for nanocrystalline copper with a mean grain size of 50 nm (see (Ashby 1972) and Methods). Experimental creep-rate data from nanocrystalline metals such as copper (25-nm grain size) and nickel (40-nm grain size (Mohamed and Li 2001) along with the theoretical, constant, Coble creep-rate lines for copper with an average grain size of 50 nm (green and blue circles in Fig. 15). The reported creep properties of nanocrystalline copper and nickel fall within the Coble region. This is mainly due to grain-boundary diffusional processes: that is, vacancy diffusion and self-diffusion in copper and nickel, occurring through both the grain boundaries and the lattice are faster at elevated temperatures and, hence, the diffusional creep controls the creep behaviour (Atul H. Chokshi 2009). Therefore, in these conventional nanocrystalline copper and nickel metals, the grain coarsening creates powerful kinetics that constantly evolves the microstructure. By contrast, the creep rates of our nanocrystalline Cu–10 at% Ta show a marked departure from convention, with the measured creep rates primarily in the dislocation–climb region (as shown by the triangles in Fig. 15 b). In other words, the diffusional creep processes have been suppressed (or were absent) in our nanocrystalline Cu–10 at% Ta alloy.

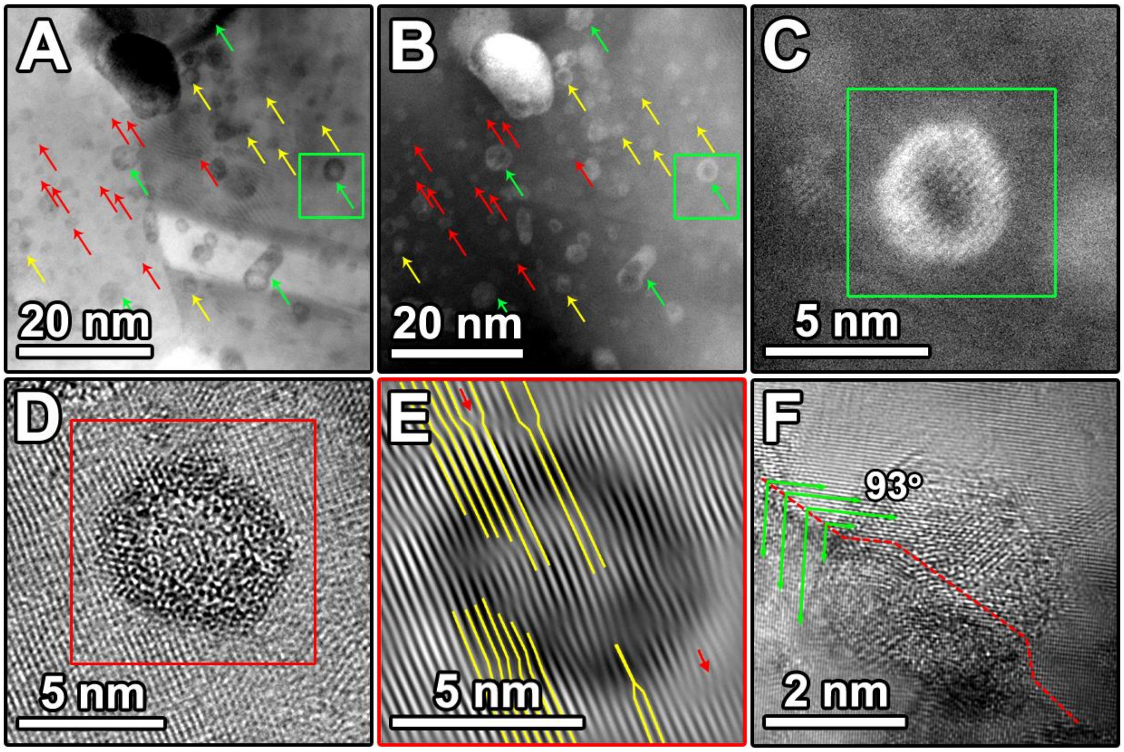

Figure 16: TEM characterization of Ta-based nanocluster in as-received NC-Cu-10at.%Ta (a) the bright-field STEM (BF-STEM) image highlighting the high number density of nanoclusters of various sizes. The colored arrows are used to designate the sizes of the different coherent/semi-coherent nanoclusters (red arrows ~1nm, yellow ~2.5nm, green ≥ 4nm radius). (b) HAADF-STEM image accentuating Ta-rich clusters based on Z-contrast and (c) higher magnification of the same. The BF-STEM (d) highlighting the core-shell structure of the nanocluster. (e) Inverse Fast Fourier Transform (FFT) image highlighting the threading dislocations and half plans between the matrix semi-coherent clusters. (f) 3nm particle residing at a high angle GB (K. A. Darling et al. 2016a).

To understand the observed enhancement of the creep property, we turn our attention to the large number (density of 6.5×10^{23} m^{-3}) of coherent or semi-coherent (diameters of 1–4 nm) nanoclusters (see Figs. 16a-b). These small nanoclusters have a core–shell-type structure that can be seen in Figs. 16b-c, which shows that the contrast within and across the individual nanoclusters varies, indicating a compositional gradient. In addition, the High Angle Annular Dark Field Scanning Transmission Electron Microscopy (HAADF-

STEM) image (Fig. 13b) points to the shell portion of the particle being tantalum-rich, with the core generating less contrast, possibly owing to an element with a lower atomic number or to structural defects that would not generate contrast (such as vacancies). The High Resolution Transmission Electron Microscopy (HR-TEM) image of the nanocluster (Fig. 13d) provides further evidence that the loss in contrast could be partly due to the presence of vacancies within the core region. The inverse fast Fourier transform image of one such nanocluster is shown in Fig. 16e. Note the distortion of the lattice as it approaches and enters the nanocluster, with the yellow arrows indicating the insertion of extra half planes of atoms into the lattice to minimize distortion. Finally, Fig. 16f shows a HR-TEM characterization of semi-coherent bonding between the nanocluster and the copper matrix at a high-angle (93°) grain boundary with an average misfit strain of 5.8%, indicating strong interfacial bonding that can lead to enhanced mechanical properties. Quasi-static and dynamic strengths of greater than 1.2 GPa have previously been measured for the nanocrystalline Cu–10 at% Ta alloy (see previous chapter); these strengths are greater than double that predicted by Hall–Petch hardening for nanocrystalline copper and presented with an apparent linear temperature dependence of flow stress(K. A. Darling et al. 2015b). Similarly, core-shell type nanoclusters have recently been reported in ODS ferritic alloys (Hirata et al. 2011) and Mo-alloys (G. Liu et al. 2013), and are responsible for the excellent strength and ductility therein.

To understand the underlying mechanisms of creep resistance and to determine the enhancement of the creep property induced by the nanoclusters, atomistic simulations and post-HR-TEM characterizations were performed (See Fig. 17). First, the HR-TEM characterizations of post-deformed creep samples (at 600 °C and 50% yield stress) were performed, as shown in Fig. 17. The stability of the nanoclusters, which is crucial for enhanced properties, can be seen in Fig. 17b as the coarsening rate of nanoclusters during creep at elevated temperatures is negligible, which is mainly owing to coherency of such dispersions. Further, due to highly stabilized nanoclusters, the bowing of the GB as the boundary interacts with numerous nanoclusters can clearly be identified in a high resolution BF-STEM image of the post-creep sample, as shown in Fig. 17c. That means clusters located at GBs are likely to increase the barrier strength for both GB sliding and rotation, both of which are crucial creep mechanisms in NC-metals. In addition, the nanoclusters pin the GBs, i.e. Zener pinning(Manohar, Ferry, and Chandra 1998), thereby preventing significant grain coarsening, which is consistent with the atomistic calculations (Figs. 18a-b). Here, atomistic simulations were performed using a molecular dynamic code LAMMPS (Plimpton 1995) along with an embedded atom potential (Pun et al. 2015) (see Methodology section).

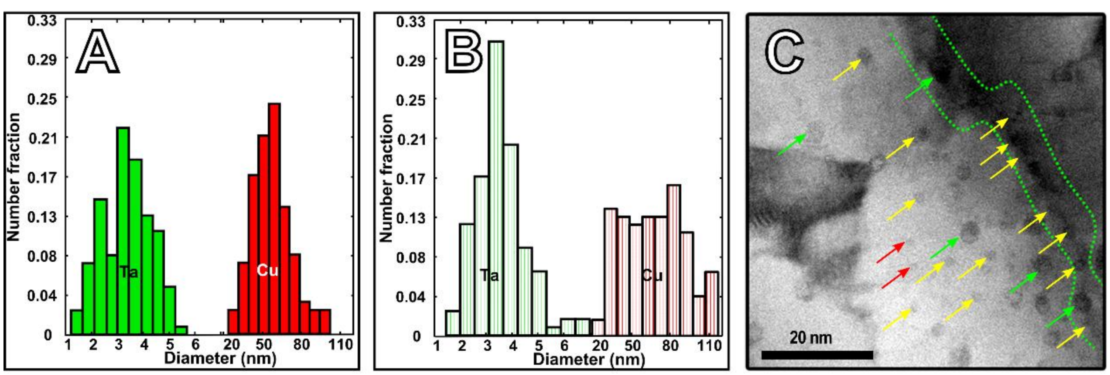

Figure 17: TEM images showing the microstructures and grain distributions indicating stability in NC-Cu-10at.%Ta after creep testing. Number distributions averaged over 300 grains of both the Cu matrix (red) and Ta particles (green) (a) before and (b) after the creep testing. The Cu grains and Ta particles have a nearer identical distribution before and after the creep testing. (c) The high resolution BF-STEM image showing the bowing of the GB as it interacts with Ta clusters. The color-coded arrows highlight the varying sizes of Ta (red arrows < 1 nm, yellow arrows < 1-2 nm, and green arrows > 4 nm diameter) (K. A. Darling et al. 2016a).

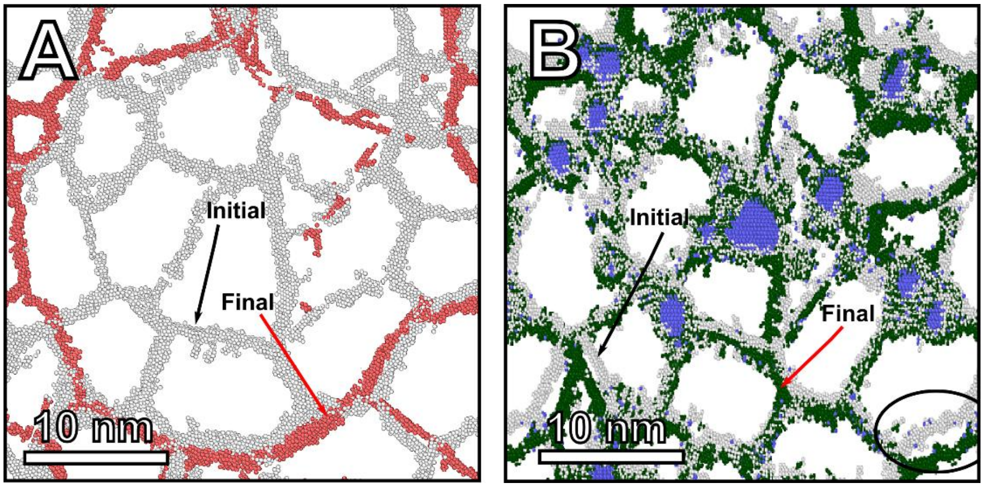

Figure 18: Modeling data indicating stability in NC Cu-10at.%Ta after creep testing. (a-b) provides 2-D slices through 3-D atomistic creep simulations of pure NC-Cu and NC-Cu-10at.%Ta at 600 ˚C and 295 MPa of applied stress, respectively. White atoms represent the initial GB configurations (avg. grain size 8nm, both cases), while red and green atoms represent the extent of coarsening associated with plastic deformation under constant load and temperature conditions. In (b), Ta atoms (blue in color) formulate a random distribution of GB clusters and localized growth is observed (circled in black) due to insufficient Zener pinning in some grains (K. A. Darling et al. 2016a).

5.6 Conclusions

Thus, highly stabilized nanoclusters with strong structural affinity within the matrix and along the GB are the governing mechanisms for the unusual combinations of materials properties, i.e., high strength, extreme thermal stability, and creep resistance. In summary, this report points to a new beginning for innovative fundamental and applied science in designing NC-alloys with a multitude of simultaneously enhanced properties, i.e., creep resistance of single crystals but with the additional benefit of much higher strength. Further, the presented research on NC-Cu-10at.%Ta alloys proves immiscible based systems produced from non-equilibrium processing represent a new archetype from which advanced applications and new fundamental mechanisms can be derived in an area still viewed by many as one of the grand challenges facing researchers.

CHAPTER 6

6 ROLE OF TA ON TWINNABILITY IN NANOCRYSTALLINE CU-TA ALLOYS

6.1 Introduction

Metals with a mean grain size *(d)* below 100 nm, i.e., nanocrystalline (NC) materials, have garnered significant interest due to their superior mechanical properties as compared to coarse-grained materials (Gleiter 2000). A large number of experimental and computational studies have explored how grain boundary mediated plasticity and microstructural size effects, affect the mechanical behavior of NC materials (Meyers, Mishra, and Benson 2006; Dao et al. 2007; Q. Wei et al. 2008). For example, the Hall-Petch (Hall 1954; Petch 1953) relationship describes the experimentally-observed increase in yield strength with decreasing grain size down to diameters as small as 20 nm (Gleiter 2000; Meyers, Mishra, and Benson 2006); this behavior is generally followed by a plateau/negative slope region for grain sizes below a critical size (e.g., 8-15 nm for Cu (Schiøtz, Di Tolla, and Jacobsen 1998)). This inverse Hall-Petch effect has been directly attributed to changes in the governing deformation mechanisms away from traditional dislocation glide and pile-up processes (A. H. Chokshi et al. 1989). Fundamental changes in deformation mechanisms are also known to cause many other intriguing and unexpected physical responses of NC metals, including altered strain rate and pressure dependence of deformation (Hornbuckle et al. 2015), superplasticity (Sherby and Wadsworth 1989), and low temperature creep (M. A. Bhatia, Mathaudhu, and Solanki 2015), to name a few (see (Tschopp et al. 2014)). Generally, these unique deviations in behavior are solely attributed to a continual reduction in grain size and an increase in the fraction of grain boundaries and triple junctions, which leads to experimentally reported mechanisms of deformation twinning, GB rotation/sliding and viscous flow (M. Chen et al. 2003; X. Z. Liao et al. 2004; Zhu, Liao, and Wu 2012). Plastic instability (Kumar, Van Swygenhoven, and Suresh 2003a; Meyers, Mishra, and Benson 2006; Ovid'ko 2007; Dao et al. 2007) due to loss in the strain hardening behavior and grain growth (under both monotonic and cyclic loading) (Gianola et al. 2006; Malow and Koch 1997; Hibbard et al. 2002) have also been observed in various pure NC materials at small grain sizes. The ability to utilize such unique deformation responses advantageously depends heavily on our ability to recognize and to engineer them within NC metals. That is, by restricting or promoting specific deformation mechanisms, it may be possible to elicit or tune unprecedented physical responses in these materials.

Recently, quasistatic and dynamic yield strengths of greater than 1 GPa were measured in bulk samples of a NC Cu–Ta, which could not be explained by grain size strengthening alone (K. A. Darling, Tschopp, Guduru, et al. 2014). The increase in strength was attributed to the thermal decomposition of a non-equilibrium Cu rich Cu-Ta solid solution over a range of temperatures (700–900 °C), which led to the formation of a high density of small coherent Ta-rich atomic clusters (~2 nm in diameter) (K. A. Darling, Tschopp, Guduru, et al. 2014). The presence of these Ta precipitates within grains and along grain boundaries resulted in strength levels approximately two times higher than those predicted by Hall–Petch hardening alone (K. A. Darling et al. 2015b). These studies suggest that the presence of Ta-based clusters play a commanding role in defining the deformation response as compared to the NC grain size alone. However, there is no direct experimental evidence to date of how and why Ta has such a pronounced effect. This work shows for the first time that the mean Ta particle size and distribution, much like grain size, can be used to tailor the governing deformation mechanisms in nanocrystalline immiscible alloys.

In this chapter, the role that Ta particles play in altering the slip and deformation twinning response in previously reported NC Cu-Ta alloys is examined along with the microstructural evolution in alloys with a varying Ta concentration using a combination of generalized stacking fault energy (GSFE) surfaces along with high resolution transmission electron microscopy (TEM) characterization. The GSFE curves are often employed to measure and understand the competition between dislocation slip and twinning, often referred to as the *twinnability* of the material (T. Cai et al. 2014b). Here, large-scale atomic/molecular massively parallel simulator (LAMMPS) (Plimpton 1995) along with a semi-empirical embedded atom potential (EAM) developed by Pun et al. (Pun et al. 2015) was used to compute the GSFE energy curves. This EAM potential was parameterized using an extensive database of energies and configurations from density functional theory (DFT) calculations of energy differences between various crystal structures of pure Cu and pure Ta, the formation energies of coherent Cu-Ta interfaces, and the binding energy of several ordered compounds, such as $L1_2$-Cu_3Ta, $L1_0$-CuTa, $L1_1$-CuTa, B_2-CuTa and $L1_2$-Ta_3Cu (Pun et al. 2015). More details on the validation of the EAM potential at different temperatures can be found in Pun et al. (Pun et al. 2015).

6.2 Methodology

The relaxed GSFE curves (Figure 16a) were computed in LAMMPS using a rectangular slab structure having x, y, and z axes oriented along the $[112]$, $[11\bar{1}]$, and $[\bar{1}10]$ directions, respectively, with a $(11\bar{1})$ plane stacking sequence of

ABCAB|CABC, see Figure 16b. The simulation cell/supercell dimensions were 17.7 nm x 12.5 nm x 1 nm (Figure 16g and 16h). To compute GSFE curves, a 3 nm vacuum was added along the y direction while a periodic boundary condition was maintained along the other two directions. Then the upper half crystal of the $(11\bar{1})$ plane was displaced along the x direction by a partial Burger's distance of $\frac{a}{\sqrt{6}}$ to create a stable stacking fault ($\boldsymbol{\gamma_{ssf}}$) with a stacking sequence of *ABCAB|ABCA*, as shown in Figure 16d. From this point, either a trailing partial of the dissociated dislocation is nucleated or another partial dislocation of leading type on the adjacent plan is nucleated to form a microtwin (Figure 16f). For the emission of a trailing partial, Rice (Rice 1992) showed that the required critical stress is a function of energy difference ($\boldsymbol{\gamma_{usf}}$-$\boldsymbol{\gamma_{ssf}}$) and the stacking sequence can be restored to *ABCAB|CABC* (Figure 16b). In the next step, the displacement was carried out on the adjacent $(11\bar{1})$ plane along the $[112]$ direction to create a microtwin (twin fault, $\boldsymbol{\gamma_{utf}}$) with a stacking sequence of *ABCABA|CAB*, see Figure 16f. During each incremental shear displacement, the structure was relaxed using a conjugate gradient algorithm with force and energy criteria of 10^{-12} meV/Å and 10^{-12} meV, respectively. To quantify the role of Ta on predominant deformation mechanisms (twin versus slip transition), the GSFE curves were computed for the Cu matrix with distinct Ta particle sizes, ranging from 0 to 10 nm in radius. While the Cu-Ta system is known to be a phase separated (immiscible) material (Subramanian and Laughlin 1989), GSFE curves for several non-equilibrium Cu-Ta solid solution (up to 10 at.% Ta) were also computed, because these solid solutions can be expected to experimentally occur and persist over moderate temperature ranges (K. A. Darling, Tschopp, VanLeeuwen, et al. 2014a). In the case of solid solution Cu-Ta, Ta atoms were free to relax in all directions whereas Cu atoms were free to move along the $[11\bar{1}]$ direction only.

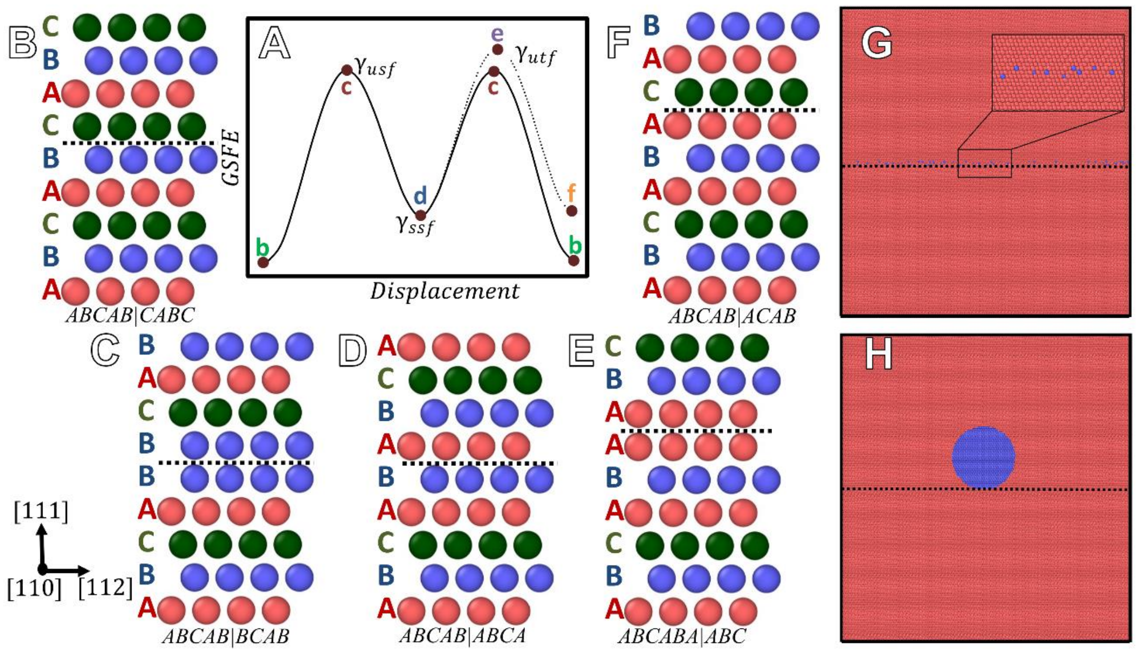

Figure 19: Simulation details. (a) Illustrative model for the generalized stacking fault energy calculation: (b) a perfect crystal with *ABCAB|CABC* stacking; (c) an unstable stacking fault (γ_{usf}) with *ABCAB|BCAB* stacking; (d) a stable stacking fault (γ_{ssf}) with *ABCAB|ABCA* stacking left behind by the leading partial; (e) an unstable twinning fault (γ_{utf}) with *ABCABA|ABC* stacking; (f) 2 layers microtwin with *ABCABA|CAB* stacking; (g) supercell with a random doping of Ta atoms; and (h) supercell with one Ta particle. Note that the red, blue and green atoms are A, B and C stacking, respectively. In (g) and (h) the red and blue atoms correspond to Copper and Tantalum atoms respectively. The dotted line in this figure represents the shear plane. For a twin fault to nucleate, the shear plane has to move by one atomic layer (M. Bhatia et al. 2016).

6.3 Results and Discussion

All GSFE curves with different Ta solute concentrations and Ta particle sizes are presented in Figures 20a & 20b, respectively. The first local maximum corresponds to the unstable stacking fault energy (γ_{usf}), which is correlated to the energy barrier for the leading partial to propagate. In the case of Cu-Ta solid solutions, the γ_{usf} decreases with the addition of Ta solute. In contrast, the value of $\boldsymbol{\gamma_{usf}}$ was found to increase with the addition of Ta particles to the Cu matrix. Overall, in both cases, the stable stacking fault energy and unstable twinning fault energy ($\gamma_{\mathbf{ssf}}$ and $\gamma_{\mathbf{utf}}$, respectively) increase with the addition of Ta. The ratios $\alpha = \boldsymbol{\gamma_{ssf}/\gamma_{usf}}$ and $\beta = \boldsymbol{\gamma_{utf}/\gamma_{usf}}$ can provide insight into the observed changes in all three intrinsic properties ($\gamma_{\mathbf{usf}}$, $\gamma_{\mathbf{ssf}}$, and $\gamma_{\mathbf{utf}}$) for different solute concentrations or particle sizes, as shown in Figure 21a. If the ratio α, which is a ratio of the stable and unstable stacking fault energies, is close to one, then the energy barrier for a trailing partial is very low and the stacking fault width is very small, e.g., Al (α = ~0.97) (Tadmor and Hai 2003). On the other hand and in the case of a pure Cu, the ratio α was found to be 0.24 (Figure 21a, red star), i.e., the energy barrier for a trailing partial is higher and, hence, the stacking fault width or extended partial can be observed across a grain size of 50 nm (Schiøtz and Jacobsen 2003a). However, the ratio α (Figure 21a) increases with the addition of Ta as a solid solution or in particle form, i.e., the stacking fault width decreases with a decrease in the energy barrier for the trailing partial (Figure 20). Further, as the particle size increases, it is expected that the particle interface transitions from coherent to semi-coherent with respect to Cu matrix (JOHN D. Eshelby 1957); this results in the ratio α increasing from 0.24 with no Ta to 0.30 for a Cu matrix with a 2 nm radius particle, see Figure 21a. Similarly, as shown in Figure 21a, a transition from twinning towards slip-dominated mechanisms occurs when the ratio α increases to approximately 0.69 for a 5.4 nm radius particle and 0.57 for the NC Cu–6% Ta solid solution.

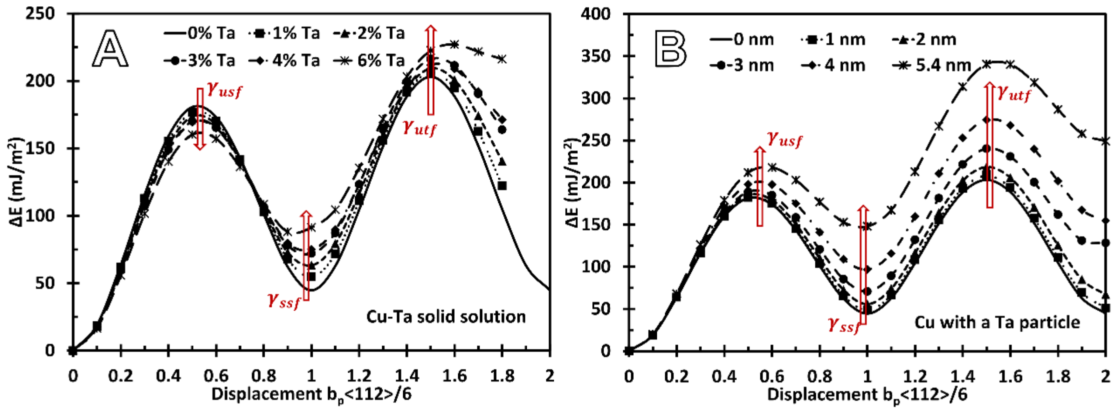

Figure 20: GSFE as a function of shear displacement along the [112] direction for (a) Cu-Ta solid solution alloys and (b) Cu matrix with various size Ta particles (radius). In both cases we observed an increase in γ_{ssf} and γ_{utf} with addition Ta (M. A. Bhatia et al. 2016).

The ratio of the unstable twinning fault energy to the unstable stacking fault energy, $\beta = \gamma_{utf}/\gamma_{usf}$, can also help explain the role of Ta on deformation twinning in NC Cu-Ta alloys. For pure Cu, the ratio β is close to unity (~1.11), i.e., the energy barrier for a twin fault is smaller and hence, nucleating a twin fault is relatively easy. However, as the value of β increases, the energy barrier (Figure 21) as well as the stress required to nucleate twin increases. In the present study, the ratio β increases with both increasing Ta solute concentrations or increasing Ta particle sizes (Figure 21a). For example, Figure 17a shows that the ratio β is 1.11, 1.18, and 1.60 for Cu with no Ta, Cu with 2 nm radius semi-coherent Ta particle, and Cu with 5.4 nm radius Ta particle size, respectively. This suggests that, similar to grain size as discussed in Zhu et al. (Zhu, Liao, and Wu 2012; X. Z. Liao et al. 2004), Ta particles can be used to tailor twinnability, with coherent particles increasing the density of deformation twinning and incoherent particles promoting dislocation-based plasticity. This is also true for the dissolved Ta content in solid solution. This has practical significance as the deformation response and microstructure of these materials will depend heavily on the choice of bulk consolidation processing variables such as composition, temperature, and or pressure/degree of deformation.

TEM observations confirm this hypothesis. Figure 21 shows TEM results which compares the twin and dislocation contents in two different NC Cu-Ta alloys synthesized and consolidated through high energy ball milling and equal channel angular processing. For additional processing details and sample preparation details refer to the supplementary documents. Figures 21b–e show ECAE processed bulk samples for NC Cu–10 at.% Ta (800 °C, Fig. 3b–3c) and NC Cu–1 at.% Ta (700 °C, Fig. 18d–18e), where the lighter areas represent Cu and darker areas represent the Ta phase. These two processing conditions were chosen as the mean grain size and their distributions are comparable (NC Cu–10% Ta has a mean grain size of 118 nm and NC Cu–1% Ta has a mean grain size of 126 nm). As the grain sizes of the alloys are comparable, the effect of Ta concentration on the deformation mechanism can be isolated. While both alloys contain Ta-rich particles, the NC Cu–10 at.% Ta alloy has a higher density of both smaller (diameter < 10 nm) and larger particles (diameter of 50–100 nm) compared to the NC Cu–1 at.% Ta sample (Hornbuckle et al. 2015). Using HRTEM characterization along <110> zone axis, its shown that (Figure 21c), the Ta based particles (outlined using yellow dotted lines) can be seen at the end of a twin (outlined using blue dotted lines) blocking the twin boundary from growing on either end. On the other hand, the twin boundaries (outlined using blue dotted lines) in Figure 18e are not constrained by the Ta based particles. For more details, please refer to Figure 22 which includes FFT images to indicate the nature of the feature (i.e.) twin boundaries. The average twin density per unit area obtained over multiple regions is ~1 x 10^{12} m^{-2} for NC Cu–10 at.% Ta and is ~4 x

10^{12} m^{-2} for the NC Cu–1 at.% Ta sample. These experimental observations are in good agreement with the computational results where the NC Cu–10 at.% Ta alloy is expected to exhibit dislocation-dominated plasticity and the NC Cu–1 at.% Ta alloy is expected to exhibit twin-dominated deformation.

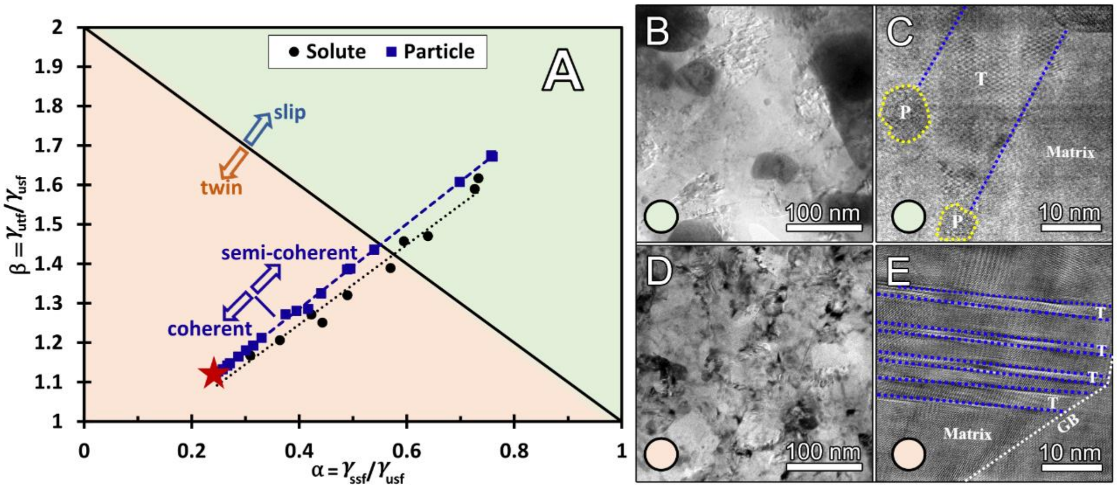

Figure 21: (a) Transition of deformation from slip to deformation twinning with increasing concentration of Ta (circle) and increasing particle size (diamond) in α-β coordinates. Note: Red star is a point with no Ta. Points under the ideal black line can form twins while over the line, twinning is difficult. As the concentration of Ta as well as the Ta particle size increases, there is a transition from twinning to slip. Around a 2 nm radius particle size, there is a transition from a coherent boundary to a semi-coherent boundary for the particle as predicted by Eshelby (JOHN D. Eshelby 1957). TEM/HRTEM micrographs of (b,c) NC Cu–10 at.% Ta (processed at 800 °C) and (d,e) NC Cu–1 at.% Ta (processed at 700 °C). While the deformation in (b,c) is primarily dislocation-mediated (restricted by Ta particles, yellow outline), deformation in (d,e) occurs through twinning. The HRTEM images were taken in <110> zone axis (M. A. Bhatia et al. 2016).

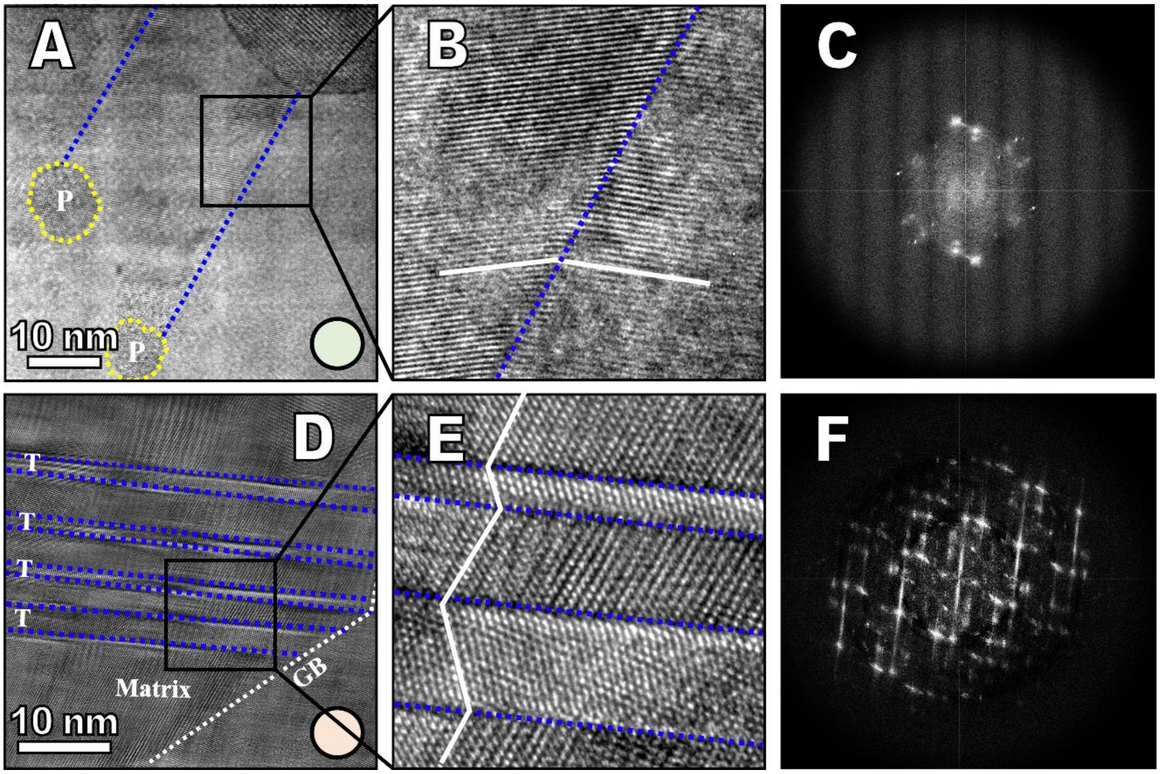

Figure 22: High resolution transmission electron microscopy images (zone axis <110>) and corresponding FFTs from (a-c) Cu-10 at. % Ta processed at 800 °C and (d-f) Cu-1 at.% Ta processed at 700 °C. The twinning process in case of Cu-10 at. % Ta alloy is restricted due to the presence of Ta nano-particles (indicated by yellow dotted lines) whereas in the case of Cu-1 at. % Ta alloy, twinning is favored. The extra spots in the FFT are due to the ion-milling damage (M. A. Bhatia et al. 2016).

Last, the role of Ta on homogeneous and heterogeneous twin nucleation as compared to dislocation nucleation in NC Cu–Ta can be inferred from the ratios α and β computed from GSFE calculations. As described by Cai et al. (T. Cai et al. 2014a), the homogeneous twinning ability (T_{OR}, OR stands for crystal orientation) in NC Cu due to the influence of orientation and GSFE is given by

$$T_{OR} = tan^{-1}\left(\frac{\beta-1}{\alpha-1}\right) + \frac{\pi}{4} \tag{2}$$

Tadmor and Hai (Tadmor and Hai 2003) proposed a simple criterion for inhomogeneous or heterogeneous nucleation of twins from crack tips in the absence of strain rate and temperature. This criterion is expected to be valid because thermal activation does not play an important role in deformation twinning (Christian and Mahajan 1995). Moreover, extending to high rates, materials twin more easily at high strain rates compared to lower strain rates, so this criterion is expected to be the lower bound for predicting twin nucleation (Christian and Mahajan 1995). Hence, twins nucleate at the tips of moving cracks where stresses and strain rates are high (Reid 1981). Therefore, twinnability from an ideal crack tip (T_{CT}) without temperature and strain rate is

$$T_{CT} = [1.136 - 0.151\alpha]/\sqrt{\beta} \qquad (3)$$

Similarly, Asaro and Suresh (Asaro and Suresh 2005) proposed a criterion for heterogeneous twin nucleation (T_{GB}) from a grain boundary, i.e.,

$$T_{GB} = \sqrt{(3 + 2\alpha)/\beta} \qquad (4)$$

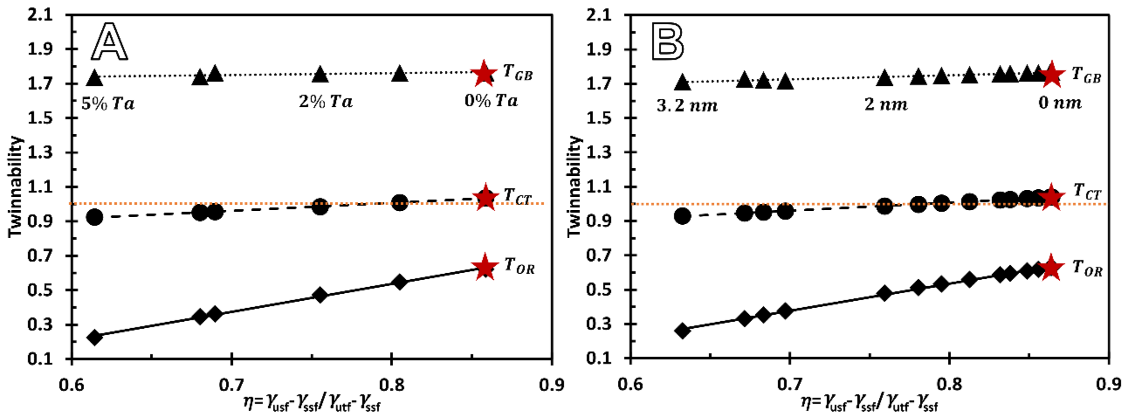

Figure 23: Twinnability as a function of intrinsic twinnability factor η for (a) solid solution of Ta atoms and (b) different sizes of tantalum particle. Red star points indicate pure Cu (no Ta). Diamond points are for homogeneous twins, while circles and triangles are for heterogeneous twins from a crack tip and a grain boundary, respectively. With an increase in the concentration of Ta, there is a decrease in homogeneous twins (M. A. Bhatia et al. 2016).

In all three cases, the condition when T > 1 favors a twin partial emission over the trailing partial. For pure Cu, the twinning criteria values are 1.76, 1.03, and 0.62 for T_{GB}, T_{CT}, and T_{OR}, respectively; these agree well with published literature values of 1.55, 0.95, and 0.58 for T_{GB} (Asaro and Suresh 2005), T_{CT} (Tadmor and Hai 2003) and T_{OR} (T. Cai et al. 2014a), respectively. Hence, heterogeneous deformation twins nucleate from crack tips and grain boundaries. Further, the above three criteria for twinning tendency from different nucleation sites can be understood through an intrinsic twinnability factor η ($\eta = \gamma_{usf} - \gamma_{ssf}/\gamma_{utf} - \gamma_{ssf}$), which only depends on the material's intrinsic properties γ (stacking fault energies, Figure 2). Figure 4 shows the effect of Ta concentration on the twinnability for homogeneous (T_{OR}) twin formation, which is more predominant than for heterogeneous (T_{CT} and T_{GB}) twin formation, i.e., $T_{OR} \propto \beta/\alpha$; whereas T_{CT} & $T_{GB} \propto \alpha/\beta$ (where β>1 and α<1). Hence, as the percentage of Ta increases (right to left on Figure 4), the rate of decrease in twinnability is greater for a homogeneous twins (T_{OR})

compared to heterogeneous twins (T_{CT} and T_{GB}) for both solid solution (Figure 23a) and Ta particle size (Figure 23b). Our result predicts that the formation of trailing partials is favored over that of twinning partials from crack tips ($T_{CT} < 1$) for a given Ta particle size of 1.8 nm in radius ($T_{CT} = 0.94$) and for 3 at.% Ta atoms ($T_{CT} = 0.95$). There is no transition from a twinning partial to trailing partial in case of heterogeneous twin nucleation at the grain boundary.

6.4 Conclusions

In summary, the role of Ta on the transition from twinning to slip dominated deformation mechanisms in Cu-Ta alloys through atomistic simulations and TEM experiments is elucidated. In particular, the computed GSFE curves showed that as Ta content increases, there is a shift from a twin-dominated towards a dislocation-dominated deformation mechanism. Thus, similar to grain size as discussed in Zhu et al. (Zhu, Liao, and Wu 2012; X. Z. Liao et al. 2004), Ta particles can be used to tailor twinnability, with coherent particles increasing the density of deformation twinning and incoherent particles promoting dislocation-based plasticity. Furthermore, heterogeneous twinnability from microstructural defects such as grain boundaries decreases with an increase in Ta content. The observed effect of Ta on plasticity is consistent with the TEM observations.

CHAPTER 7

7 SUMMARY AND FUTURE WORK

Nanocrystalline materials are good contenders for engineering applications however the plastic and thermal instability renders it impractical for these applications. In this dissertation, we have systematically analyzed the deformation and mechanical response at extreme conditions of one such stable alloy system, NC-Cu-Ta which shows promise. This understanding will aid in the design and development of a class of super-strong nanocrystalline alloys with a multitude of optimized properties at elevated temperatures. The several insights gathered from this dissertation include:

(i) NC-Cu-Ta alloys exhibit tremendous thermal stability even at elevated temperatures where the Ta nanoclusters pin the grain boundaries through Zener pinning mechanism which was verified by in-situ heating experiments and atomistic simulations.

(ii) The quasistatic and high strain rate behavior of these alloys at elevated temperatures in compression supersedes the behavior exhibited by conventional nanocrystalline materials where GB dominated mechanisms lead to instability at temperatures as low as 0.4 T_m.

(iii) The long term deformation behavior (creep) is also exceptional for these alloys and the creep resistance offered by the NC-Cu-10at.%Ta at 600 °C (0.64 Tm) is 6-8 orders of magnitude higher than the conventional NC alloys reported for 1.5–2 times higher temperature and an order of magnitude higher stress.

(iv) The role of Ta on deformation mechanisms in Cu-Ta alloys was probed through atomistic simulations and TEM experiments. Atomistic and TEM characterizations reveal that Ta particles can be used to tailor twinnability, with coherent particles increasing the density of deformation twinning and incoherent particles promoting dislocation-based plasticity. Furthermore, heterogeneous twinnability from microstructural defects such as grain boundaries decreases with an increase in Ta content.

While there has been a pursuit to develop alloys that are strong, there is the inherent obstacle to develop alloys which are ductile as well due to the strength-ductility tradeoff. Nanocrystalline materials are excellent in terms of their mechanical strength, however their ability to deform through dislocation motion is restricted due to which achieving NC alloys with considerable ductility remains challenging. As seen from the previous sections, NC-Cu-Ta alloy system offers potential from the strength and stability at elevated conditions. By tailoring the microstructure of this alloy system, an optimum strength-ductility combination can also be achieved despite what will remain greater than all known NC materials.

From the previous chapters, we saw that Ta concentration and processing plays a critical role in determining the mode of deformation in the alloys. To identify an optimum strength-ductility alloy a set of NC-Cu-Ta alloys with varying Ta concentrations were processed and subjected to mechanical testing and strength-ductility response was evaluated. Fig. 24, a typical strength-ductility map of NC-Cu-Ta alloys with varying Ta concentrations and data from literature for the known Cu alloys. The yield strength of NC-Cu-10at.%Ta processed at 700 °C and tested at RT is about 1 GPa, and the ductility is negligible. When consolidation temperature (ECAE) changes from 700 to 900 ºC the yield strength changes from to 1040 MPa to 680 MPa, while the ductility increases from 1% to 6%. Thus by controlling the processing parameters and solute concentration, it is possible to achieve a composition with nanocrystalline grains which shows sufficient strength and ductility (projected Cu-Ta).

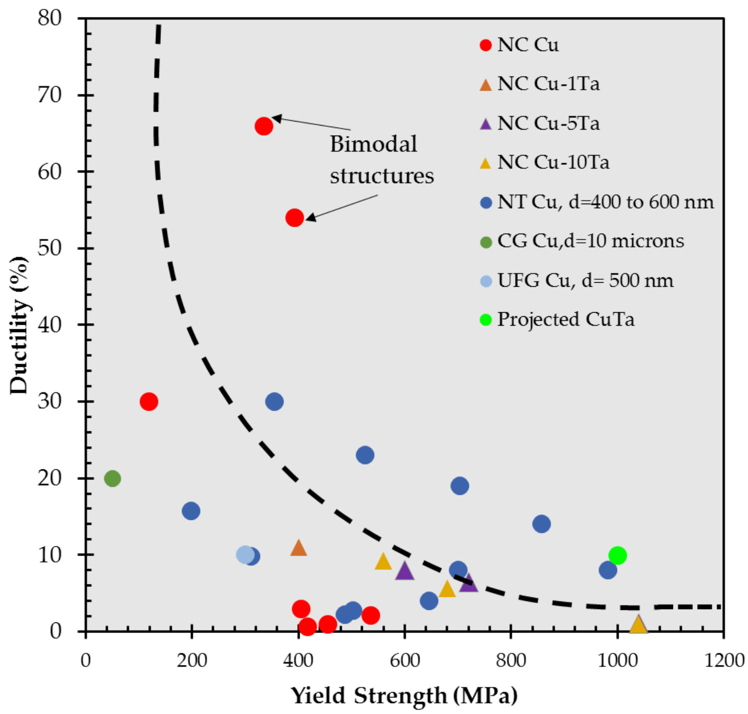

Figure 24: Plot of strength versus ductility for NC Cu and alloys. NC-Cu-Ta offers promise in comparison to pure NC Cu and through tailoring the microstructure via processing, an alloy with the optimal Ta concentration which has sufficient strength and ductility can be deduced. NC Cu data taken from (Sanders, Eastman, and Weertman 1997; M. Legros et al. 2000; Y. Wang et al. 2002; Lu et al. 2000; Y. M. Wang et al. 2003), NT Cu and UFG Cu from (Lu et al. 2009; Dao et al. 2006),and CG Cu from (Lu et al. 2009). NC Cu-Ta data is from the current study.

The strengthening can be attributed to the high density of Ta nanoclusters, the change in the grain size and Ta concentration influences the degree of strengthening (Chapters 3 to 5). Grains with a considerable size within the NC/UFG regime can help in maintaining the strength whilst allowing ductility. In addition, there will be sufficient dislocation storage inside the grains owing it to their sizes. Due to their inherent microstructural stability by Zener pinning, plastic and thermal instability is non-existent in these high-strength materials, thereby unleashing the potential to accommodate uniform elongation through the material. The future goal is to effectively tune the microstructure by varying the Ta concentration and processing temperature to achieve nominal strength-ductility combinations in Cu-Ta alloy system. Furthermore this methodology can be adapted and used for other material systems as well. Several techniques exist for improving strength and ductility in materials (Y. Wang et al. 2002). In this case, the processing technique, namely equal channel angular extrusion (ECAE) produces nanostructured materials with a sufficient amount of stored dislocation content. Also from the previous chapter, it is known that presence of Ta inhibits the formation of twins in these alloys, with the propensity decreasing with the increase of Ta concentration from 1 at.% to 10 at. %. Further, twinning indicates that the microstructure deforms at a higher stress which can lead to the observed high strength. These interfaces also can act as a strong barrier to the dislocation motion. So, a material system with a Ta concentration of about 5 at.% or lower will have the capability to retain nanocrystalline microstructure at extreme conditions, exhibit high strength and show moderate ductility which will greater than all observed NC material systems. Furthermore, the results from this systematic studies highlighted in the previous chapters which probes the microstructural evolution and mechanical behavior of these stabilized alloys will aid in developing a strength optimized alloy which shows exceptional response under extreme conditions.

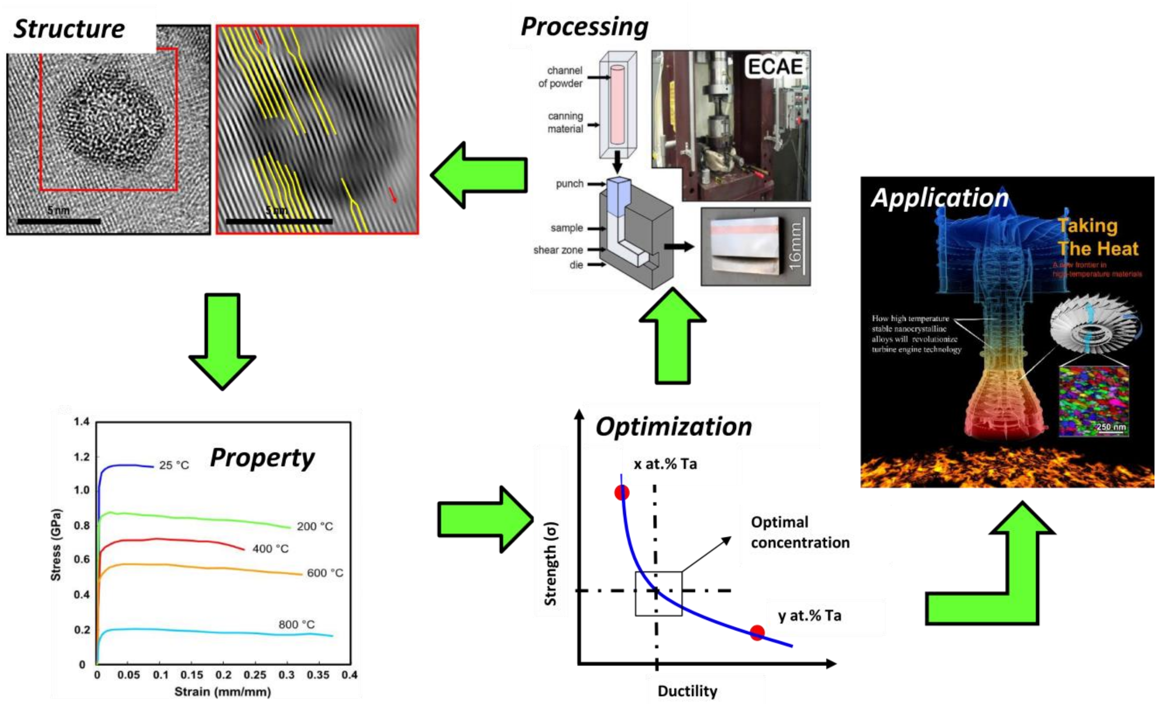

Figure 25: Schematic for developing strong microstructurally stable nanocrystalline materials which have a potential to replace current generation high-temperature components. Compression data from (K. A. Darling et al. 2015a), structure micrographs from (K. A. Darling et al. 2016a),and processing schematic from (Tschopp et al. 2014).

The ultimate goal is to develop stronger NC materials with a multitude of simultaneous properties such as high strength, ductility, creep and fatigue resistance which shows promise for high temperature applications such as turbines. These alloys will in turn improve the efficiency and life thereby reducing the carbon footprint. This methodology is not exclusive to Cu-Ta system and can be extended to develop material systems which have an exotic microstructure comprising of nanoclusters which determine strength and stability.

REFERENCES

Akbarpour, MR, and HS Kim. 2015. “Microstructure, Grain Growth, and Hardness during Annealing of Nanocrystalline Cu Powders Synthesized via High Energy Mechanical Milling.” *Materials & Design* 83: 644–650.

Alavudeen, A., N. Venkateshwaran, and J. T. Winowlin Jappes. 2006. *A Textbook of Engineering Materials and Metallurgy*. Firewall Media.

Ames, Markus, Jürgen Markmann, Rudolf Karos, Andreas Michels, Andreas Tschöpe, and Rainer Birringer. 2008. “Unraveling the Nature of Room Temperature Grain Growth in Nanocrystalline Materials.” *Acta Materialia* 56 (16): 4255–66. doi:10.1016/j.actamat.2008.04.051.

Asaro, Robert J., and Subra Suresh. 2005. “Mechanistic Models for the Activation Volume and Rate Sensitivity in Metals with Nanocrystalline Grains and Nano-Scale Twins.” *Acta Materialia* 53 (12): 3369–3382.

Ashby, M. F. 1972. “A First Report on Deformation-Mechanism Maps.” *Acta Metallurgica* 20 (7): 887–97. doi:10.1016/0001-6160(72)90082-X.

Ashby, M. F., R. Bullough, and C. S. Hartley. 2013. *Dislocation Modelling of Physical Systems: Proceedings of the International Conference, Gainesville, Florida, USA, June 22-27, 1980*. Elsevier.

Atwater, Mark A., Ronald O. Scattergood, and Carl C. Koch. 2013. “The Stabilization of Nanocrystalline Copper by Zirconium.” *Materials Science and Engineering: A* 559 (January): 250–56. doi:10.1016/j.msea.2012.08.092.

Atwater, Mark, and Kris Darling. 2012. “A Visual Library of Stability in Binary Metallic Systems: The Stabilization of Nanocrystalline Grain Size by Solute Addition: Part 1.” Final ARL-TR-6007. Aberdeen Proving Ground, MD: Army Research Laboratory.

Ball, A, and R. E Smallman. 1966. “The Operative Slip System and General Plasticity of NiAl-II.” *Acta Metallurgica* 14 (11): 1517–26. doi:10.1016/0001-6160(66)90173-8.

Bate, P. 2001. “The Effect of Deformation on Grain Growth in Zener Pinned Systems.” *Acta Materialia* 49 (8): 1453–61. doi:10.1016/S1359-6454(01)00033-7.

Bhatia, M. A., S. N. Mathaudhu, and K. N. Solanki. 2015. “Atomic-Scale Investigation of Creep Behavior in Nanocrystalline Mg and Mg–Y Alloys.” *Acta Materialia* 99 (October): 382–91. doi:10.1016/j.actamat.2015.07.068.

Bhatia, M. A., M. Rajagopalan, K. A. Darling, M. A. Tschopp, and K. N. Solanki. 2016. "The Role of Ta on Twinnability in Nanocrystalline Cu–Ta Alloys." *Materials Research Letters* 0 (0): 1–7. doi:10.1080/21663831.2016.1201160.

Bhatia, MA, M Rajagopalan, KA Darling, MA Tschopp, and KN Solanki. 2016. "The Role of Ta on Twinnability in Nanocrystalline Cu–Ta Alloys." *Materials Research Letters*, 1–7.

Boyce, Brad L., and Henry A. Padilla Ii. 2011. "Anomalous Fatigue Behavior and Fatigue-Induced Grain Growth in Nanocrystalline Nickel Alloys." *Metallurgical and Materials Transactions A* 42 (7): 1793–1804. doi:10.1007/s11661-011-0708-x.

Cahn, John W., Yuri Mishin, and Akira Suzuki. 2006. "Coupling Grain Boundary Motion to Shear Deformation." *Acta Materialia* 54 (19): 4953–75. doi:10.1016/j.actamat.2006.08.004.

Cahn, John W., and Jean E. Taylor. 2004. "A Unified Approach to Motion of Grain Boundaries, Relative Tangential Translation along Grain Boundaries, and Grain Rotation." *Acta Materialia* 52 (16): 4887–98. doi:10.1016/j.actamat.2004.02.048.

Cai, B., Q. P. Kong, L. Lu, and K. Lu. 1999. "Interface Controlled Diffusional Creep of Nanocrystalline Pure Copper." *Scripta Materialia* 41 (7): 755–59. doi:10.1016/S1359-6462(99)00213-4.

Cai, T., Z. J. Zhang, P. Zhang, J. B. Yang, and Z. F. Zhang. 2014a. "Competition between Slip and Twinning in Face-Centered Cubic Metals." *Journal of Applied Physics* 116 (16): 163512.

———. 2014b. "Competition between Slip and Twinning in Face-Centered Cubic Metals." *Journal of Applied Physics* 116 (16): 163512. doi:10.1063/1.4898319.

Chellali, M. R., Z. Balogh, L. Zheng, and G. Schmitz. 2011. "Triple Junction and Grain Boundary Diffusion in the Ni/Cu System." *Scripta Materialia* 65 (4): 343–46. doi:10.1016/j.scriptamat.2011.05.002.

Chen, M., E. Ma, K. J. Hemker, H. Sheng, Y. Wang, and X. Cheng. 2003. "Deformation Twinning in Nanocrystalline Aluminum." *Science* 300 (5623): 1275–77.

Chen, Z., F. Liu, H. F. Wang, W. Yang, G. C. Yang, and Y. H. Zhou. 2009. "A Thermokinetic Description for Grain Growth in Nanocrystalline Materials." *Acta Materialia* 57 (5): 1466–75. doi:10.1016/j.actamat.2008.11.025.

Chen, Z., F. Liu, X. Q. Yang, and C. J. Shen. 2012. "A Thermokinetic Description of Nanoscale Grain Growth: Analysis of the Activation Energy Effect." *Acta Materialia* 60 (12): 4833–44. doi:10.1016/j.actamat.2012.05.029.

Chen, Zheng, Feng Liu, Wei Yang, Haifeng Wang, Gencang Yang, and Yaohe Zhou. 2009. "Influence of Grain Boundary Energy on the Grain Size Evolution in Nanocrystalline Materials." *Journal of Alloys and Compounds* 475 (1–2): 893–97. doi:10.1016/j.jallcom.2008.08.040.

Cheng, S., J. Xie, A. D. Stoica, X. -L. Wang, J. A. Horton, D. W. Brown, H. Choo, and P. K. Liaw. 2009. "Cyclic Deformation of Nanocrystalline and Ultrafine-Grained Nickel." *Acta Materialia* 57 (4): 1272–80. doi:10.1016/j.actamat.2008.11.011.

Choi, In-Chul, Yong-Jae Kim, Moo-Young Seok, Byung-Gil Yoo, Ju-Young Kim, Yinmin Wang, and Jae-il Jang. 2013. "Nanoscale Room Temperature Creep of Nanocrystalline Nickel Pillars at Low Stresses." *International Journal of Plasticity* 41: 53–64.

Chokshi, A. H., A. Rosen, J. Karch, and H. Gleiter. 1989. "On the Validity of the Hall-Petch Relationship in Nanocrystalline Materials." *Scripta Metallurgica* 23 (10): 1679–83. doi:10.1016/0036-9748(89)90342-6.

Chokshi, Atul H. 2009. "Unusual Stress and Grain Size Dependence for Creep in Nanocrystalline Materials." *Scripta Materialia* 61 (1): 96–99. doi:10.1016/j.scriptamat.2009.03.009.

Chookajorn, Tongjai, Heather A. Murdoch, and Christopher A. Schuh. 2012. "Design of Stable Nanocrystalline Alloys." *Science* 337 (6097): 951–54. doi:10.1126/science.1224737.

Christian, J.W., and S. Mahajan. 1995. "Deformation Twinning." *Progress in Materials Science* 39 (1–2): 1–157. doi:10.1016/0079-6425(94)00007-7.

Coble, RL. 1963. "A Model for Boundary Diffusion Controlled Creep in Polycrystalline Materials." *Journal of Applied Physics* 34 (6): 1679–1682.

Connolley, T., P. E. Mchugh, and M. Bruzzi. 2005. "A Review of Deformation and Fatigue of Metals at Small Size Scales." *Fatigue & Fracture of Engineering Materials & Structures* 28 (12): 1119–52. doi:10.1111/j.1460-2695.2005.00951.x.

Cserháti, Cs, I. A. Szabó, and D. L. Beke. 1998. "Size Effects in Surface Segregation." *Journal of Applied Physics* 83 (6): 3021–27. doi:10.1063/1.367125.

Dake, Jules M., and Carl E. Krill III. 2012. "Sudden Loss of Thermal Stability in Fe-Based Nanocrystalline Alloys." *Scripta Materialia* 66 (6): 390–93. doi:10.1016/j.scriptamat.2011.11.040.

Dao, M., L. Lu, R. J. Asaro, J. T. M. De Hosson, and E. Ma. 2007. "Toward a Quantitative Understanding of Mechanical Behavior of Nanocrystalline Metals." *Acta Materialia* 55 (12): 4041–65. doi:10.1016/j.actamat.2007.01.038.

Dao, M., L. Lu, Y. F. Shen, and S. Suresh. 2006. “Strength, Strain-Rate Sensitivity and Ductility of Copper with Nanoscale Twins.” *Acta Materialia* 54 (20): 5421–32. doi:10.1016/j.actamat.2006.06.062.

Darling, K. A., E. L. Huskins, B. E. Schuster, Q. Wei, and L. J. Kecskes. 2015a. “Mechanical Properties of a High Strength Cu–Ta Composite at Elevated Temperature.” *Materials Science and Engineering: A* 638 (June): 322–28. doi:10.1016/j.msea.2015.04.069.

———. 2015b. “Mechanical Properties of a High Strength Cu–Ta Composite at Elevated Temperature.” *Materials Science and Engineering: A* 638 (June): 322–28. doi:10.1016/j.msea.2015.04.069.

Darling, K. A., M. Rajagopalan, M. Komarasamy, M. A. Bhatia, B. C. Hornbuckle, R. S. Mishra, and K. N. Solanki. 2016a. “Extreme Creep Resistance in a Microstructurally Stable Nanocrystalline Alloy.” *Nature* 537 (7620): 378–81. doi:10.1038/nature19313.

Darling, K. A., M. Rajagopalan, M. Komarasamy, M. A. Bhatia, B. C. Hornbuckle, R. Mishra, and K. N. Solanki. 2016b. “Extreme Creep Resistance in a Microstructurally Stable Nanocrystalline Alloy.” doi:10.1038/nature19313.

Darling, K. A., A. J. Roberts, Y. Mishin, S. N. Mathaudhu, and L. J. Kecskes. 2013. “Grain Size Stabilization of Nanocrystalline Copper at High Temperatures by Alloying with Tantalum.” *Journal of Alloys and Compounds* 573 (October): 142–50. doi:10.1016/j.jallcom.2013.03.177.

Darling, K. A., M. A. Tschopp, R. K. Guduru, W. H. Yin, Q. Wei, and L. J. Kecskes. 2014. “Microstructure and Mechanical Properties of Bulk Nanostructured Cu–Ta Alloys Consolidated by Equal Channel Angular Extrusion.” *Acta Materialia* 76 (September): 168–85. doi:10.1016/j.actamat.2014.04.074.

Darling, K. A., M. A. Tschopp, B. K. VanLeeuwen, M. A. Atwater, and Z. K. Liu. 2014a. “Mitigating Grain Growth in Binary Nanocrystalline Alloys through Solute Selection Based on Thermodynamic Stability Maps.” *Computational Materials Science* 84 (March): 255–66. doi:10.1016/j.commatsci.2013.10.018.

———. 2014b. “Mitigating Grain Growth in Binary Nanocrystalline Alloys through Solute Selection Based on Thermodynamic Stability Maps.” *Computational Materials Science* 84 (March): 255–66. doi:10.1016/j.commatsci.2013.10.018.

Darling, K. A., B. K. VanLeeuwen, C. C. Koch, and R. O. Scattergood. 2010. “Thermal Stability of Nanocrystalline Fe–Zr Alloys.” *Materials Science and Engineering: A* 527 (15): 3572–80. doi:10.1016/j.msea.2010.02.043.

Darling, Kris A., Suveen Mathaudhu, and Laszlo Kecskes. 2012. “Demonstration of Ultra High-Strength Nanocrystalline Copper Alloys for Military Applications.”

Detor, A.J., and C.A. Schuh. 2007. “Microstructural Evolution during the Heat Treatment of Nanocrystalline Alloys.” *Journal of Materials Research* 22 (11): 3233–48. doi:10.1557/jmr.2007.0403.

Detor, Andrew J, and Christopher A Schuh. 2007. “Grain Boundary Segregation, Chemical Ordering and Stability of Nanocrystalline Alloys: Atomistic Computer Simulations in the Ni–W System.” *Acta Materialia* 55 (12): 4221–4232.

Duhamel, Cécilie, Yves Brechet, and Yannick Champion. 2010. “Activation Volume and Deviation from Cottrell–Stokes Law at Small Grain Size.” *International Journal of Plasticity* 26 (5): 747–57. doi:10.1016/j.ijplas.2009.10.003.

Eshelby, J. D. 1957. “The Determination of the Elastic Field of an Ellipsoidal Inclusion, and Related Problems.” *Proceedings of the Royal Society of London A: Mathematical, Physical and Engineering Sciences* 241 (1226): 376–96. doi:10.1098/rspa.1957.0133.

Eshelby, JOHN D. 1957. “The Determination of the Elastic Field of an Ellipsoidal Inclusion, and Related Problems.” In *Proceedings of the Royal Society of London A: Mathematical, Physical and Engineering Sciences*, 241:376–396. The Royal Society. http://rspa.royalsocietypublishing.org/content/royprsa/241/1226/376.full.pdf.

Fan, G. J., Y. D. Wang, L. F. Fu, H. Choo, P. K. Liaw, Y. Ren, and N. D. Browning. 2006. “Orientation-Dependent Grain Growth in a Bulk Nanocrystalline Alloy during the Uniaxial Compressive Deformation.” *Applied Physics Letters* 88 (17): 171914. doi:10.1063/1.2200589.

Färber, B., E. Cadel, A. Menand, G. Schmitz, and R. Kirchheim. 2000. “Phosphorus Segregation in Nanocrystalline Ni–3.6 At.% P Alloy Investigated with the Tomographic Atom Probe (TAP).” *Acta Materialia* 48 (3): 789–96. doi:10.1016/S1359-6454(99)00397-3.

Farrokh, Babak, and Akhtar S Khan. 2009a. “Grain Size, Strain Rate, and Temperature Dependence of Flow Stress in Ultra-Fine Grained and Nanocrystalline Cu and Al: Synthesis, Experiment, and Constitutive Modeling.” *International Journal of Plasticity* 25 (5): 715–732.

Farrokh, Babak, and Akhtar S. Khan. 2009b. “Grain Size, Strain Rate, and Temperature Dependence of Flow Stress in Ultra-Fine Grained and Nanocrystalline Cu and Al: Synthesis, Experiment, and Constitutive Modeling.” *International Journal of Plasticity* 25 (5): 715–32. doi:10.1016/j.ijplas.2008.08.001.

Frolov, T., K. A. Darling, L. J. Kecskes, and Y. Mishin. 2012. “Stabilization and Strengthening of Nanocrystalline Copper by Alloying with Tantalum.” *Acta Materialia* 60 (5): 2158–68. doi:10.1016/j.actamat.2012.01.011.

Gama, Bazle A, Sergey L Lopatnikov, and Jr Gillespie John W. 2004. “Hopkinson Bar Experimental Technique: A Critical Review.” *Applied Mechanics Reviews* 57 (4): 223–50. doi:10.1115/1.1704626.

Giamei, Anthony F. 2013. “Development of Single Crystal Superalloys: A Brief History.” *Advanced Materials and Processes* 171 (9): 26–30.

Gianola, D. S., S. Van Petegem, M. Legros, S. Brandstetter, H. Van Swygenhoven, and K. J. Hemker. 2006. “Stress-Assisted Discontinuous Grain Growth and Its Effect on the Deformation Behavior of Nanocrystalline Aluminum Thin Films.” *Acta Materialia* 54 (8): 2253–63. doi:10.1016/j.actamat.2006.01.023.

Gleiter, H. 2000. “Nanostructured Materials: Basic Concepts and Microstructure.” *Acta Materialia* 48 (1): 1–29. doi:10.1016/S1359-6454(99)00285-2.

Gong, M.M., F. Liu, and K. Zhang. 2011. “Thermodynamic Stability of Binary Nanocrystalline Alloys: Analysis of Solute and Excess Vacancy.” *Applied Physics A: Materials Science and Processing* 105 (4): 927–34. doi:10.1007/s00339-011-6501-2.

Gutkin, M. Yu., and I. A. Ovid’ko †. 2004. “Nanocracks at Grain Boundaries in Nanocrystalline Materials.” *Philosophical Magazine Letters* 84 (10): 655–63. doi:10.1080/09500830512331329123.

Hall, E. O. 1954. “Variation of Hardness of Metals with Grain Size.” *Nature* 173 (4411): 948–49. doi:10.1038/173948b0.

Hasnaoui, A, H Van Swygenhoven, and P. M Derlet. 2002. “On Non-Equilibrium Grain Boundaries and Their Effect on Thermal and Mechanical Behaviour: A Molecular Dynamics Computer Simulation.” *Acta Materialia* 50 (15): 3927–39. doi:10.1016/S1359-6454(02)00195-7.

Hibbard, G. D, J. L McCrea, G Palumbo, K. T Aust, and U Erb. 2002. “An Initial Analysis of Mechanisms Leading to Late Stage Abnormal Grain Growth in Nanocrystalline Ni.” *Scripta Materialia* 47 (2): 83–87. doi:10.1016/S1359-6462(02)00098-2.

Hirata, A., T. Fujita, Y. R. Wen, J. H. Schneibel, C. T. Liu, and M. W. Chen. 2011. “Atomic Structure of Nanoclusters in Oxide-Dispersion-Strengthened Steels.” *Nature Materials* 10 (12): 922–26. doi:10.1038/nmat3150.

Hirth, John Price, and Jens Lothe. 1982. *Theory of Dislocations*. Krieger Publishing Company.

Hornbuckle, B. C., T. Rojhirunsakool, M. Rajagopalan, T. Alam, G. P. Purja Pun, R. Banerjee, K. N. Solanki, Y. Mishin, L. J. Kecskes, and K. A. Darling. 2015. “Effect of Ta Solute Concentration on the Microstructural Evolution in

Immiscible Cu-Ta Alloys." *JOM* 67 (12): 2802–9. doi:10.1007/s11837-015-1643-x.

Howe, James M. 1997. *Interfaces in Materials: Atomic Structure, Thermodynamics and Kinetics of Solid-Vapor, Solid-Liquid and Solid-Solid Interfaces*. Wiley-Interscience.

Huang, YK, AA Menovsky, and FR De Boer. 1993. "Calorimetric Analysis of the Grain Growth in Nanocrystalline Copper Samples." *Nanostructured Materials* 2 (6): 587–595.

Hugo, R. C., H. Kung, J. R. Weertman, R. Mitra, J. A. Knapp, and D. M. Follstaedt. 2003. "In-Situ TEM Tensile Testing of DC Magnetron Sputtered and Pulsed Laser Deposited Ni Thin Films." *Acta Materialia* 51 (7): 1937–43. doi:10.1016/S1359-6454(02)00599-2.

Humphreys, F. J., and M. Hatherly. 2004. "Chapter 9 - Recrystallization of Two-Phase Alloys." In *Recrystallization and Related Annealing Phenomena (Second Edition)*, edited by F. J. HumphreysM. Hatherly, 285–319. Oxford: Elsevier. http://www.sciencedirect.com/science/article/pii/B978008044164150013X.

Ii, H. A. Padilla, and B. L. Boyce. 2010. "A Review of Fatigue Behavior in Nanocrystalline Metals." *Experimental Mechanics* 50 (1): 5–23. doi:10.1007/s11340-009-9301-2.

Jin, M., A. M. Minor, E. A. Stach, and J. W. Morris Jr. 2004. "Direct Observation of Deformation-Induced Grain Growth during the Nanoindentation of Ultrafine-Grained Al at Room Temperature." *Acta Materialia* 52 (18): 5381–87. doi:10.1016/j.actamat.2004.07.044.

Kato, Masaharu. 2009. "Thermally Activated Dislocation Depinning at a Grain Boundary in Nanocrystalline and Ultrafine-Grained Materials." *Materials Science and Engineering: A* 516 (1–2): 276–82. doi:10.1016/j.msea.2009.03.035.

Kirchheim, Reiner. 2002. "Grain Coarsening Inhibited by Solute Segregation." *Acta Materialia* 50 (2): 413–19. doi:10.1016/S1359-6454(01)00338-X.

Koch, Carl C. 2007. "Structural Nanocrystalline Materials: An Overview." *Journal of Materials Science* 42 (5): 1403–1414.

Koch, Carl C., Ronald O. Scattergood, Mostafa Saber, and Hasan Kotan. 2013. "High Temperature Stabilization of Nanocrystalline Grain Size: Thermodynamic versus Kinetic Strategies." *Journal of Materials Research* 28 (13): 1785–91. doi:10.1557/jmr.2012.429.

Koch, C.C., R.O. Scattergood, K.A. Darling, and J.E. Semones. 2008. "Stabilization of Nanocrystalline Grain Sizes by Solute Additions." *Journal of Materials Science* 43 (23–24): 7264–72. doi:10.1007/s10853-008-2870-0.

Koju, R. K., K. A. Darling, L. J. Kecskes, and Y. Mishin. 2016. "Zener Pinning of Grain Boundaries and Structural Stability of Immiscible Alloys." *JOM*, April, 1–9. doi:10.1007/s11837-016-1899-9.

Kumar, K. S., S. Suresh, M. F. Chisholm, J. A. Horton, and P. Wang. 2003. "Deformation of Electrodeposited Nanocrystalline Nickel." *Acta Materialia* 51 (2): 387–405. doi:10.1016/S1359-6454(02)00421-4.

Kumar, K. S, H Van Swygenhoven, and S Suresh. 2003a. "Mechanical Behavior of Nanocrystalline Metals and Alloys." *Acta Materialia*, The Golden Jubilee Issue. Selected topics in Materials Science and Engineering: Past, Present and Future, 51 (19): 5743–74. doi:10.1016/j.actamat.2003.08.032.

———. 2003b. "Mechanical Behavior of Nanocrystalline Metals and Alloys." *Acta Materialia*, The Golden Jubilee Issue. Selected topics in Materials Science and Engineering: Past, Present and Future, 51 (19): 5743–74. doi:10.1016/j.actamat.2003.08.032.

Lee, Woei-Shyan, and Chi-Feng Lin. 1998. "Plastic Deformation and Fracture Behaviour of Ti–6Al–4V Alloy Loaded with High Strain Rate under Various Temperatures." *Materials Science and Engineering: A* 241 (1–2): 48–59. doi:10.1016/S0921-5093(97)00471-1.

Legros, M., B. R. Elliott, M. N. Rittner, J. R. Weertman, and K. J. Hemker. 2000. "Microsample Tensile Testing of Nanocrystalline Metals." *Philosophical Magazine A* 80 (4): 1017–26. doi:10.1080/01418610008212096.

Legros, Marc, Daniel S. Gianola, and Kevin J. Hemker. 2008. "In Situ TEM Observations of Fast Grain-Boundary Motion in Stressed Nanocrystalline Aluminum Films." *Acta Materialia* 56 (14): 3380–93. doi:10.1016/j.actamat.2008.03.032.

Lennon, A. M., and K. T. Ramesh. 2000. "The Thermoviscoplastic Response of Polycrystalline Tungsten in Compression." *Materials Science and Engineering: A* 276 (1–2): 9–21. doi:10.1016/S0921-5093(99)00517-1.

Li, B. Q., M. L. Sui, B. Li, E. Ma, and S. X. Mao. 2009. "Reversible Twinning in Pure Aluminum." *Physical Review Letters* 102 (20): 205504.

Li, Jianguo, Tao Suo, Chongxiang Huang, Yulong Li, Hongtao Wang, and Jiabin Liu. 2016. "Adiabatic Shear Localization in Nanostructured Face Centered Cubic Metals under Uniaxial Compression." *Materials & Design* 105: 262–267.

Liao, X. Z., Y. H. Zhao, S.G. Srinivasan, Y.T. Zhu, R. Z. Valiev, and D.V. Gunderov. 2004. “Deformation Twinning in Nanocrystalline Copper at Room Temperature and Low Strain Rate.” *Applied Physics Letters* 84 (4): 592–94. doi:10.1063/1.1644051.

Liao, XZ, F. Zhou, EJ Lavernia, SG Srinivasan, MI Baskes, DW He, and YT Zhu. 2003. “Deformation Mechanism in Nanocrystalline Al: Partial Dislocation Slip.” *Applied Physics Letters* 83: 632.

Liu, Feng, and Reiner Kirchheim. 2004. “Grain Boundary Saturation and Grain Growth.” *Scripta Materialia* 51 (6): 521–25. doi:10.1016/j.scriptamat.2004.05.042.

Liu, G., G. J. Zhang, F. Jiang, X. D. Ding, Y. J. Sun, J. Sun, and E. Ma. 2013. “Nanostructured High-Strength Molybdenum Alloys with Unprecedented Tensile Ductility.” *Nature Materials* 12 (4): 344–50. doi:10.1038/nmat3544.

Liu, K. W., and F. Mücklich. 2001. “Thermal Stability of Nano-RuAl Produced by Mechanical Alloying.” *Acta Materialia* 49 (3): 395–403. doi:10.1016/S1359-6454(00)00340-2.

Lu, L., X. Chen, X. Huang, and K. Lu. 2009. “Revealing the Maximum Strength in Nanotwinned Copper.” *Science* 323 (5914): 607–10. doi:10.1126/science.1167641.

Lu, L., L. B. Wang, B. Z. Ding, and K. Lu. 2000. “High-Tensile Ductility in Nanocrystalline Copper.” *Journal of Materials Research* 15 (2): 270–73. doi:10.1557/JMR.2000.0043.

Ma, E. 2004. “Recent Progress in Improving Ductility of Ultra-High Strength Nanostructured Metals.” *Metals and Materials International* 10 (6): 527–31. doi:10.1007/BF03027414.

Malow, T. R, and C. C Koch. 1997. “Grain Growth in Nanocrystalline Iron Prepared by Mechanical Attrition.” *Acta Materialia* 45 (5): 2177–86. doi:10.1016/S1359-6454(96)00300-X.

Manohar, PA, M Ferry, and T Chandra. 1998. “Five Decades of the Zener Equation.” *ISIJ International* 38 (9): 913–924.

Meyers, M. A., A. Mishra, and D. J. Benson. 2006. “Mechanical Properties of Nanocrystalline Materials.” *Progress in Materials Science* 51 (4): 427–556. doi:10.1016/j.pmatsci.2005.08.003.

Millett, Paul C., R. Panneer Selvam, and Ashok Saxena. 2007. “Stabilizing Nanocrystalline Materials with Dopants.” *Acta Materialia* 55 (7): 2329–36. doi:10.1016/j.actamat.2006.11.028.

Mohamed, Farghalli A, and Yong Li. 2001. "Creep and Superplasticity in Nanocrystalline Materials: Current Understanding and Future Prospects." *Materials Science and Engineering: A* 298 (1): 1–15.

Mughrabi, Hael, and Heinz Werner Höppel. 2010. "Cyclic Deformation and Fatigue Properties of Very Fine-Grained Metals and Alloys." *International Journal of Fatigue*, Emerging Frontiers in Fatigue, 32 (9): 1413–27. doi:10.1016/j.ijfatigue.2009.10.007.

Murdoch, Heather A, and Christopher A Schuh. 2013. "Estimation of Grain Boundary Segregation Enthalpy and Its Role in Stable Nanocrystalline Alloy Design." *Journal of Materials Research* 28 (16): 2154–2163.

Ovid'ko, I. A. 2007. "Review on the Fracture Processes in Nanocrystalline Materials." *Journal of Materials Science* 42 (5): 1694–1708. doi:10.1007/s10853-006-0968-9.

Palumbo, G., S. J. Thorpe, and K. T. Aust. 1990. "On the Contribution of Triple Junctions to the Structure and Properties of Nanocrystalline Materials." *Scripta Metallurgica et Materialia* 24 (7): 1347–50. doi:10.1016/0956-716X(90)90354-J.

Panzarino, Jason F., Jesus J. Ramos, and Timothy J. Rupert. 2015. "Quantitative Tracking of Grain Structure Evolution in a Nanocrystalline Metal during Cyclic Loading." *Modelling and Simulation in Materials Science and Engineering* 23 (2): 25005. doi:10.1088/0965-0393/23/2/025005.

Petch, N. J. 1953. "The Cleavage Strength of Polycrystals." *J. Iron Steel Inst. Lond.* 173: 25–28.

Plimpton, Steve. 1995. "Fast Parallel Algorithms for Short-Range Molecular Dynamics." *Journal of Computational Physics* 117 (1): 1–19. doi:10.1006/jcph.1995.1039.

Pollock, Tresa M., and Sammy Tin. 2006. "Nickel-Based Superalloys for Advanced Turbine Engines: Chemistry, Microstructure and Properties." *Journal of Propulsion and Power* 22 (2): 361–74. doi:10.2514/1.18239.

Pun, GP Purja, KA Darling, LJ Kecskes, and Y Mishin. 2015. "Angular-Dependent Interatomic Potential for the Cu–Ta System and Its Application to Structural Stability of Nano-Crystalline Alloys." *Acta Materialia* 100: 377–391.

Rajagopalan, Jagannathan, Jong H. Han, and M. Taher A. Saif. 2007. "Plastic Deformation Recovery in Freestanding Nanocrystalline Aluminum and Gold Thin Films." *Science* 315 (5820): 1831–34. doi:10.1126/science.1137580.

Rajagopalan, M., K. Darling, S. Turnage, R. K. Koju, B. Hornbuckle, Y. Mishin, and K. N. Solanki. 2017. "Microstructural Evolution in a Nanocrystalline Cu-Ta Alloy: A Combined in-Situ TEM and Atomistic Study." *Materials & Design* 113 (January): 178–85. doi:10.1016/j.matdes.2016.10.020.

Reed, Roger C. 2008. *The Superalloys: Fundamentals and Applications*. Cambridge University Press.

Reid, C. N. 1981. “The Association of Twinning and Fracture in Bcc Metals.” *Metallurgical Transactions A* 12 (3): 371–377.

Ribis, J., and Y. de Carlan. 2012. “Interfacial Strained Structure and Orientation Relationships of the Nanosized Oxide Particles Deduced from Elasticity-Driven Morphology in Oxide Dispersion Strengthened Materials.” *Acta Materialia* 60 (1): 238–52. doi:10.1016/j.actamat.2011.09.042.

Rice, James R. 1992. “Dislocation Nucleation from a Crack Tip: An Analysis Based on the Peierls Concept.” *Journal of the Mechanics and Physics of Solids* 40 (2): 239–271.

Rinaldi, A., P. Peralta, C. Friesen, and K. Sieradzki. 2008. “Sample-Size Effects in the Yield Behavior of Nanocrystalline Nickel.” *Acta Materialia* 56 (3): 511–17. doi:10.1016/j.actamat.2007.09.044.

Rojhirunsakool, Tanaporn, Kristopher A Darling, Mark A Tschopp, Ganga P Purja Pun, Yuri Mishin, Rajarshi Banerjee, and Laszlo J Kecskes. 2015. “Structure and Thermal Decomposition of a Nanocrystalline Mechanically Alloyed Supersaturated Cu–Ta Solid Solution.” *MRS Communications* 5 (2): 333–339.

Rupert, T. J., D. S. Gianola, Y. Gan, and K. J. Hemker. 2009. “Experimental Observations of Stress-Driven Grain Boundary Migration.” *Science* 326 (5960): 1686–90. doi:10.1126/science.1178226.

Rupert, Timothy J. 2016. “The Role of Complexions in Metallic Nano-Grain Stability and Deformation.” *Current Opinion in Solid State and Materials Science*.

Saada, G. 2005. “Hall–Petch Revisited.” *Materials Science and Engineering: A*, Dislocations 2004An International Conference on the Fundamentals of Plastic Deformation, 400–401 (July): 146–49. doi:10.1016/j.msea.2005.02.091.

Saber, Mostafa, Hasan Kotan, Carl C. Koch, and Ronald O. Scattergood. 2013a. “Thermodynamic Stabilization of Nanocrystalline Binary Alloys.” *Journal of Applied Physics* 113 (6): 63515. doi:10.1063/1.4791704.

———. 2013b. “A Predictive Model for Thermodynamic Stability of Grain Size in Nanocrystalline Ternary Alloys.” *Journal of Applied Physics* 114 (10): 103510. doi:10.1063/1.4821040.

Sanders, P. G., J. A. Eastman, and J. R. Weertman. 1997. “Elastic and Tensile Behavior of Nanocrystalline Copper and Palladium.” *Acta Materialia* 45 (10): 4019–25. doi:10.1016/S1359-6454(97)00092-X.

Schiøtz, Jakob, Francesco D. Di Tolla, and Karsten W. Jacobsen. 1998. “Softening of Nanocrystalline Metals at Very Small Grain Sizes.” *Nature* 391 (6667): 561–63. doi:10.1038/35328.

Schiøtz, Jakob, and Karsten W. Jacobsen. 2003a. “A Maximum in the Strength of Nanocrystalline Copper.” *Science* 301 (5638): 1357–1359.

———. 2003b. “A Maximum in the Strength of Nanocrystalline Copper.” *Science* 301 (5638): 1357–59. doi:10.1126/science.1086636.

Shan, Zhiwei, E. A. Stach, J. M. K. Wiezorek, J. A. Knapp, D. M. Follstaedt, and S. X. Mao. 2004. “Grain Boundary-Mediated Plasticity in Nanocrystalline Nickel.” *Science* 305 (5684): 654–57. doi:10.1126/science.1098741.

Shaw, Leon L, and Hong Luo. 2007. “Deformation Behavior and Mechanisms of a Nanocrystalline Multi-Phase Aluminum Alloy.” *Journal of Materials Science* 42 (5): 1415–1426.

Shen, T. D., and C. C. Koch. 1996. “Formation, Solid Solution Hardening and Softening of Nanocrystalline Solid Solutions Prepared by Mechanical Attrition.” *Acta Materialia* 44 (2): 753–61. doi:10.1016/1359-6454(95)00178-6.

Sherby, Oleg D., and Jeffrey Wadsworth. 1989. “Superplasticity—Recent Advances and Future Directions.” *Progress in Materials Science* 33 (3): 169–221. doi:10.1016/0079-6425(89)90004-2.

Simões, S., R. Calinas, P.j. Ferreira, F. Viana, M.t. Vieira, and M.f. Vieira. 2008. “TEM and SEM in-Situ Annealing of Nanocrystalline Copper Thin Films.” *Microscopy and Microanalysis* 14 (Supplement S3): 49–52. doi:10.1017/S1431927608089368.

Simões, Sonia, Rosa Calinas, P.J. Ferreira, M. Teresa Vieira, Filomena Viana, and Manuel F. Vieira. 2008. “Effect of Annealing Conditions on the Grain Size of Nanocrystalline Copper Thin Films.” *Materials Science Forum* 587–588: 483–87. doi:10.4028/www.scientific.net/MSF.587-588.483.

“Sina_Shahandeh_TMS2010.pdf.” 2015. Accessed July 29. http://iranscholars.org/wiki/images/3/36/Sina_Shahandeh_TMS2010.pdf.

Stukowski, Alexander. 2010. “Visualization and Analysis of Atomistic Simulation Data with OVITO–the Open Visualization Tool.” *Modelling and Simulation in Materials Science and Engineering* 18 (1): 15012. doi:10.1088/0965-0393/18/1/015012.

Subramanian, P. R., and D. E. Laughlin. 1989. “The Cu-Ta (Copper-Tantalum) System.” *Bulletin of Alloy Phase Diagrams* 10 (6): 652–55. doi:10.1007/BF02877637.

Sun, P. L., E. K. Cerreta, G. T. Gray, and J. F. Bingert. n.d. "The Effect of Grain Size, Strain Rate, and Temperature on the Mechanical Behavior of Commercial Purity Aluminum." *Metallurgical and Materials Transactions A* 37 (10): 2983–94. doi:10.1007/s11661-006-0180-1.

Suo, Tao, Yulong Li, Feng Zhao, Xueling Fan, and Weiguo Guo. 2013. "Compressive Behavior and Rate-Controlling Mechanisms of Ultrafine Grained Copper over Wide Temperature and Strain Rate Ranges." *Mechanics of Materials* 61 (July): 1–10. doi:10.1016/j.mechmat.2013.02.003.

Swygenhoven, H. Van, and A. Caro. 1997. "Plastic Behavior of Nanophase Ni: A Molecular Dynamics Computer Simulation." *Applied Physics Letters* 71 (12): 1652–54. doi:10.1063/1.119785.

Tadmor, E. B., and S. Hai. 2003. "A Peierls Criterion for the Onset of Deformation Twinning at a Crack Tip." *Journal of the Mechanics and Physics of Solids* 51 (5): 765–793.

Tao, J. M., X. K. Zhu, R. O. Scattergood, and C. C. Koch. 2013. "The Thermal Stability of High-Energy Ball-Milled Nanostructured Cu." *Materials & Design* 50 (September): 22–26. doi:10.1016/j.matdes.2013.02.083.

Terwilliger, C. D., and Yet-Ming Chiang. 1995. "Size-Dependent Solute Segregation and Total Solubility in Ultrafine Polycrystals: Ca in TiO2." *Acta Metallurgica et Materialia* 43 (1): 319–28. doi:10.1016/0956-7151(95)90288-0.

Trelewicz, Jason R., and Christopher A. Schuh. 2007. "The Hall–Petch Breakdown in Nanocrystalline Metals: A Crossover to Glass-like Deformation." *Acta Materialia* 55 (17): 5948–58. doi:10.1016/j.actamat.2007.07.020.

Tschopp, M. A., H. A. Murdoch, L. J. Kecskes, and K. A. Darling. 2014. "'Bulk' Nanocrystalline Metals: Review of the Current State of the Art and Future Opportunities for Copper and Copper Alloys." *JOM* 66 (6): 1000–1019. doi:10.1007/s11837-014-0978-z.

Upmanyu, M, D. J Srolovitz, L. S Shvindlerman, and G Gottstein. 2002. "Molecular Dynamics Simulation of Triple Junction Migration." *Acta Materialia* 50 (6): 1405–20. doi:10.1016/S1359-6454(01)00446-3.

Valiev, R. Z., M. J. Zehetbauer, Y. Estrin, H. W. Höppel, Y. Ivanisenko, H. Hahn, G. Wilde, H. J. Roven, X. Sauvage, and T. G. Langdon. 2007. "The Innovation Potential of Bulk Nanostructured Materials." *Advanced Engineering Materials* 9 (7): 527–33. doi:10.1002/adem.200700078.

Valiev, Ruslan Z., Kenong Xia, and Terence G. Langdon. 2009. "Processing by Severe Plastic Deformation:an Ancient Skill Adapted for the Modern World."

International Journal of Materials Research 100 (12): 1623–31. doi:10.3139/146.110233.

Van Swygenhoven, H, A Caro, and D Farkas. 2001. “A Molecular Dynamics Study of Polycrystalline Fcc Metals at the Nanoscale: Grain Boundary Structure and Its Influence on Plastic Deformation.” *Materials Science and Engineering: A*, Dislocations 2000: An International Conference on the Fundamentals of Plastic Deformation, 309–310 (July): 440–44. doi:10.1016/S0921-5093(00)01794-9.

Van Swygenhoven, H., P. M. Derlet, and A. G. Frøseth. 2004. “Stacking Fault Energies and Slip in Nanocrystalline Metals.” *Nature Materials* 3 (6): 399–403. doi:10.1038/nmat1136.

———. 2006a. “Nucleation and Propagation of Dislocations in Nanocrystalline Fcc Metals.” *Acta Materialia* 54 (7): 1975–83. doi:10.1016/j.actamat.2005.12.026.

———. 2006b. “Nucleation and Propagation of Dislocations in Nanocrystalline Fcc Metals.” *Acta Materialia* 54 (7): 1975–83. doi:10.1016/j.actamat.2005.12.026.

Van Swygenhoven, H., P. M. Derlet, and A. Hasnaoui. 2002. “Atomic Mechanism for Dislocation Emission from Nanosized Grain Boundaries.” *Physical Review B* 66 (2): 24101. doi:10.1103/PhysRevB.66.024101.

Wang, Y. M., K. Wang, D. Pan, K. Lu, K. J. Hemker, and E. Ma. 2003. “Microsample Tensile Testing of Nanocrystalline Copper.” *Scripta Materialia* 48 (12): 1581–86. doi:10.1016/S1359-6462(03)00159-3.

Wang, Yinmin, Mingwei Chen, Fenghua Zhou, and En Ma. 2002. “High Tensile Ductility in a Nanostructured Metal.” *Nature* 419 (6910): 912–15. doi:10.1038/nature01133.

Wei, Q., T. Jiao, S. N. Mathaudhu, E. Ma, K. T. Hartwig, and K. T. Ramesh. 2003. “Microstructure and Mechanical Properties of Tantalum after Equal Channel Angular Extrusion (ECAE).” *Materials Science and Engineering: A* 358 (1–2): 266–72. doi:10.1016/S0921-5093(03)00305-8.

Wei, Q., B. E. Schuster, S. N. Mathaudhu, K. T. Hartwig, L. J. Kecskes, R. J. Dowding, and K. T. Ramesh. 2008. “Dynamic Behaviors of Body-Centered Cubic Metals with Ultrafine Grained and Nanocrystalline Microstructures.” *Materials Science and Engineering: A*, Mechanical Behavior of Nanostructured Materials, a Symposium Held in Honor of Carl Koch at the TMS Annual Meeting 2007, Orlando, Florida, 493 (1–2): 58–64. doi:10.1016/j.msea.2007.05.126.

Wei, Yujie, Allan F. Bower, and Huajian Gao. 2008a. “Recoverable Creep Deformation and Transient Local Stress Concentration due to Heterogeneous Grain-Boundary Diffusion and Sliding in Polycrystalline Solids.” *Journal of the Mechanics and Physics of Solids* 56 (4): 1460–83. doi:10.1016/j.jmps.2007.08.007.

———. 2008b. “Enhanced Strain-Rate Sensitivity in Fcc Nanocrystals due to Grain-Boundary Diffusion and Sliding.” *Acta Materialia* 56 (8): 1741–52. doi:10.1016/j.actamat.2007.12.028.

Weissmüller, J. 1993. “Alloy Effects in Nanostructures.” *Nanostructured Materials*, Proceedings of the First International Conference on Nanostructured Materials, 3 (1–6): 261–72. doi:10.1016/0965-9773(93)90088-S.

Weissmüller, J., W. Krauss, T. Haubold, R. Birringer, and H. Gleiter. 1992. “Atomic Structure and Thermal Stability of Nanostructured Y-Fe Alloys.” *Nanostructured Materials* 1 (6): 439–47. doi:10.1016/0965-9773(92)90076-A.

Weissmüller, Jörg. 1994. “Alloy Thermodynamics in Nanostructures.” *Journal of Materials Research* 9 (1): 4–7. doi:10.1557/JMR.1994.0004.

Witkin, David, Bing Q. Han, and Enrique J. Lavernia. n.d. “Mechanical Behavior of Ultrafine-Grained Cryomilled Al 5083 at Elevated Temperature.” *Journal of Materials Engineering and Performance* 14 (4): 519–27. doi:10.1361/105994905X56232.

Wu, X. L., K. M. Youssef, C. C. Koch, S. N. Mathaudhu, L. J. Kecskés, and Y. T. Zhu. 2011. “Deformation Twinning in a Nanocrystalline Hcp Mg Alloy.” *Scripta Materialia* 64 (3): 213–16. doi:10.1016/j.scriptamat.2010.10.024.

Xiao, Chenghe, R. A. Mirshams, S. H. Whang, and W. M. Yin. 2001. “Tensile Behavior and Fracture in Nickel and Carbon Doped Nanocrystalline Nickel.” *Materials Science and Engineering: A* 301 (1): 35–43. doi:10.1016/S0921-5093(00)01392-7.

Yamakov, V., D. Wolf, S. R. Phillpot, A. K. Mukherjee, and H. Gleiter. 2004. “Deformation-Mechanism Map for Nanocrystalline Metals by Molecular-Dynamics Simulation.” *Nature Materials* 3 (1): 43–47. doi:10.1038/nmat1035.

Yamashita, Masaki, and Koji Kakehi. 2006. “Tension/Compression Asymmetry in Yield and Creep Strengths of Ni-Based Superalloy with a High Amount of Tantalum.” *Scripta Materialia* 55 (2): 139–42. doi:10.1016/j.scriptamat.2006.03.048.

Zhang, J. X., J. C. Wang, H. Harada, and Y. Koizumi. 2005. “The Effect of Lattice Misfit on the Dislocation Motion in Superalloys during High-Temperature Low-Stress Creep.” *Acta Materialia* 53 (17): 4623–33. doi:10.1016/j.actamat.2005.06.013.

Zhang, Kai, J. R. Weertman, and J. A. Eastman. 2005. “Rapid Stress-Driven Grain Coarsening in Nanocrystalline Cu at Ambient and Cryogenic Temperatures.” *Applied Physics Letters* 87 (6): 61921. doi:10.1063/1.2008377.

Zhao, F. X., X. C. Xu, H. Q. Liu, and Y. L. Wang. 2014. “Effect of Annealing Treatment on the Microstructure and Mechanical Properties of Ultrafine-Grained

Aluminum." *Materials & Design* 53 (January): 262–68. doi:10.1016/j.matdes.2013.06.075.

Zhou, LZ, JT Guo, GS Li, LY Xiong, SH Wang, and CG Li. 1997. "Investigation of Annealing Behavior of Nanocrystalline NiAl." *Materials & Design* 18 (4): 373–377.

Zhu, Y. T., X. Z. Liao, and X. L. Wu. 2012. "Deformation Twinning in Nanocrystalline Materials." *Progress in Materials Science* 57 (1): 1–62. doi:10.1016/j.pmatsci.2011.05.001.

Zhu, Y. T., X. L. Wu, X. Z. Liao, J. Narayan, L. J. Kecskés, and S. N. Mathaudhu. 2011. "Dislocation–twin Interactions in Nanocrystalline Fcc Metals." *Acta Materialia* 59 (2): 812–21. doi:10.1016/j.actamat.2010.10.028.